

REMARKS

In the OFFICE ACTION dated September 23, 2003, the Examiner withdrew claims 11-22 from further consideration. Applicant cancels these claims.

Claims 1-10, 23 and 24 have been rejected under 35 U.S.C. § 112, first paragraph, as being non-enabled. Applicant amends the claims to more particularly point out that the claimed invention is a composition of matter that is composed of an “eye-specific gene” that is located within a receptor-specific delivery vehicle. The delivery vehicle includes a liposome that has been decorated with a plurality of targeting agents that are specific for the blood-retinal barrier and ocular cell membrane. The targeting agents are attached to the surface of the liposome by way of conjugation agents. The reference to “therapeutic” gene has been deleted from the claims. Accordingly, there is no need for applicant to positively demonstrate a therapeutic result or otherwise enable an invention for gene therapy.

The term “therapeutic” gene, as used in the specification, is intended to provide guidance to one of ordinary skill in the art regarding the types of genes that are suitable for encapsulation in the receptor-specific delivery vehicle. The use of “therapeutic” in defining the types of genes that are suitable for encapsulation should not be viewed as a requirement that the receptor-specific delivery vehicle (including the gene) must meet some undefined threshold of therapeutic value that might be considered suitable for gene therapy purposes in humans. Instead, the nature of the invention simply involves delivery of eye-specific genes to ocular cells wherein the genes that are delivered are known by those of skill in the art to be of potential therapeutic or diagnostic value in treating eye disorders.

It should be noted that the claimed invention is not limited to a composition for use in gene therapy. As set forth in Paragraphs 12 and 39 of the specification, the genes that are encapsulated in the receptor-specific liposome are those that may be used in the diagnosis and treatment of eye diseases. The specification provides sufficient details for

one of ordinary skill in the art to make the claimed composition. In Paragraph 39, a list of about eighteen exemplary “eye-specific” genes is provided along with a general teaching that any of the common genes used in diagnosis and therapy of the eye may be used. In addition, the examples demonstrate how two exemplary reporter genes (β -galactosidase and luciferase) are combined with receptor-specific liposomes to deliver such reporter genes to ocular cells.

The Examiner is correct that there had been no success stories associated with gene therapy approaches when the Verma et al. article appeared in 1997. Like many other researchers at that time, Verma et al. recognized that the “Achilles” heel of gene therapy is how to successfully target and deliver the therapeutic agent. The present application, which was filed some 4 years after Verma et al., provides a delivery vehicle that is substantially different from the systems described by Verma et al. The viral vectors and cationic lipids in use at the time of Verma et al. are completely different from the targeting ligand-conjugated liposomes claimed by applicant. Applicant encloses herewith seven articles that demonstrate the successes which have been achieved using receptor-specific liposomes to deliver genes to cells including ocular cells.

The invention, as now claimed, does not require undue experimentation nor is it unpredictable. The skilled artisan does not have to empirically determine what genes can be encapsulated in the receptor-specific liposome. The genes that can be used are defined in the specification as being eye-specific genes that are already known and proven to have therapeutic or diagnostic value. The invention is not a gene therapy method, but rather a composition for use in a gene delivery method. Accordingly, there is no need for the skilled artisan to determine how much of the gene needs to be administered to the patient in order to achieve a “therapeutic effect”. In order to use the claimed invention, the skilled artisan need only know how to deliver the receptor-specific liposome to the ocular cells. Delivery to ocular cells *in vitro* is accomplished by simple admixture with the cells. Delivery *in vivo* is accomplished by combining the receptor-specific liposomes with saline or other suitable carrier and injecting the preparation intravenously.

The issues of unpredictability and experimentation are only relevant to an invention that is claiming a method for treating eye disorders with gene therapy. The invention, as now claimed, more particularly points out that the present invention is directed to compositions that are useful for delivering eye-specific genes to ocular cells. The end result of such delivery is not claimed and therefore need not be enabled. The invention, if desired, can be for diagnostic or therapeutic purposes.

Claims 1-10, 23 and 24 have also been rejected under 35 U.S.C. § 112, first paragraph as containing subject matter that is not sufficiently described in the specification. Again, applicant has amended the claims to delete the term “therapeutic” from the claims. The claims invention covers receptor-specific liposomes that are targeted to the blood-retinal barrier and ocular cell membrane. Further, the liposome contains a gene that is “eye-specific” as set forth in the specification. Such “eye-specific” genes are those that are known by those of skill in the art to be therapeutic or diagnostic with respect to eye diseases. As mentioned above, applicant provides numerous examples of the types of “eye-specific” genes that are suitable for encapsulation. Since the claimed invention is not a method for gene therapy, it is neither necessary nor required that applicant show reduction to practice of a successful gene therapy treatment. It is only necessary for applicant to demonstrate that the receptor-specific liposome is useful in that it does deliver genes (therapeutic or diagnostic) to ocular cells with a non-invasive intravenous administration. This is a novel advance, since all prior methods for gene delivery to the eye involved injecting the gene directly into the eyeball of the patient. The examples in the specification provide this demonstration (reduction to practice) of the invention, as now claimed.

Claims 1-10, 23 and 24 have been rejected under 35 U.S.C. § 112, second paragraph, as being indefinite. Applicant amends the claims to delete the term “sufficient amount” that has been objected to as being vague. Also, “said nanocontainer” has been deleted since it lacks antecedent basis. In addition, the specification has been amended to indicate what is meant by the various acronyms that are used to identify exemplary eye-

Serial No. 10/025,732

-11-

Docket No. 0180.0029

specific genes. The claims have been amended accordingly to delete the use of acronyms.

With regards to the use of improper Markush language in claims 3 and 10, these claims have been amended and new claims 25-29 have been added to remove the improper Markush language.

Claims 6 and 23 have been rejected because "said liposome" lacks antecedent basis. The antecedent basis for "said liposome" is found in the element that is initially described in claims 1 and 23 as "a liposome having an exterior surface and an internal compartment." Applicant amends claims 6 and 23 to remove any question of antecedent basis by referring to "said exterior surface of said liposome." Applicant submits that it would be incorrect to remedy the rejection as suggested by the Examiner because "said liposome" refers to only one of four elements that make up the "receptor-specific liposome" set forth in the preamble of the claim.

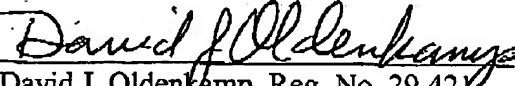
Applicant amends claim 9 as suggested by the Examiner to provide proper antecedent basis throughout the claim.

In view of the above amendments and remarks, applicant respectfully requests that this application be reexamined and that the claims, as amended, be allowed.

Please charge any fees that may be due for the filing of this AMENDMENT or credit any overpayments to Deposit Account No. 50-1811.

Respectfully Submitted,

Dated: December 22 2003


David J. Oldenkamp, Reg. No. 29,421
SHAPIRO & DUPONT LLP
233 Wilshire Boulevard, Suite 700
Santa Monica, California 90401
(310) 319-5411 (Telephone)
(310) 319-5401 (Facsimile)

Index of Cited References

1. Zhang, Y. et al. "Antisense Gene Therapy of Brain Cancer with an Artificial Virus Gene Delivery System," MOLECULAR THERAPY Vol. 6, No. 1, pps. 67-72 (2002).
2. Zhang, Y. et al. "Intravenous Nonviral Gene Therapy Causes Normalization of Striatal Tyrosine Hydroxylase and Reversal of Motor Impairment in Experimental Parkinsonism," HUMAN GENE THERAPY 14:1-12 (2003).
3. Zhang, Y. et al. "Organ-specific gene expression in the rhesus monkey eye following intravenous non-viral gene transfer," MOLECULAR VISION 2003; 9:465-72.
4. Zhang, Y. et al. "Global Non-Viral Gene Transfer to the Primate Brain Following Intravenous Administration," MOLECULAR THERAPY Vol. 7, No. 1 (2003).
5. Zhu, C. et al. "Widespread Expression of an Exogenous Gene in the Eye after Intravenous Administration," INVESTIGATIVE OPHTHALMOLOGY & VISUAL SCIENCE, Vol. 43, No. 9, pps. 3075-3080 (2002).
6. Zhang, Y. et al. "Absence of Toxicity of Chronic Weekly Intravenous Gene Therapy with Pegylated Immunoliposomes," PHARMACEUTICAL RESEARCH, Vol. 20, No. 11, pps. 1779-1785 (2003).
7. Shi, N. et al. "Receptor-Mediated Gene Targeting to Tissues *In Vivo* Following Intravenous Administration of Pegylated Immunoliposomes," PHARMACEUTICAL RESEARCH, Vol. 18, No. 8, pps. 1091-1095 (2001).

Antisense Gene Therapy of Brain Cancer with an Artificial Virus Gene Delivery System

Yun Zhang, Chunni Zhu, and William M. Pardridge*

Department of Medicine, UCLA School of Medicine, Los Angeles, California 90024, USA

**To whom correspondence and reprint requests should be addressed. Fax: (310) 206-5163. E-mail: wpardridge@mednet.ucla.edu.*

Therapeutic genes are delivered to the nuclear compartment of cancer cells following intravenous administration with a non-immunogenic "artificial virus" gene delivery system that uses receptor-specific monoclonal antibodies (MAb) to navigate the biological barriers between the blood and the nucleus of the cancer cell. Mice implanted with intracranial U87 human glial brain tumors are treated with a nonviral expression plasmid encoding antisense mRNA against the human epidermal growth factor receptor gene (*EGFR*). The plasmid DNA is packaged within the interior of polyethylene glycol-modified (PEGylated) immunoliposomes, and delivered to the brain tumor with MAbs that target the mouse transferrin receptor (TRFR) and the human insulin receptor (INSR). The mouse TRFR MAb enables transport across the tumor vasculature, which is of mouse brain origin, and the INSR MAb causes transport across the plasma membrane and the nuclear membrane of the human brain cancer cell. The lifespan of the mice treated weekly with an intravenous administration of the *EGFR* antisense gene therapy packaged within the artificial virus is increased 100% relative to mice treated either with a luciferase gene or with saline.

Key Words: gene therapy, liposomes, blood-brain barrier, brain cancer, insulin receptor, transferrin receptor, epidermal growth factor receptor

INTRODUCTION

Most solid cancers, including brain cancers, are dependent on the epidermal growth factor receptor (*EGFR*) [1,2], and antisense gene therapy directed at the gene *EGFR* is a potential treatment strategy. The delivery of therapeutic genes to solid cancers is hindered by the tumor microvascular barrier, which in brain forms the blood-brain barrier (BBB). Viral vectors for gene therapy do not cross the BBB; therefore, it is necessary to administer the vector by means of intracerebral injection. However, this has limited success owing to poor diffusion of the vector from the injection site, which prevents distribution of the therapeutic gene to most cells within the brain cancer [3]. The preexisting immunity to viral vectors is another difficulty, as a single injection of the virus into the brain causes inflammation and demyelination in humans and primates [4,5]. The principal nonviral gene transfer technology uses complexes of plasmid DNA and cationic lipids or cationic proteins. However, these complexes aggregate in physiological saline and are not suitable for gene transfer to the brain following intravenous administration. The problems in gene transfer presented by either viral vectors or DNA/cationic complexes are eliminated with the use of a polyethylene glycol-modified (PEGylated) immunoliposome (PIL) gene delivery system that is capable of transport across the BBB

and can be administered by intravenous injection [6-8]. This targeted gene delivery system uses an "artificial virus" wherein the therapeutic gene encoded in a nonviral expression plasmid is encapsulated within the interior of an 85 nm PIL (Fig. 1A). The PIL construct is unrelated to cationic liposomes, as the plasmid DNA is encapsulated in the interior of a spherical liposome with a net anionic charge [7]. The surface of the PIL gene delivery system contains one or more peptidomimetic monoclonal antibodies (MAb). These targeting antibodies bind to specific receptor systems to facilitate transport of the PIL across the multiple biological barriers separating the blood from the nuclear compartment of the cancer cell. With this approach, a therapeutic gene can be delivered to the nucleus of a cancer cell following an intravenous injection.

In this investigation, experimental human brain cancer develops in severe combined immunodeficient (SCID) mice following the intracerebral injection of U87 human glioma cells. The brain cancer is treated weekly with an intravenous injection of a plasmid encoding antisense mRNA to human *EGFR*. This plasmid DNA encoding the *EGFR* antisense mRNA is designated clone 882. When the plasmid is encapsulated within the interior of the PIL and delivered to human U87 glioma cells in tissue culture, there is a 70% reduction in thymidine incorporation into

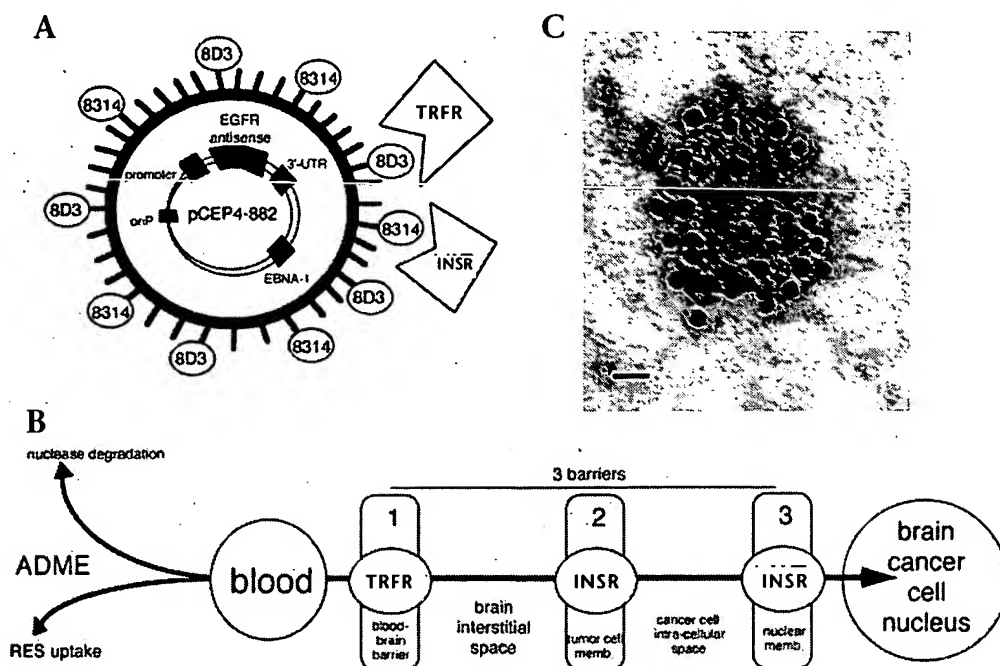


FIG. 1. Gene delivery across biological barriers. (A) The 85 nm PEGylated immunoliposome (PIL) includes approximately 2000 strands of 2000 Da PEG conjugated to the surface of the liposome to minimize rapid uptake by the RES. Approximately 2% of the PEG strands are tethered at the tips of the strands with either the 8D3 or the 83-14 MAb to cause binding of the PIL to either the mouse TRFR or the human INSR, respectively. The expression plasmid (clone 882) is derived from the pCEP4 plasmid, encodes *EGFR* antisense mRNA, and is driven by the SV40 promoter [9]. (B) Multiple barriers must be circumvented before a therapeutic gene injected in the bloodstream can distribute to the nuclear compartment of the cancer cell. The 8D3 MAb to the TRFR causes receptor-mediated transcytosis of the PIL across the tumor microvascular barrier, or BBB. The 83-14 MAb to the INSR mediates transport of the PIL across the tumor cell plasma membrane and the nuclear membrane of the tumor cell [9]. (C) Electron microscopy of the PIL conjugated with the INSR MAb, and complexed with a conjugate of 10 nm gold and an anti-mouse secondary antibody. Magnification bar, 20 nm.

the cells and a 79% reduction in the level of immunoreactive EGFR protein [9]. In this study, clone 882 plasmid DNA is encapsulated within the interior of the PIL targeted with both the rat 8D3 MAb to the mouse transferin receptor (TRFR) and the mouse 83-14 MAb to the human insulin receptor (INSR; Fig. 1A). The brain tumor, composed of human U87 glioma cells, is perfused by a microvasculature of mouse brain origin. The 8D3 MAb causes receptor-mediated transcytosis of the PIL across the tumor BBB by targeting the endogenous mouse TRFR on the tumor microvascular endothelium (Fig. 1B) [8]. The 83-14 MAb causes receptor-mediated endocytosis of the PIL into the U87 tumor cell [9]. In addition, confocal microscopy studies show that the INSR MAb also targets the PIL across the nuclear barrier (Fig. 1B) [9]. The PIL that is conjugated with both the 8D3 MAb and the 83-14 MAb is designated the 8D3/83-14 PIL (Fig. 1A).

The expression plasmid encoding the *EGFR* antisense gene is encapsulated within the interior of the 85 nm PIL (Fig. 1A). The PIL acts as a nanocontainer or artificial virus and shields the therapeutic DNA from the ubiquitous endonucleases present *in vivo*. The surface of the liposome is conjugated with several thousand strands of 2000 Da polyethylene glycol (PEG²⁰⁰⁰). The PEG polymers extend

from the surface of the liposome [6]. About 2% of the PEG strands are tethered at the tip with the targeting MAb, and there are typically 35–50 MAb molecules per individual liposome [6–8]. The PEG strands prevent the absorption of serum proteins to the surface of the liposome [10], which reduces the uptake of the PIL by cells lining the reticulo-endothelial system (RES; Fig. 1B). PEGylation of the liposome gives it prolonged blood residence time and optimized properties of absorption, distribution, and metabolism (ADME) [10], similar to other drugs (Fig. 1B). An effective *in vivo* gene transfer vehicle must have the dual properties of stability in the bloodstream and ability to navigate the biological barriers separating the blood from the nucleus of the target cell (Fig. 1B).

RESULTS AND DISCUSSION

The PEG-extended MAb molecules projecting from the surface of the PIL were revealed by electron microscopy (Fig. 1C). The PIL has a diameter of nearly 100 nm, which approximates the size of many viruses. The average number of 83-14 or 8D3 MAb molecules conjugated per liposome is computed from trace amounts of [³H]8D3 MAb or [¹²⁵I]-83-14 MAb (37 ± 2 and 35 ± 3 , respectively). The

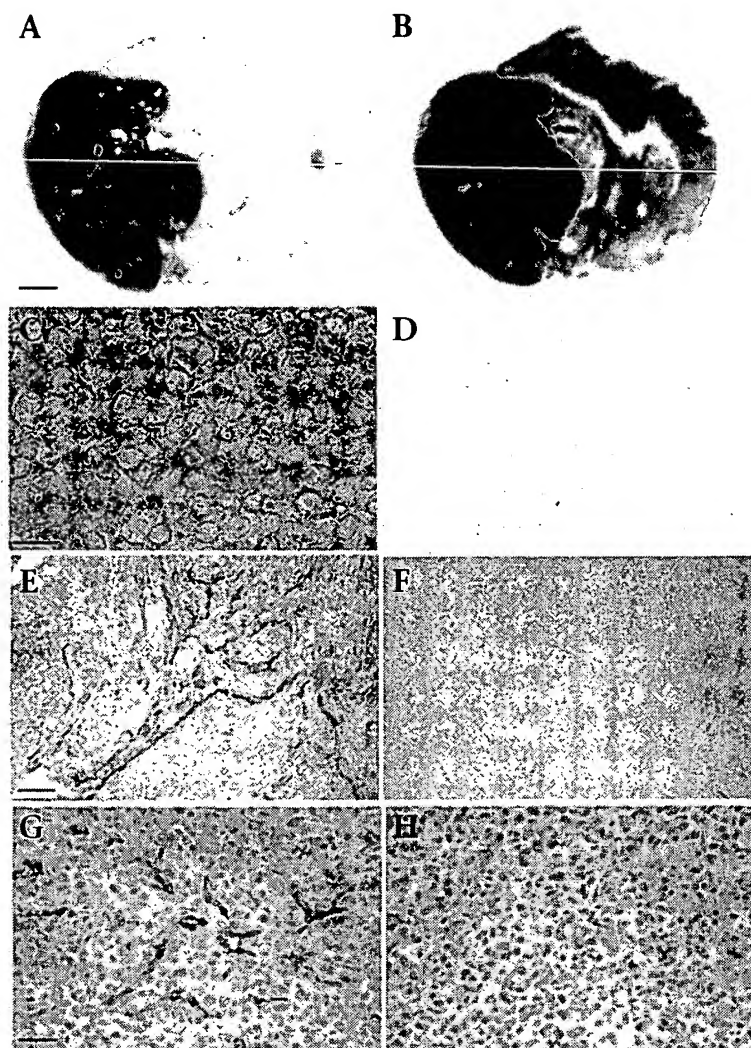


FIG. 2. Immunocytochemistry of frozen sections of mouse brain using the 528 MAb to the human EGFR (A), the 83-14 MAb to the INSR (C), the rat 8D3 MAb to the mouse TRFR (E, G), mouse IgG_{2a} (D), and rat IgG (F, H). (A) Abundant expression of the immunoreactive EGFR in the tumor with minimal expression in normal mouse brain. (B) Frozen section of mouse brain corresponding to (A) counterstained with hematoxylin. The sections in (A) and (B) show the size of the brain tumor at death. (C) Expression of the INSR on the plasma membrane of the tumor cells, whereas the mouse IgG_{2a} isotype control (D) shows no staining of the tumor cells. Abundant expression of the mouse TRFR on the microvasculature perfusing the tumor (E, G), whereas the rat IgG control antibody (F, H) shows no staining of the tumor or tumor vessels. Panels (B) and (E–H) are counter-stained, and (A), (C), and (D) are not counter-stained. The magnification is the same in (A) and (B), (C) and (D), (E) and (F), and (G) and (H), respectively; the magnification bars in (A), (C), (E), and (G) are 1 mm, 11 μ m, 114 μ m, and 29 μ m, respectively.

plasma membrane of the brain tumor cells *in situ* express INSR, as shown by immunocytochemistry of tumor sections with the 83-14 MAb (Fig. 2C). The microvessels perfusing the tumors are strongly immunoreactive for the mouse TRFR, as shown by immunocytochemistry with the 8D3 MAb (Fig. 2E), although the 8D3 MAb does not react with the human TRFR on the U87 cell plasma membrane (Fig. 2G). Therefore, the mouse TRFR and the human INSR, which mediate uptake of the PIL into the tumor, and the target EGFR, are all expressed in these experimental brain tumors *in vivo* (Fig. 2).

The expression of an exogenous gene within the experimental tumor is demonstrated with a luciferase expression plasmid, designated clone 790 [9]. This pCEP4-derived plasmid is identical to the clone 882 plasmid expressing the EGFR antisense mRNA, except for the expressed gene [9]. The clone 882 plasmid DNA contains the EBNA-1/oriP replication system, which promotes persistence of gene expression and enables extrachromosomal replication of the plasmid DNA at the time of cell division [12]. Gene expression in human U87 glioma cells persists for up to 21 days after a single addition of the PIL gene delivery system to the cells [9]. The clone 790 plasmid is encapsulated within the 8D3/83-14 conjugated PIL and is injected intravenously to tumor-bearing mice at 5 and 12 days after tumor implantation. On days 16–19 after tumor implantation, the luciferase enzyme activity is measured in both the brain tumor and the contralateral normal mouse brain (Fig. 3). Luciferase enzyme activity decreases with a $t_{1/2}$ of 1.02 ± 0.02 days and 1.31 ± 0.52 days in tumor brain and normal mouse brain, respectively. The peak luciferase enzyme activity in brain is observed 2 days after injection [6,8], and the extrapolated luciferase enzyme activity in the brain tumor at 2 days after injection

average DNA encapsulation per liposome preparation is computed from trace amounts of [32 P]DNA ($21 \pm 1\%$ (mean \pm SE), $n = 12$). The doses administered by tail vein per mouse (in a final volume of 400 μ L saline) are as follows: plasmid DNA, 5.2 ± 0.4 μ g; lipid, 2.4 ± 0.2 μ mol; 8314 MAb, 125 ± 13 μ g; 8D3 MAb, 139 ± 17 μ g; PEG, 200 ± 20 μ g. The PIL administered is 80% lipid, 11% protein, 9% carbohydrate, and 0.2% DNA. This dose of an 11.0-kb plasmid is equivalent to 9.6×10^{11} plasmid molecules per mouse. Assuming a tumor uptake of 0.1% injected dose per gram [7,11], and 1.8×10^8 tumor cells per gram, then about five to six plasmid molecules are targeted to each tumor cell. Each plasmid may produce multiple copies of the EGFR antisense mRNA within the tumor cell.

The implanted U87 cells grow into large tumors and approximately 50% of the cranium is occupied by tumor at the time of death (Figs. 2A and 2B). These brain tumors express EGFR, as demonstrated by immunocytochemistry with the 528 MAb to the human EGFR (Fig. 2A). The

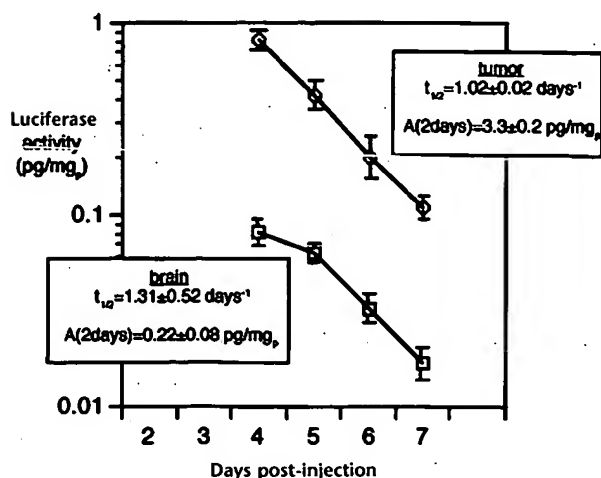


FIG. 3. Luciferase gene expression. Luciferase activity in extracts of either contralateral normal mouse brain or brain tumor is measured at 4, 5, 6, and 7 days after single intravenous injection of clone 790, the luciferase expression plasmid, packaged within the PIL targeted with both the 8D3 and 83-14 MAb. Data are mean \pm SE ($n = 3-4$ animals per group). The data are analyzed by linear regression analysis to yield the slope and y-intercept of the curve. The $t_{1/2}$ of decay in luciferase activity is computed from the slope. The peak luciferase activity at 2 days after injection [A(2days)] is computed from the slope and intercept.

tion is 15-fold greater than luciferase enzyme activity in normal mouse brain (Fig. 3). The INSR MAb, which targets the PIL across both the tumor cell plasma membrane and the tumor cell nuclear membrane [9], is inactive in normal mouse brain as the 83-14 MAb does not cross-react with the mouse insulin receptor. The TRFR MAb and the INSR MAb work in parallel to target the gene to the tumor, whereas the TRFR MAb works alone to target the gene to normal mouse brain. The higher level of gene expression in the tumor, relative to contralateral mouse brain, is attributed to the selective nuclear membrane targeting properties of the INSR MAb [9]. The insulin receptor delivers ligand to the nuclear compartment as demonstrated by either electron microscopic autoradiography or gold labeling [13,14].

The survival of the SCID mice bearing the U87 brain tumors is examined in three groups of mice treated with saline, clone 790 plasmid DNA expressing the luciferase mRNA and packaged within the 8D3/83-14 PIL, and clone 882 plasmid DNA expressing the *EGFR* antisense mRNA and packaged within the 8D3/83-14 PIL. Clone 882, expressing *EGFR* antisense mRNA, induces a 79% reduction in immunoreactive *EGFR* in the U87 glioma cells [9]. In this study, an aggressive tumor model is used in which the initiation of intravenous gene therapy was delayed until large brain tumors were already formed. In this model, 500,000 U87 brain tumor cells are implanted at day 0 and treatment is not initiated until day 5 after tumor implantation. At 5 days after implantation of 500,000 U87

cells in mouse brain, the entire caudate-putamen nucleus is occupied by tumors of up to 3 mm in diameter [15]. At the time of death, the tumor diameter is approximately 6 mm, and tumor tissue occupies half of the intracranial volume (Fig. 2B). The luciferase or *EGFR* antisense gene therapy is administered intravenously at days 5, 12, 19, and 26 after tumor implantation (Fig. 4). Both the mice treated with saline and the mice treated with the luciferase gene expired by 20–21 days and 50% in either group died by 18 days (Fig. 4). In contrast, the mice treated with the *EGFR* antisense gene packaged within the PIL delivery system have a 100% increase in survival with 50% mortality at 36 days (Fig. 4). The last dose of *EGFR* antisense gene therapy is administered at 26 days (Fig. 4).

These results demonstrate that the PIL targeted gene delivery system allows for the enhanced expression of exogenous genes within brain cancer relative to normal brain (Fig. 3). A 100% increase in lifespan is achieved with *EGFR* antisense gene therapy even though the initiation of gene therapy is delayed until large brain tumors had already formed, and therapy is terminated at 26 days (Fig. 4). *EGFR* antisense gene therapy is effective in the human U87 glioma model, although there is no amplification of *EGFR* in this cell line [15]. In contrast, *EGFR* inhibiting MAbs have no effect on wild-type U87 tumors that lack *EGFR* mutations [16]. It is possible that further increases in survival can be achieved with dual or triple gene therapy. Many brain cancers, including U87 cells, have a mutation in the tumor suppressor gene *PTEN* [17]. In addition to combining *EGFR* antisense gene therapy with *PTEN* replacement gene therapy, the combined use of gene therapy and radiation therapy may be beneficial in the

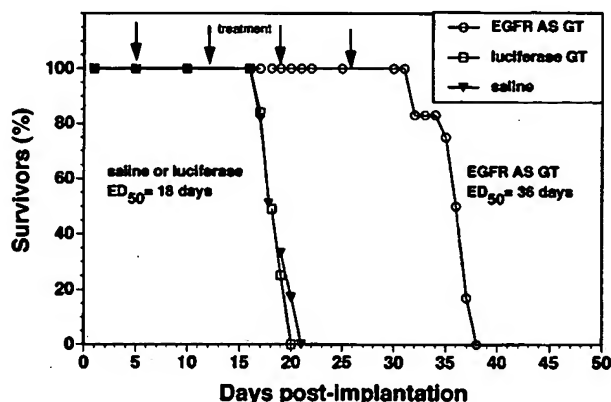


FIG. 4. Survival study. Intravenous gene therapy is initiated at 5 days, and repeated at 12, 19, and 26 days after tumor implantation. There are 12 tumor-bearing mice in each of the three groups. There is no statistical difference between the mortality in the animals treated with either saline or the luciferase expression plasmid (clone 790), although there was a 100% increase in survival of the animals that were treated with the *EGFR* antisense gene therapy (ASGT). The difference in survival in the *EGFR* antisense gene therapy group relative to the saline control, or the luciferase gene therapy group, is significant at the $P < 0.005$ level (Fisher's exact test).

treatment of brain cancer. Radiation induces an overexpression of the EGFR in brain tumors, which has a cytoprotective effect that inhibits further therapeutic effects of radiation therapy [18].

The gene delivery system used in these studies is designed specifically for brain cancer. Peptidomimetic MABs or other targeting ligands of varying tissue specificity may be selected to deliver therapeutic genes to cancers of peripheral origin. However, targeting ligands that cause not only receptor-mediated endocytosis into the tumor cell but also receptor-mediated transcytosis of the therapeutic gene across the tumor microvasculature should be selected. Without dual targeting across both the tumor cell membrane and the tumor microvascular barrier, it is unlikely that therapeutic levels of the gene will be achieved deep within the cancer cell, distal to the microvascular barrier. It may be possible to restrict gene expression to the cancer cell if the exogenous gene is driven by a promoter element taken from a gene specifically expressed in the cancer. Organ-specific gene expression is possible with the combined use of gene targeting technology and tissue-specific gene promoters [8].

This study shows that a liposomal gene delivery system can produce significant therapeutic effects in an experimental brain cancer model when used in conjunction with EGFR antisense gene therapy. The PIL gene targeting system functions as an artificial virus, and has the same size as many viral vectors (Fig. 1C). Similar to viral vectors, the gene is encapsulated in the interior of the nanocontainer [6–8], and the surface of the nanocontainer is decorated with targeting ligands that trigger receptor-mediated transcytosis across microvascular barriers [6–8] and receptor-mediated endocytosis across the tumor cell membrane [9]. The immunogenicity of the targeting MAB ligands is minimized with the use of genetically engineered, or “humanized,” antibodies. The PIL gene transfer technology allows for gene targeting to distant sites following the intravenous administration of a nonviral, non-immunogenic formulation.

MATERIALS AND METHODS

Brain tumor model. We obtained human U87 glioma cells from the American Type Culture Collection (Rockford, MD) and 500,000 cells were implanted in the caudate-putamen nucleus of adult female SCID mice under stereotaxic guidance on day 0. All animals develop large tumors, which are 4–8 mm in diameter at autopsy. The animals are treated with either saline, luciferase gene therapy, or EGFR antisense gene therapy weekly at 5, 12, 19, and 26 days. The use of vertebrate animals is in accordance with approved UCLA Animal Research Committee protocols.

Plasmid DNA. The therapeutic gene is encoded by an expression plasmid derived from the pCEP4 plasmid, that is designated clone 882, with a size of 11.0 kb (Fig. 1A). This plasmid produces a 700 nucleotide human EGFR antisense mRNA that corresponds to nucleotides 2317–3006 of the human EGFR mRNA [9]. The therapeutic gene is driven by the SV40 promoter and the transcript produced from this plasmid contains SV40 3'-untranslated region (UTR) mRNA as well as a 200-nucleotide fragment from SLC2A1 mRNA 3'-UTR, which contains an mRNA stabilizing element [9]. The plasmid also expresses the Epstein Barr nuclear antigen EBNA-1 and oriP (Fig. 1A), which is derived from the pCEP4 plasmid [9], and enables a single round of episomal replication of the plasmid with each cell mitosis [12].

PEGylated immunoliposome production and gene encapsulation. The PIL is prepared by first encapsulating 200 µg of plasmid DNA in 20 µmol of lipid with repetitive freeze/thaw cycles as described [6–8]. The lipid is 94% neutral lipid, POPC (1-palmitoyl-2-oleoyl-sn-glycerol-3-phosphocholine), 2% cationic lipid, DDAB (didodecyltrimethylammonium bromide), 3% anionic lipid, DSPE-PEG²⁰⁰⁰ (distearoylphosphatidylethanolamine conjugate of 2000 Da polyethylene glycol), and 1% anionic lipid, DSPE-PEG²⁰⁰⁰. MAL (a bi-functional PEG molecule with a DSPE moiety at one terminus of the polymer and a maleimide (MAL) group at the other terminus). Following DNA encapsulation in the large lipid vesicles, small 85–100 nm liposomes encapsulated with DNA are formed by successive extrusions through 400, 200, and 100 nm pore size polycarbonate membranes (Avestin, Ottawa, Canada), as described [6–8]. About half of the DNA is encapsulated within the liposome, and about half is exteriorized. The latter is exhaustively removed by nuclease treatment [6–8]. In parallel with the DNA encapsulation, the targeting antibodies (8D3, 83-14) are individually thiolated with 2-iminothiolane, and the thiolated antibodies are conjugated to the MAL moiety of the PEGylated liposomes overnight [6–8]. The unconjugated antibody and the nuclease digested exteriorized DNA are removed from the PIL by CL-4B gel filtration chromatography [9]. The thiolated antibody and DNA mixture contains a trace amount of [³H]8D3 MAB, [¹²⁵I]-83-14 MAB, and [³²P]DNA, and the radioactivity determinations allow for the calculation of the number of antibody molecules conjugated to the surface of each liposome and the amount of plasmid DNA encapsulated in the interior of the liposome.

Immunocytochemistry. Frozen sections of mouse brain (20 µm) are fixed in either 100% cold acetone for 20 minutes or in 4% paraformaldehyde for 10 minutes. A biotinylated horse anti-mouse IgG or a biotinylated rabbit anti-rat IgG secondary antibody is used with the ABC labeling method from Vector Labs (Burlingame, CA). The concentration of the primary antibody used is 10 µg/ml. The primary antibody used to detect the human EGFR, the human INSR, and the mouse TRFR are the 528 mouse MAB, the 83-14 mouse MAB, and the 8D3 rat MAB, respectively.

Luciferase enzyme measurement. Luciferase enzyme activity is measured in extracts of brain tumor or contralateral mouse brain with a luminometer, and expressed as pg luciferase activity per mg tissue protein [8,9].

Electron microscopy. PIL-conjugated INSR MAB are examined with a conjugate of 10 nm gold and a goat anti-mouse secondary antibody (Sigma G7652). A 4 µL aliquot of the 83-14-PIL (1.8×10^{12} liposomes) is incubated with 200 µL IgG gold conjugate (2.8×10^{12} gold particles) for 1 hour in 0.018 M Tris-buffered saline, pH 8, with 0.9% bovine serum albumin, and 17% glycerol. The mixture is applied to formvar-coated 2000 mesh copper grids, washed once with 0.05 M Tris/0.15 M NaCl, pH 7.4, counter-stained with 2% uranyl acetate, and examined directly by electron microscopy using a Jeol JEM-100CX II electron microscope at 80 kV. Negatives, taken at a $\times 29,000$, are scanned and enlarged in Adobe Photoshop 5.5 on a G4 Power Macintosh.

ACKNOWLEDGMENTS

This work was supported by funds from Accelerate Brain Cancer Cure (ABC²), Inc., and the United States Department of Defense.

RECEIVED FOR PUBLICATION MARCH 15; ACCEPTED MAY 8, 2002.

REFERENCES

- Nicholson, R. I., Gee, J. M. W., and Harper, M. E. (2001). EGFR and cancer prognosis. *Eur. J. Cancer* 37: S9–S15.
- Wong, A. J., et al. (1987). Increased expression of the epidermal growth factor receptor gene in malignant gliomas is invariably associated with gene amplification. *Proc. Natl. Acad. Sci. USA* 84: 6899–6903.
- Ram, Z., et al. (1997). Therapy of malignant brain tumors by intratumoral implantation of retroviral vector-producing cells. *Nat. Med.* 3: 1354–1361.
- Dewey, R. A., et al. (1999). Chronic brain inflammation and persistent herpes simplex virus 1 thymidine kinase expression in survivors of syngeneic glioma treated by adenovirus-mediated gene therapy: implications for clinical trials. *Nat. Med.* 5: 1256–1263.
- Driesse, M. J., et al. (1998). Intracerebral injection of adenovirus harboring the HSVtk gene combined with ganciclovir administration: toxicity study in non-human primates. *Gene Ther.* 5: 1122–1129.

6. Shi, N., and Pardridge, W. M. (2000). Non-invasive gene targeting to the brain. *Proc. Natl. Acad. Sci. USA* 97: 7567-7572.
7. Shi, N., Boado, R. J., and Pardridge, W. M. (2001). Receptor-mediated gene targeting to tissues in the rat in vivo. *Pharm. Res.* 18: 1091-1095.
8. Shi, N., Zhang, Y., Zhu, C., Boado, R. J., and Pardridge, W. M. (2001). Brain-specific expression of an exogenous gene following intravenous administration. *Proc. Natl. Acad. Sci. USA* 98: 12754-12759.
9. Zhang, Y., Lee, H. J., Boado, R. J., and Pardridge, W. M. (2002). Receptor-mediated delivery of an antisense gene to human brain cancer cells. *J. Gene Med.* 4: 183-194.
10. Papahadjopoulos, D., et al. (1991). Sterically stabilized liposomes: improvements in pharmacokinetics and antitumor therapeutic efficacy. *Proc. Natl. Acad. Sci. USA* 88: 11460-11464.
11. Lee, H. J., Engelhardt, B., Lesley, J., Bickel, U., and Pardridge, W. M. (2000). Targeting rat anti-mouse transferrin receptor monoclonal antibodies through the blood-brain barrier in the mouse. *J. Pharmacol. Exp. Ther.* 292: 1048-1052.
12. Makrides, S. (1999). Components of vectors for gene transfer and expression in mammalian cells. *Protein Expr. Purif.* 17: 181-202.
13. Podlecki, D. A., et al. (1987). Nuclear translocation of the insulin receptor. A possible mediator of insulin's long term effects. *J. Biol. Chem.* 262: 3362-3368.
14. Shah, N., Zhang, S., Harada, S., Smith, R. M., and Jarett, L. (1995). Electron microscopic visualization of insulin translocation into the cytoplasm and nuclei of intact H35 hepatoma cells using covalently linked Nanogold-insulin. *Endocrinology* 136: 2825-2835.
15. Lal, S., et al. (2000). An implantable guide-screw system for brain tumor studies in small animals. *J. Neurosurg.* 92: 326-333.
16. Mishima, K., et al. (2001). Growth suppression of intracranial xenografted glioblastomas overexpressing mutant epidermal growth factor receptors by systemic administration of monoclonal antibody (mAb) 806, a novel monoclonal antibody directed to the receptor. *Cancer Res.* 61: 5349-5354.
17. Flynn, P., Wong, M., Zaval, M., Dean, N. M., and Stokoe, D. (2000). Inhibition of PDK-1 activity causes a reduction in cell proliferation and survival. *Curr. Biol.* 10: 1439-1442.
18. Lammering, G., et al. (2001). Epidermal growth factor receptor as a genetic therapy target for carcinoma cell radiosensitization. *J. Natl. Cancer Inst.* 93: 921-929.

Intravenous Nonviral Gene Therapy Causes Normalization of Striatal Tyrosine Hydroxylase and Reversal of Motor Impairment in Experimental Parkinsonism

YUN ZHANG, FREDERIC CALON, CHUNNI ZHU, RUBEN J. BOADO, and WILLIAM M. PARDRIDGE

ABSTRACT

Brain gene-targeting technology is used to reversibly normalize tyrosine hydroxylase (TH) activity in the striatum of adult rats, using the experimental 6-hydroxydopamine model of Parkinson's disease. The TH expression plasmid is encapsulated inside an 85-nm PEGylated immunoliposome (PIL) that is targeted with either the OX26 murine monoclonal antibody (MAb) to the rat transferrin receptor (TfR) or with the mouse IgG2a isotype control antibody. TfRMAB-PIL, or mIgG2a-PIL, is injected intravenously at a dose of 10 μ g of plasmid DNA per rat. TfRMAB-PIL, but not mIgG2a-PIL, enters the brain via the transvascular route. The targeting TfRMAB enables the nanocontainer carrying the gene to undergo both receptor-mediated transcytosis across the blood-brain barrier (BBB) and receptor-mediated endocytosis into neurons behind the BBB by accessing the TfR. With this approach, the striatal TH activity ipsilateral to the intracerebral injection of the neurotoxin was normalized and increased from 738 ± 179 to 5486 ± 899 pmol/hr per milligram of protein. The TH enzyme activity measurements were corroborated by TH immunocytochemistry, which showed that the entire striatum was immunoreactive for TH after intravenous gene therapy. The normalization of striatal biochemistry was associated with a reversal of apomorphine-induced rotation behavior. Lesioned animals treated with the apomorphine exhibited 20 ± 5 and 6 ± 2 rotations/min, respectively, after intravenous administration of the TH plasmid encapsulated in mIgG2a-PIL and TfRMAB-PIL. These studies demonstrate that it is possible to normalize brain enzyme activity by intravenous administration and nonviral gene transfer.

OVERVIEW SUMMARY

Parkinson's disease (PD) results from neurodegeneration in the nigral-striatal pathway of the brain, leading to a deficiency in the striatum of tyrosine hydroxylase (TH), the rate-limiting enzyme in dopamine synthesis. One strategy for gene therapy of PD is the restoration of striatal TH activity. The present work uses the experimental 6-hydroxydopamine model of PD, which causes a 90% reduction in striatal TH enzyme activity ipsilateral to the intracerebral toxin injection. Lesioned rats are treated with a nonviral TH expression plasmid administered intravenously. The TH gene is encapsulated in an "artificial virus" composed of 85-nm PEGylated immunoliposomes targeted to the brain with a monoclonal antibody to the rat transferrin receptor. The targeted nonviral gene transfer enables delivery of the therapeutic gene across the blood-brain barrier and across the

neuronal plasma membrane. Three days after a single intravenous administration of the TH gene, the striatal TH activity is normalized in association with a 70% reduction in apomorphine-induced rotation behavior.

INTRODUCTION

GENE THERAPY of Parkinson's disease (PD) aims to prevent striatal neurodegeneration and restore striatal tyrosine hydroxylase (TH) enzyme activity (Mouradian and Chase, 1997; Mandel *et al.*, 1999). Striatal TH enzyme activity is partially restored in experimental models of PD by intracerebral injection of viral vectors encoding the TH gene (During *et al.*, 1994; Kaplitt *et al.*, 1994; Mandel *et al.*, 1998). However, viral vectors must be administered intracerebrally via penetration of the skull bone. The viruses cannot be administered intravenously

because the viruses do not cross the brain capillary endothelial wall, which forms the blood-brain barrier (BBB) *in vivo*. The intracerebral injection of the viral vector causes transduction of a small part of the striatum at the tip of the injection needle. Higher fractions of the striatum may be transduced by multiple injections of high viral titers in either rat brain (Leone *et al.*, 2000; Kirik *et al.*, 2002) or primate brain (Bankiewicz *et al.*, 2000; Kordower *et al.*, 2000).

The entire volume of the striatum may be transduced after transvascular delivery of the therapeutic gene subsequent to intravenous administration of the gene. The transvascular route to the striatum would be possible with the development of a gene-targeting system that is capable of transport across the BBB. Gene-targeting technology has been developed that enables widespread expression within the brain of nonviral plasmid DNA after intravenous administration (Shi *et al.*, 2000, 2001a,b). Plasmid DNA encoding the therapeutic gene is encapsulated inside a nanocontainer composed of a PEGylated immunoliposome (PIL), which is targeted across both the BBB and the neuronal cell membrane by receptor-specific monoclonal antibodies (MAbs). Delivery of the therapeutic gene across the BBB has the potential to transduce virtually every cell of the striatum, because every neuron in the brain is perfused by its own blood vessel. With the PIL gene-targeting system, it is possible to deliver an exogenous gene throughout the entire CNS after intravenous administration. Gene expression can be restricted to the brain by the use of brain-specific promoters (Shi *et al.*, 2001a). Prior work with this gene-targeting technology yielded a therapeutic result in an experimental brain cancer model, with a 100% increase in survival time for the animals treated by intravenous antisense gene therapy (Zhang *et al.*, 2002a). The present studies attempt to normalize the striatal TH activity and motor impairment in the experimental 6-hydroxydopamine model of PD in the rat. The full-length rat TH cDNA is incorporated in a pGL2-derived expression plasmid that is driven by the simian virus 40 (SV40) promoter and contains a cis stabilizing element in the 3'-untranslated region (UTR) of the mRNA. The plasmid DNA is encapsulated in the interior of the PIL, which is targeted to brain with the murine OX26 MAb to the rat transferrin receptor (TfR). Owing to the expression of the TfR at both the rodent and human BBB (Jefferies *et al.*, 1984; Pardridge *et al.*, 1987) and the neuronal plasma membrane (Mash *et al.*, 1991), TfRMAb-targeted PIL undergoes receptor-mediated transcytosis across the BBB followed by receptor-mediated endocytosis into neurons behind the BBB.

MATERIALS AND METHODS

Materials

1-Palmitoyl-2-oleoyl-*sn*-glycerol-3-phosphocholine (POPC) and didodecyltrimethylammonium bromide (DDAB) were purchased from Avanti-Polar Lipids (Alabaster, AL). Distearoylphosphatidylethanolamine (DSPE)-PEG 2000 was obtained from Shearwater Polymers (Huntsville, AL), where PEG 2000 is 2000-Da polyethylene glycol. DSPE-PEG 2000-maleimide (MAL) was custom synthesized by Shearwater Polymers. [α - 32 P]dCTP (3000 Ci/mmol) and L-[3,5- 3 H]ty-

rosine (51.5 Ci/mmol) were from NEN Life Science Products (Boston, MA). *N*-Succinimidyl[2,3- 3 H]propionate ([3 H]NSP, 101 Ci/mmol) and protein G-Sepharose CL-4B were purchased from Amersham Pharmacia Biotech (Arlington Heights, IL). The nick translation system was from Life Technologies (Rockville, MD). 6-Hydroxydopamine (6-OHDA), apomorphine, pargyline, catalase, (6*R*)-5,6,7,8-tetrahydrobiopterin (BH₄), β -NADPH, L-tyrosine, charcoal, the mouse MAb against rat tyrosine hydroxylase, horse serum, mouse IgG1 isotype control, and glycerol-gelatin were purchased from Sigma (St. Louis, MO); 2-iminothiolane (Traut's reagent) and bichoninic acid (BCA) protein assay reagents were obtained from Pierce (Rockford, IL). Mouse myeloma ascites containing mouse IgG2a (mIgG2a) isotype control was from the Cappel Division of ICN Pharmaceuticals (Aurora, OH). The anti-transferrin receptor monoclonal antibody (TfRMAb) used in these studies is the murine OX26 MAb to the rat TfR, which is a mouse IgG2a. The OX26 MAb is specific for the rat TfR, and is not active in human cells. The anti-insulin receptor MAb used for gene targeting to human cells is the murine 83-14 MAb to the human insulin receptor (HIR). TfRMAb, HIRMAb, and mIgG2a were individually purified by protein G affinity chromatography from hybridoma-generated ascites. COS-1 cells were obtained from the American Type Culture Collection (Manassas, VA). The biotinylated horse anti-mouse IgG, Vectastain ABC kit, 3-amino-9-ethylcarbazole (AEC) substrate kit, peroxidase kit, and hematoxylin QS counterstain were purchased from Vector Laboratories (Burlingame, CA). Optimal cutting temperature (O.C.T.) compound (Tissue-Tek) was purchased from Sakura FineTek (Torrance, CA). LipofectAMINE was obtained from Invitrogen (San Diego, CA).

Construction of tyrosine hydroxylase expression plasmids

The complete open reading frame (ORF) of rat (r) TH in the pBabe plasmid was obtained from D. Bredesen (Buck Center, Novato, CA) (Anton *et al.*, 1994). The rat TH ORF was isolated by double digestion with *Dra*I and *Acc*65I, which cleaved at sites located 26 nucleotides upstream and 13 nucleotides downstream of the rat TH ORF, respectively. The ~1.5-kb rTH fragment was purified by gel electrophoresis followed by centrifugation with a Spin-X filter unit (Costar; Corning, Acton, MA). The DNA was blunt ended with Klenow DNA polymerase, and subcloned in Bluescript (pBS; Stratagene, San Diego, CA) at the *Eco*RV site to form a plasmid named pBS-rTH. The identity of rat TH and its orientation in pBS-rTH were determined by DNA sequencing, using M13 forward and reverse primers. The rat TH cDNA was subcloned in pGL2 promoter-derived mammalian expression vectors described previously and designated clones 734 and 753 (Dwyer *et al.*, 1996). The pGL2 promoter plasmid was obtained from Promega (Madison, WI), and the pGL2-derived clones are driven by the SV40 promoter; clone 753 contains a 200-nucleotide cis element taken from nucleotides 2100–2300 of the bovine GLUT1 mRNA 3'-untranslated region (UTR), which causes stabilization of the mRNA (Boado and Pardridge, 1998). pBS-TH was linearized with *Not*I and blunt ended with Klenow DNA polymerase. The 1.5-kb rat TH was released with *Hind*III and purified by gel electrophoresis and Spin-X centrifugation. In par-

allele, the luciferase reporter gene in clones 734 and 753 was deleted with *HindIII* and *EcoNI* (blunt) and purified. The rat TH DNA fragment was ligated into clones 734 and 753 with T4 DNA ligase and *Escherichia coli* DH5 α was transformed. Positive clones were investigated by restriction endonuclease mapping using *PstI*, which releases the TH insert, and DNA sequencing, using the pGL2-1 sequencing primer (Promega). The pGL2-rTH expression vector derived from clone 734 was designated clone 878, and the pGL2-rTH expression vector containing the GLUT1 cis-stabilizing sequence, and derived from clone 753, was designated clone 877. The SV40-rTH expression cassettes were released from clones 877 and 878 and further subcloned in the pCEP4 expression vector to form clones 908 and 883, respectively. The pCEP4 vectors contain the Epstein-Barr virus replication origin (oriP) and nuclear antigen (EBNA-1), which enable extrachromosomal replication in human cells. Clones 877 and 878 were digested with *XhoI*, *SalI*, and *ScaI* to release the ~2.9-kb SV40-rTH fragments. In parallel, the pCEP4 vector was digested with *SalI* and *XhoI* to release the CMV-cassette and purified as previously described (Boado and Pardridge, 1998). The SV40-rTH expression cassettes were ligated into pCEP4. Positive clones were identified by restriction endonuclease mapping with *NruI* and *HindIII*, and confirmed by DNA sequencing as previously described for GLUT1 reporter genes (Boado and Pardridge, 1998). All four TH expression plasmids (877, 878, 883, and 908) are driven by the SV40 promoter. Clones 877 and 908 contain the GLUT1 3'-UTR cis stabilizing element, and clones 883 and 908 contain the EBNA-1/oriP cis/trans elements for extrachromosomal replication in human cells. The pGL2-derived TH clones, 877 and 878, are approximately 6.0 kb in size, and the pCEP4-derived TH clones, 883 and 908, are approximately 11.0 kb in size (Boado and Pardridge, 1998). Maxiprep DNA was purified and plasmid DNA was ^{32}P labeled as described previously (Zhang *et al.*, 2002b).

Expression of the TH gene in cell culture was first evaluated by LipofectAMINE transfection of either C6 rat glial cells or COS-1 cells, which were cultivated in Dulbecco's modified Eagle's medium (DMEM) with 10% calf serum or in DMEM with high glucose (4.5 g/liter) and 10% fetal bovine serum (FBS), respectively. Plasmid DNA was amplified with a QIAfilter plasmid Maxiprep kit (Qiagen, Chatsworth, CA) and COS-1 or C6 glial cells were transfected with LipofectAMINE as described previously (Shusta *et al.*, 2002). Cells were seeded on 60- or 100-mm dishes at a density of 80,000 cells/cm 2 and the LipofectAMINE-plasmid DNA (10:1, w/w) was added in medium without serum for 4 hr. The complex was then removed, and fresh medium with serum was added and the cells were incubated for 48 hr before extraction and measurement of TH enzyme activity as described below.

PEGylated liposome synthesis and plasmid DNA encapsulation

POPC (18.8 μmol), DDAB (0.4 μmol), DSPE-PEG 2000 (0.6 μmol), and DSPE-PEG 2000-maleimide (0.2 μmol) were dissolved in chloroform followed by evaporation, as described previously (Zhang *et al.*, 2002b). The lipids were dispersed in 0.2 ml of 0.05 M Tris-HCl buffer (pH 7.0) and vortexed for 1 min followed by 2 min of bath sonication. Supercoiled DNA

was ^{32}P labeled with [α - ^{32}P]dCTP by nick translation as described previously (Shi *et al.*, 2000). Unlabeled plasmid DNA (250 μg) and 1 μCi of ^{32}P -labeled plasmid DNA were added to the lipids. The dispersion was frozen in ethanol-dry ice for 5 min and thawed at room temperature for 25 min, and this freeze-thaw cycle was repeated five times to produce large vesicles with the DNA loosely entrapped inside. The large vesicles were converted into small (85-nm-diameter) liposomes by extrusion. The liposome dispersion was diluted to a lipid concentration of 40 mM, followed by extrusion five times each through two stacks each of 200- and 100-nm pore size polycarbonate membranes, by using a hand-held LipoFast-Basic extruder (Avestin, Ottawa, Canada), as described previously (Shi *et al.*, 2001a). The mean vesicle diameters were determined by quasielastic light scattering by using a Microtrac ultrafine particle analyzer (Leeds-Northrup, St. Petersburg, FL), as described previously (Huwylar *et al.*, 1996).

Approximately half of the DNA is interiorized in the small liposomes and about half is exteriorized. The plasmid DNA absorbed to the exterior of the liposomes was quantitatively removed by nuclease digestion (Shi *et al.*, 2000). For digestion of the unencapsulated DNA, 5 units of pancreatic endonuclease I and 5 units of exonuclease III were added in 5 mM MgCl $_2$ to the liposome-DNA mixture after extrusion (Monnard *et al.*, 1997). After incubation at 37°C for 1 hr, the reaction was stopped by adding 20 mM EDTA. The extent to which the nuclease digestion removed the exteriorized plasmid DNA was determined by agarose gel electrophoresis and ethidium bromide staining of aliquots taken before and after nuclease treatment, as described previously (Shi *et al.*, 2000). The entrapped plasmid DNA is completely resistant to high local concentrations of nuclease. The DNA encapsulated within the PEGylated liposome is designated PEGylated liposome-DNA.

MAb conjugation to the PEGylated liposome-DNA

TfRMAb, HIRMAb, or mIgG2a was thiolated and individually conjugated to the MAL moiety of the PEGylated liposome-DNA to produce a PEGylated immunoliposome (PIL) with the desired receptor (R) specificity. PIL conjugated with the OX26 MAb is designated TfRMAb-PIL and PIL conjugated with the mIgG2a isotype control is designated mIgG2a-PIL. Either MAb or mIgG2a was radiolabeled with [^3H]NSP as described previously (Pardridge *et al.*, 1992). ^3H -Labeled MAb had a specific activity of >0.11 $\mu\text{Ci}/\mu\text{g}$ and a trichloroacetic acid (TCA) precipitability of >97%. The MAb (3.0 mg, 20 nmol) was thiolated with a 40:1 molar excess of 2-iminothiolane (Traut's reagent), as described previously (Huwylar *et al.*, 1996). The thiolated MAb, which contained a trace amount of ^3H -labeled MAb, was conjugated to the PEGylated liposome overnight and unconjugated MAb (and oligonucleotides produced by nuclease treatment) were separated from the PIL by Sepharose CL-4B column chromatography as described previously (Shi *et al.*, 2000). The number of MAb molecules conjugated per liposome was calculated from the total ^3H -labeled MAb counts per minute in the liposome pool and the specific activity of the labeled MAb, assuming 100,000 lipid molecules per liposome, as described previously (Zhang *et al.*, 2002b). The average number of MAb molecules conjugated per liposome was 52 ± 8 (mean \pm SD, $n = 4$ syn-

theses). The final percentage entrapment of 250 μg of plasmid DNA in the liposome preparation was computed from the ^{32}P radioactivity and was $35.6 \pm 2.1\%$ (mean \pm SD, $n = 4$ syntheses), or 89 μg of plasmid DNA.

The PIL solution was sterilized for use in tissue culture by passage through a 0.22- μm pore size Millex-GV filter (Millipore, Bedford, MA). The PIL is not structurally altered by this filtration step (Zhang *et al.*, 2002b).

Electron microscopy

IgG-conjugated PIL carrying plasmid DNA was examined with a conjugate of 10-nm gold and a goat anti-mouse secondary antibody (G7652; Sigma). A 5- μl aliquot of the 83-14-PIL (5×10^{12} liposome-conjugated MAbs) was incubated with 72 μl of IgG-gold conjugate (1×10^{12} gold particles) for 1 hr in 0.05 M Tris-buffered saline, pH 6.9, with 0.7% bovine serum albumin, 5% FBS, and 12% glycerol in a total volume of 125 μl . Gold-conjugated secondary antibody bound to the PIL was separated from unbound gold conjugate by passage through a 0.7×10 cm column of Sepharose CL-4B (Bio-Rad, Hercules, CA). An aliquot (10 μl) of the eluate was applied to Formvar-coated 2000 mesh copper grids, washed twice with 0.05 M Tris–0.15 M NaCl, pH 7.4, counterstained with 2% uranyl acetate for 1 min, and then examined directly by electron microscopy using a JEOL JEM-100CX II electron microscope at 80 kV. Negatives, taken at a magnification of $\times 29,000$, were scanned and enlarged in Adobe Photoshop 5.5 on a G4 Power Macintosh.

TH gene expression in cultured brain cells with the PIL gene-targeting system

Human U87 glioma cells or rat RG-2 glioma cells were plated on 60-mm collagen-treated dishes with minimal essential medium (MEM) or with F12 Ham's medium containing 10% FBS, respectively. When the cells reached 60% confluence, the medium was removed by aspiration, and 6 ml of fresh medium containing 10% FBS was added to the cells, followed by the addition of 142 μl of HIRMAb-PIL carrying clone 877 DNA (4 μg of plasmid DNA per dish) or TfRMAb-PIL carrying clone 877 DNA (4 μg of plasmid DNA per dish). The cells were incubated for 2, 4, or 6 days, with three dishes at each time point, for measurement of TH enzyme activity. This time course was based on prior work describing the temporal changes in gene expression in cultured cells exposed to TfRMA-targeted PEGylated liposomes (Zhang *et al.*, 2003).

6-Hydroxydopamine model

Adult male Sprague-Dawley rats (supplied by Harlan Breeders, Indianapolis, IN) weighing 200–250 g were anesthetized with ketamine (50 mg/kg) and xylazine (4 mg/kg) intraperitoneally. Animals received unilateral 6-OHDA injections into the right medial forebrain bundle (Armstrong *et al.*, 2002; Meshul *et al.*, 2002). Each animal received pargyline 30–60 min before surgery (50 mg/kg in normal saline, administered intraperitoneally). After pargyline administration, 4 μl of 6-OHDA (2 $\mu\text{g}/\mu\text{l}$; prepared freshly in ascorbic acid [0.2 $\mu\text{g}/\mu\text{l}$]) was injected over a 4-min period with a 10- μl Hamilton sy-

ringe, using the following stereotaxic coordinates: -4.4 mm anterior to the bregma, -1.0 mm lateral to the bregma, and 7.8 mm below the dura. The syringe needle was left in place for 2 min after the injection to allow for diffusion of the toxin. Three weeks after the lesion had been made, rats were tested for apomorphine-induced contralateral turning, using apomorphine (0.5 mg/kg) injected intraperitoneally. Full (360°), contralateral rotations only were counted over 20 min, starting 5 min after apomorphine administration, and rats turning more than 120 times in 20 min, or 6 rotations/min (rpm), were treated 1 week later by TH gene therapy. Rats were individually identified so that the rotations per minute 1 week before and 3 days after treatment could be compared for each rat.

For each experiment, successfully lesioned rats were divided into two groups: (1) control group—each rat received 10 μg of clone 877 DNA encapsulated in mIgG2a-PIL; (2) treatment group—each rat received 1, 5, or 10 μg of clone 877 DNA encapsulated in TfRMAb-PIL. PIL was administered via the femoral vein; 3 days later the rats were tested for apomorphine-induced rotation behavior and then killed. In each group, rat brains were removed and used for either TH immunocytochemistry assays or TH biochemistry assays. A time-response study was performed, wherein animals were not killed until 6 and 9 days after the single intravenous injection of clone 877 DNA encapsulated in TfRMAb-PIL. A dose-response study was also performed, wherein animals were killed 3 days after the single intravenous injection of clone 877 DNA encapsulated in TfRMAb-PIL at a dose of 1, 5, or 10 μg of DNA per rat. In these animals, the brain was removed for measurement of TH enzyme activity in the contralateral and ipsilateral striatum.

Tyrosine hydroxylase assay

The TH activity assay was performed according to Reinhard *et al.* (1986) and Horellou *et al.* (1989), with modifications. TH converts L-[3,5- ^3H]tyrosine to both $^3\text{H}_2\text{O}$ and L-dopa in a 1:1 stoichiometric relationship, and the two metabolites are separated by charcoal, which selectively binds the amino acids. For cultured cells, at the end of incubation, the growth medium was removed. The cells were washed three times with cold wash buffer (5 mM potassium phosphate buffer), and then 400 μl of sonication buffer (wash buffer with 0.2% Triton X-100) was added to each dish. The cells were collected and, after a short vortex, the cells were sonicated for 30 sec with a Branson Ultrasonics (Danbury, CT) sonifier cell disruptor model 185. The cell homogenate was centrifuged at $10,000 \times g$ for 10 min at 4°C , and the supernatant was removed for TH assays. For TH assays in rat organs, the liver, the frontal cortex, and the dorsal striatum in both lesioned (ipsilateral) and nonlesioned (contralateral) sides of brain were frozen in dry ice. The tissue was transferred to a chilled glass tissue grinder containing 0.5 ml of cold wash buffer, and was homogenized with 10–15 strokes at 4°C followed by centrifugation at $10,000 \times g$ for 20 min, and the supernatant was removed for TH assays.

The tissue supernatants (200 μl) were added to 100 μl of assay buffer [final concentration 0.5 mM NADPH, 1 mM BH_4 , 2600 units of catalase, 20 μM $\text{Fe}(\text{NH}_4)_2(\text{SO}_4)_2$, 10 μM L-tyrosine, L-[^3H]tyrosine [40–50 $\mu\text{Ci}/\text{ml}$], 50 mM potassium phos-

phate] to start the incubation at 37°C for 45 min. The reaction was stopped by the addition of 1 ml of 7.5% charcoal in 1.0 M HCl. The mixture was vortexed for 2 sec and centrifuged at 500 × g for 10 min. The supernatant was counted for the radioactivity of the $^3\text{H}_2\text{O}$ product, using a Packard (Meriden, CT) Tri-Carb 2100TR liquid scintillation analyzer. The supernatant radioactivity was measured in parallel with assays blanks, and all assay measurements were at least 10-fold above the assay blank. The protein concentration in the cell extract was determined with the BCA protein assay reagent. The counts per minute were converted to picomoles of L-dopa on the basis of the [^3H]tyrosine specific activity, and the results were expressed as picomoles of L-dopa per hour per milligram protein.

Immunocytochemistry

Tyrosine hydroxylase immunocytochemistry was performed by the avidin-biotin complex (ABC) immunoperoxidase method (Vector Laboratories). Brains were removed immediately after sacrifice, cut through the striatum into coronal slabs, embedded in O.C.T. medium, and frozen in dry ice powder. Frozen sections (20 μm) of rat brain were cut on a Mikron HM505E cryostat, and were fixed in 4% paraformaldehyde for 20 min at 4°C. Endogenous peroxidase was blocked with 0.3% H_2O_2 in 0.3% horse serum-phosphate-buffered saline (PBS) for 30 min. Nonspecific binding of proteins was blocked with 10% horse serum in 0.1% Triton X-100-PBS for 30 min. Sections were then incubated in either mouse anti-TH MAb (0.2 $\mu\text{g}/\text{ml}$) or mouse IgG1 isotype control (0.2 $\mu\text{g}/\text{ml}$) overnight at 4°C. After wash in PBS, sections were incubated in biotinylated horse anti-mouse IgG for 30 min and then in ABC for 30 min. After development in AEC, sections were mounted with glycerol-gelatin with or without light counterstaining with hematoxylin.

Statistical analyses

Statistically significant differences in TH enzyme activity in different brain regions and treatment groups were determined by analysis of variance (ANOVA) with the Bonferroni correction, using program 7D of the BMDP Statistical Software package developed by the UCLA Biomedical Computing Series. A p value of <0.05 was considered significant.

RESULTS

Evaluation of TH expression plasmid activity in COS cells and C6 glioma cells transfected with LipofectAMINE

The four TH expression plasmids were combined with the LipofectAMINE and individually added to either COS-1 or C6 rat glioma cells, and TH enzyme activity was measured 48 hr later (Fig. 1). A similar pattern of TH gene expression was observed in both cell lines, although the TH enzyme activity in COS-1 cells was 10-fold greater than in C6 cells, consistent with the selective activation of genes driven by the SV40 promoter in COS-1 cells. In either cell line, pGL2-derived plasmid 877 produced the highest level of TH enzyme activity. Therefore, clone 877 was selected for subsequent encapsulation in TfRMAb-PIL for *in vivo* gene therapy in rats with experimentally induced PD.

Transfection of cultured cells with the PIL gene-targeting system

The encapsulation of clone 877 plasmid DNA within the PIL gene-targeting system is depicted in Fig. 2A. The targeting MAb molecules tethered to the tips of the PEG strands on the

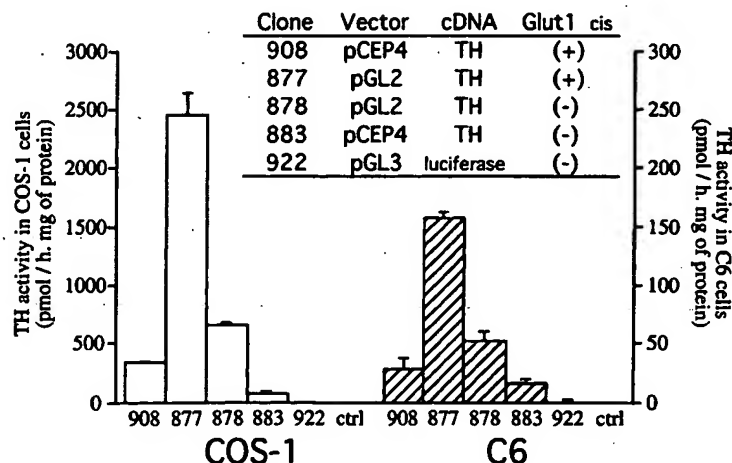


FIG. 1. Tyrosine hydroxylase (TH) activity in either COS-1 cells or C6 rat glioma cells transfected with one of five different expression plasmids in cell culture with LipofectAMINE. Clones 883 and 908 are derived from pCEP4, which contains EBNA1/oriP elements, and clones 877 and 878 are derived from pGL2, which lacks the EBNA1/oriP elements. Clones 877 and 908 contain a 200-base pair cis element taken from the 3'-untranslated region (UTR) of the GLUT1 glucose transporter mRNA, and this cis element causes stabilization of the transcript (Boado and Pardridge, 1998). Clone 922 is a pGL3 luciferase expression plasmid and this clone produced no measurable TH enzyme activity in either cell line (control, ctrl). Data represent means \pm SE ($n = 4$ dishes per point).

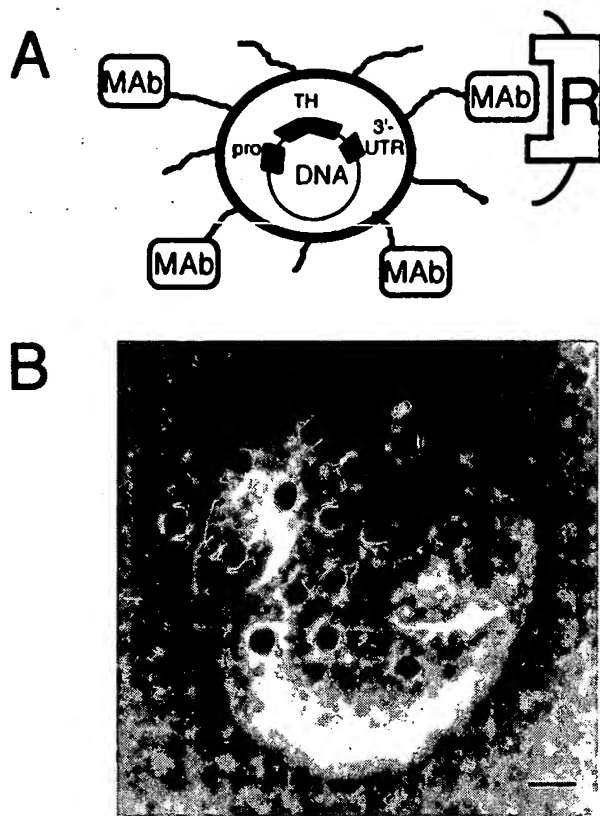


FIG. 2. (A) Plasmid DNA encapsulated in the interior of the PEGylated immunoliposome (PIL) with a receptor (R)-specific targeting monoclonal antibody (MAB). The targeting MAB is conjugated to 1–2% of the polyethylene glycol (PEG) strands that project from the surface of the liposome. There are about 2000 strands of 2000-Da PEG conjugated to the liposome surface. The PEG strands inhibit uptake of the PIL by the reticuloendothelial systems *in vivo* and prolong the blood residence time of the PIL *in vivo* (Shi *et al.*, 2000). The tyrosine hydroxylase (TH) gene is driven by an SV40 promoter (pro) and contains a cis-stabilizing element in the 3'-untranslated region (UTR). (B) Transmission electron microscopy of a PIL. The mouse IgG molecules tethered to the tips of the 2000-Da polyethylene glycol (PEG) are bound by a conjugate of 10-nm gold and an anti-mouse secondary antibody. The position of the gold particles illustrates the relationship of the PEG-extended MAB and the liposome. Magnification bar: 20 nm.

PIL are visualized by electron microscopy, using an anti-mouse secondary antibody conjugated with 10-nm gold (Fig. 2B). Because the targeting MAB molecules are species specific (Zhang *et al.*, 2002c), clone 877 plasmid DNA was targeted to human U87 glioma cells, with the PIL conjugated with 83-14 MAB to the human insulin receptor (HIR). Conversely, rat RG-2 glioma cells were transduced with the PIL conjugated with OX26 murine MAB to the rat transferrin receptor (rTfR). Clone 877 plasmid DNA was encapsulated in either TfRMAB-PIL or HIRMAb-PIL and 4 μ g of plasmid DNA was applied to each 60-mm culture dish containing either RG-2 or U87 cells, respectively. The level of TH enzyme activity in either U87 cells or RG-2 cells increased with time of incubation and peaked 4 days after the single application of the PIL formulation at time

0 (Fig. 3). TH enzyme activity in rat RG-2 cells targeted with the OX26-PIL system was comparable to the TH enzyme activity in C6 glioma cells targeted with LipofectAMINE (Figs. 1 and 3). The TH enzyme activity in human U87 glioma cells targeted with the HIRMAb-PIL delivery system was comparable to TH enzyme activity produced with LipofectAMINE in COS-1 cells (Figs. 1 and 3).

TH enzyme activity in liver of control rats treated by intravenous gene therapy

TfRMAB-PIL targeting of the TH gene was initially examined in a TfR-rich peripheral organ, liver, of control rats so as to identify the time course of gene expression. Each control rat was administered 10 μ g of clone 877 plasmid DNA encapsulated in TfRMAB-PIL and hepatic TH enzyme activity was measured 0, 1, 2, and 3 days after the single intravenous administration (Table 1). The TH activity in control rat liver increased >30-fold above basal levels by 3 days after gene administration. Therefore, 72 hr was chosen as the time point for measuring brain TH activity after intravenous TH gene therapy in rats with experimentally induced PD.

TH enzyme activity and immunoreactive TH levels in rat brain with experimentally induced parkinsonism treated by intravenous TH gene therapy

Three weeks after the intracerebral injection of 6-hydroxydopamine, rats were treated with apomorphine and rotation behavior was examined. Those rats that demonstrated contralat-

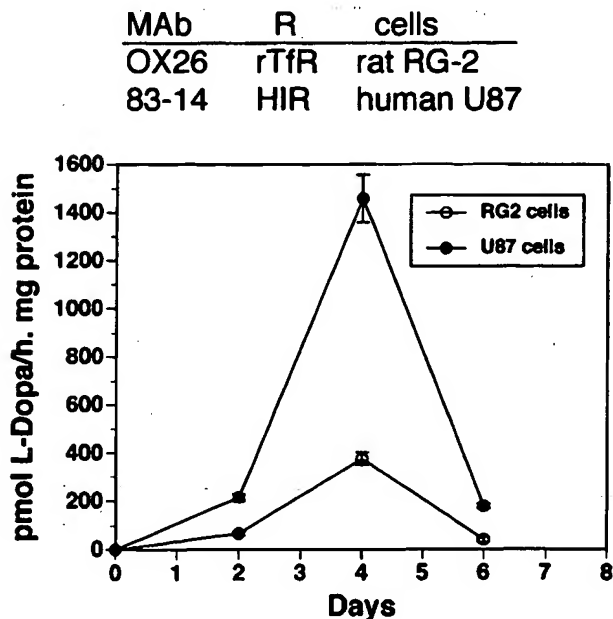


FIG. 3. Tyrosine hydroxylase activity is plotted relative to the days of incubation in cell culture of either rat RG-2 cells or human U87 glioma cells exposed to clone 877 plasmid DNA encapsulated in PIL. PIL was targeted to rat RG-2 cells with the OX26 murine MAB to the rat transferrin receptor (rTfR), and PIL was targeted to human U87 cells with the 83-14 murine MAB to the human insulin receptor (HIR). Data represent means \pm SE ($n = 4$ dishes per point).

TABLE 1. TYROSINE HYDROXYLASE ACTIVITY IN LIVER AFTER INTRAVENOUS INJECTION OF CLONE 877 PLASMID DNA ENCAPSULATED IN TfRMAB-PIL IN CONTROL RATS^a

Day post administration	TH activity (pmol L-dopa/hr per mg protein)
0	3.0 ± 0.3
1	18.2 ± 1.8
2	33.2 ± 2.7
3	103.7 ± 9.1

^aValues represent means ± SD (*n* = 3 rats per time point).

eral rotation in response to apomorphine were selected for subsequent treatment with the PIL gene-targeting system 1 week later. Rats with experimentally induced PD were treated either with clone 877 plasmid DNA encapsulated in PIL targeted with TfRMAB (designated TfRMAB-PIL) or with clone 877 plasmid DNA encapsulated in PIL targeted with mouse IgG2a isotype control antibody (designated mIgG2a-PIL). Plasmid DNA was injected intravenously at a dose of 10 µg of DNA per rat, and animals were killed 72 hr after the single intravenous injection for measurement of either TH enzyme activity in dorsal striatal or cortical homogenates or immunoreactive TH levels by immunocytochemistry. TH enzyme activity in the dorsal striatum ipsilateral to the 6-hydroxydopamine injection was reduced 87% compared with TH enzyme activity in the contralateral striatum, and TH enzyme activity was completely normalized in rats treated with clone 877 DNA encapsulated within TfR-PIL (Table 2). In contrast, intravenous administration of clone 877 DNA encapsulated in mIgG2a-PIL resulted in no increase in TH enzyme activity in the ipsilateral striatum (Table 2). TH enzyme activity in the cortex was only 2% relative to the contralateral striatum and there was no change in cortical TH enzyme activity in the lesioned animals treated with TfRMAB-PIL (Table 2).

The level of immunoreactive TH was measured by immunocytochemistry and there was a complete loss of immunoreactive TH in the dorsal striatum ipsilateral to the neurotoxin injection, although residual immunoreactive TH was detected in the ventral striatum and olfactory tubercle below the anterior commissure in some rats (Fig. 4D and F). The administration of clone 877 encapsulated within mIgG2a-PIL resulted

in no increase in the level of immunoreactive TH in the striatum (Fig. 4D-F). However, the level of immunoreactive TH was normalized in the entire striate body 3 days after an intravenous injection of clone 877 DNA encapsulated within PIL targeted to brain by TfRMAB (Fig. 4A-C).

Reversal of motor impairment after TH gene therapy

Apomorphine-induced contralateral rotation was quantified in individual rats 1 week before and 3 days after a single intravenous injection of clone 877 TH expression plasmid encapsulated in either mIgG2a-PIL (Fig. 5A) or TfRMAB-PIL (Fig. 5B). Contralateral rotations were counted for 20 min after the intraperitoneal injection of apomorphine. Total rotations in a 20-min period 3 days after treatment are plotted in Fig. 5C. The mean rotations per minute (rpm) for the animals treated with mIgG2a-PIL was 20 ± 5 (range, 13–26 rpm per animal). In contrast, the animals treated with clone 877 TH expression plasmid encapsulated within TfRMAB-PIL demonstrated a 70% reduction in rotation to 6 ± 2 rpm (mean ± SD) with a range of 3–9 rpm per individual rat.

Time-response study

The persistence of TH gene expression in the striatum ipsilateral to the lesion was determined by measurement of striatal TH enzyme activity 6 and 9 days after a single intravenous injection of clone 877 plasmid DNA (10 µg/rat) encapsulated in TfRMAB-PIL, and these data were compared with the TH measurements at 3 days. As shown in Fig. 6, striatal TH activity peaked at 3 days and had decreased by 50% by 6 days after injection. By 9 days after injection, TH activity in the ipsilateral striatum of rats treated with TfRMAB-PIL was comparable to the control levels in the lesioned striatum of animals treated with mIgG2a-PIL (Table 2).

Dose-response study

TH enzyme activity in the striatum either contralateral or ipsilateral to the lesion was measured 3 days after a single intravenous injection of clone 877 plasmid DNA encapsulated in TfRMAB-PIL at a dose of 1, 5, or 10 µg/rat (Fig. 7). TH activity in the ipsilateral striatum was proportional to the dose of plasmid DNA administered via TfRMAB-PIL, and no increases in striatal TH was observed with the 1-µg/rat dose (Fig. 7).

TABLE 2. TYROSINE HYDROXYLASE ACTIVITY IN RAT BRAIN LESIONED WITH 6-HYDROXYDOPAMINE, 3 DAYS AFTER INTRAVENOUS INJECTION OF CLONE 877 PLASMID DNA ENCAPSULATED IN EITHER TfRMAB-PIL OR mIgG2a-PIL^a

Region	TH activity (pmol L-dopa/hr per mg protein)	
	TfRMAB-PIL	mIgG2a-PIL
Ipsilateral striatum	5486 ± 899 ^b	738 ± 179
Contralateral striatum	5875 ± 550 ^b	5101 ± 443 ^b
Ipsilateral cortex	159 ± 27	101 ± 7
Contralateral cortex	121 ± 39	108 ± 51

^aValues represent means ± SD (*n* = 5 rats in each group).

^b*p* < 0.01 difference from ipsilateral striatum treated with mIgG2a-PIL (one-way ANOVA, Bonferroni correction).

DISCUSSION

The results of these studies are consistent with the following conclusions. First, striatal TH enzyme activity is normalized by intravenous injection of nonviral TH expression plasmid encapsulated inside a PIL targeted by a TfRMAB to neurons (Table 2). Second, normalization of TH enzyme activity in the striatum is paralleled by normalization of the level of immunoreactive TH protein, as measured by immunocytochemistry (Fig. 4). Third, the specificity of the gene-targeting system is a function of the MAB, because the only difference between TfRMAB-PIL and mIgG2a-PIL is the receptor specificity of the targeting MAB conjugated to the PEGylated liposome (Fig. 2A). Both TfRMAB-PIL and mIgG2a-PIL carry the clone 877 TH expression plasmid. Fourth, there is no change in TH enzyme activity in cortex and no measurable immunoreactive cortical TH as determined by immunocytochemistry performed after the intravenous injection of TH expression plasmid encapsulated in TfRMAB-PIL (Table 2 and Fig. 4). Fifth, there is a reversal of apomorphine-induced rotation behavior after intravenous TH gene therapy, with a 70% reduction in drug-induced rotation (Fig. 5). Sixth, the normalization of TH activity in brain after the single administration of a plasmid-based TH gene is time dependent, and the peak activity declines 50% by 6 days (Fig. 6). Seventh, the effect of gene therapy is dose dependent, as minimal, intermediate, and maximal effects on striatal TH activity are observed, respectively, after intravenous administration to each rat of 1, 5, and 10 μ g of TH plasmid delivered with TfRMAB-PIL (Fig. 7).

Normalization of TH enzyme activity in the ipsilateral striatum (Table 2) is consistent with the detection of immunoreactive TH throughout the ipsilateral striatum of rats treated with TfRMAB-PIL (Fig. 4). For treatment of human PD, it may be necessary to transduce at least 50% of the striate body, because the threshold of PD symptoms occurs with a 50% loss of nigral-striatal neurons (Booij *et al.*, 2001). The transduction of 50–100% of the striatum with a therapeutic gene is possible after delivery of the gene to brain via the transvascular route. All neurons in the brain are perfused by their own capillaries and PIL carrying the therapeutic gene is delivered to the “doorstep” of virtually every neuron in the brain after transport across the BBB (Pardridge, 2002).

Transduction of cell lines with retroviral vectors carrying the TH gene increases TH enzyme activity to approximately 1600 pmol/hr per 10^6 cells (Leff *et al.*, 1998). This is comparable to the TH enzyme activity in COS-1 cells transduced with LipofectAMINE and clone 877 (Fig. 1), as 10^6 cells in culture is equivalent to 1 mg of protein. A similar level of TH enzyme activity is also generated in human U87 glioma cells with the HIRMAb-PIL gene-targeting system (Fig. 3). Therefore, the level of transduction of a target cell by the PIL gene-targeting system is comparable to levels achieved with either cationic lipids or viral vectors.

Cellular targeting of the PIL gene delivery system is a function only of the receptor specificity of the targeting MAB (Shi *et al.*, 2001a,b). TfRMAB-PIL and mIgG2a-PIL have identical formulations, except that the mouse IgG2a isotype control antibody does not recognize the rat TfR. TfRMAB triggers receptor-mediated transcytosis of the PIL nanocontainer across the BBB *in vivo*. Once in the brain interstitial space, the PIL

undergoes receptor-mediated endocytosis into brain cells expressing the TfR. The TfR is widely expressed on neurons throughout the CNS (Mash *et al.*, 1991). Once inside brain cells, the fusogenic lipids of the liposome cause release of the plasmid DNA, which is then transported into the nuclear compartment for expression of the transgene. The rapid intranuclear delivery of DNA to cells by the PIL gene-targeting system has been demonstrated by confocal microscopy of fluoresceinated DNA encapsulated in PIL (Zhang *et al.*, 2002b).

TH enzyme activity is not increased in the cortex of brain after intravenous administration of TH expression plasmid encapsulated within TfRMAB-PIL (Table 2 and Fig. 4). A similar finding was made in the human TH transgenic mouse model, which shows increased TH enzyme activity in the striatum, but only minor changes in the frontal cortex (Kaneda *et al.*, 1991). The inability to mount a measurable increase in TH enzyme activity in the cortex is attributed to the absence of TH cofactor in this region of the brain (Shimoji *et al.*, 1999). The TH enzyme has an obligatory cofactor, tetrahydrobiopterin (BH₄), and the TH enzyme is not active in the absence of local production of the BH₄ cofactor (Hwang *et al.*, 1998). Studies performed in knockout mice show that the level of TH protein, measured by either enzyme activity or Western blotting, is diminished in animals lacking BH₄ (Sumi-Ichinose *et al.*, 2001). Both *in situ* hybridization and immunocytochemistry demonstrate that only monoaminergic neurons in the brain express the enzyme that is rate limiting for BH₄ synthesis, that is, GTP-cyclohydrolase (GTPCH), and there is no measurable GTPCH produced in the cortex (Nagatsu *et al.*, 1997; Hwang *et al.*, 1998). Although mRNA for GTPCH exists at a low level in the striatum (Hirayama *et al.*, 1993), the GTPCH protein is produced in nerve endings terminating in the striatum (Hwang *et al.*, 1998). GTPCH is produced in cell bodies of multiple regions of the brain outside the striatum, particularly serotonergic systems (Lentz and Kapatos, 1996). These neurons terminate in the striatum (Hwang *et al.*, 1998), and enable the striatal production of BH₄, a diffusible small molecule, within the lesioned striatum. Both GTPCH and BH₄ levels in the striatum of 6-hydroxydopamine-lesioned rat are still one-third the concentrations in nonlesioned animals (Levine *et al.*, 1981). This residual GTPCH in the striatum provides the BH₄ cofactor for TH enzyme produced by the exogenous TH gene delivered to the brain. In contrast, GTPCH is not produced in the neocortex, and it is not possible to increase TH enzyme activity in this region of the brain by administration of exogenous TH gene (Table 2). This is advantageous for the treatment of PD, because it is not desirable to augment dopamine production in cortical structures. TH enzyme activity is increased in rat glioma cells targeted with TfRMAB-PIL or in human U87 glial cancer cells targeted with HIRMAb-PIL (Fig. 3). These findings are consistent with prior studies showing that both cultured rat glioma cells and cancer cell lines produce the GTPCH enzyme (Nussler *et al.*, 1996; Vann *et al.*, 2002). A modest increase in rat liver TH activity is observed in control rats (Table 1), and this is consistent with the expression of GTPCH in liver (Nagatsu *et al.*, 1997). However, TH enzyme activity in rat liver is reduced by 98% compared with striatal TH enzyme activity (Tables 1 and 2).

Reversal of apomorphine-induced rotational behavior in the 6-hydroxydopamine lesioned rat is not seen in all studies involving transduction of the striatum with TH genes, using vi-

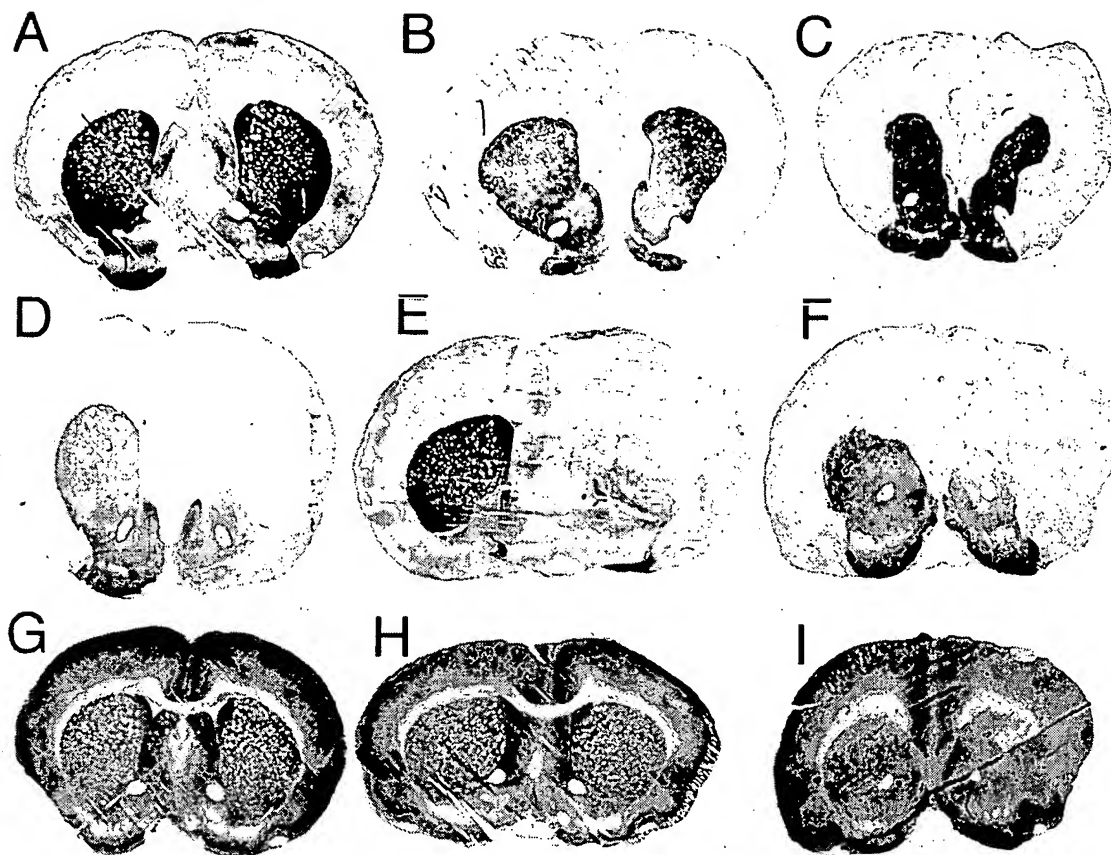


FIG. 4. Tyrosine hydroxylase immunocytochemistry of rat brain removed 72 hr after a single intravenous injection of 10 μ g per rat of clone 877 plasmid DNA encapsulated in PIL targeted with either the TfrMAB (A–C) or with the mouse IgG2a isotype control (D–F). Coronal sections are shown for three different rats from each of the two treatment groups. The 6-hydroxydopamine was injected into the medial forebrain bundle of the right hemisphere, which corresponds to right side of the figure. (G–I) Coronal sections of brain stained with hematoxylin. (G), (H), and (I) correspond to (A), (E), and (F), respectively. Immunoreactive TH is completely abolished in both the caudal and ventral striatum in the rat shown in (E), whereas there is residual immunoreactive TH in the ventral striatum and olfactory tubercle in the rats shown in (D) and (F).

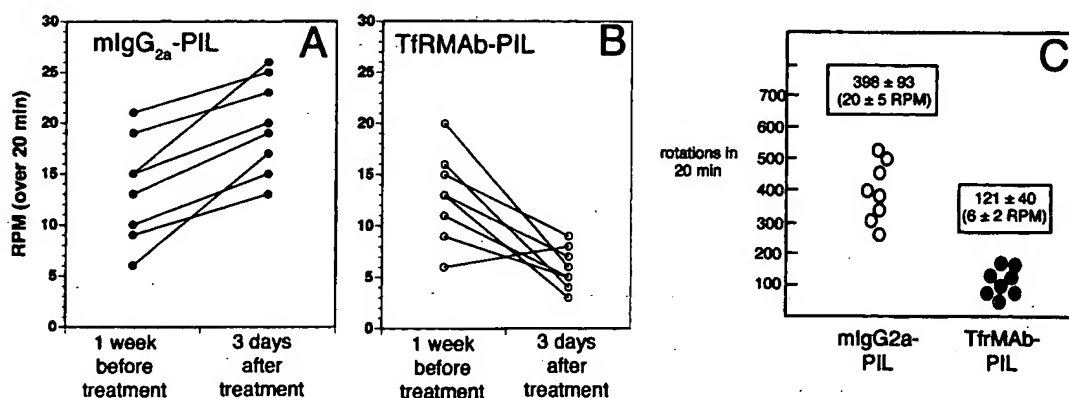


FIG. 5. (A) Apomorphine-induced rotations per minute (rpm) over a 20-min period, measured in individual rats 1 week before treatment and 3 days after a single intravenous injection of, per rat, 10 μ g of clone 877 plasmid DNA encapsulated in PIL targeted with the mouse IgG2a isotype control antibody. (B) Apomorphine-induced rotations per minute over a 20-min period measured in individual rats 1 week before treatment and 3 days after a single intravenous injection of, per rat, 10 μ g of clone 877 plasmid DNA encapsulated in PIL targeted with TfrMAB. (C) Comparison of the total rotations in the two groups 3 days after treatment. The average rotations per minute is 20 ± 5 and 6 ± 2 (mean \pm SD) in animals treated with mIgG_{2a}-PIL and TfrMAB-PIL, respectively. The difference in rotation between the two groups is significant at the $p < 0.005$ level (Student *t* test). The rotation behavior in all animals was measured 3 weeks after 6-hydroxydopamine injection, which corresponds to 1 week before PIL treatment, and 4 weeks after toxin injection, which corresponds to 3 days after treatment with the PIL.

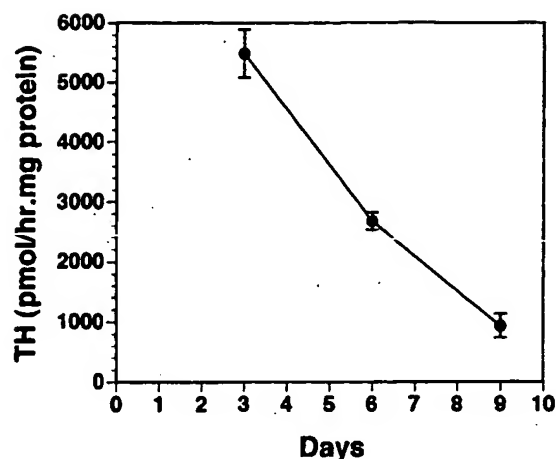


FIG. 6. The striatal tyrosine hydroxylase (TH) activity ipsilateral to the 6-hydroxydopamine lesion is plotted versus time after a single intravenous injection of, per rat, 10 μ g of clone 877 plasmid DNA encapsulated in TfRMAB-PIL on day 0. Data represent means \pm SD ($n = 3$ rats per point). The TH activity on the lesioned side 9 days after treatment with TfRMAB-PIL is comparable to the TH activity in the lesioned striatum of rats treated with mlgG2a-PIL (Table 2). The 3-day data are from Table 2.

ral vectors (Mandel *et al.*, 1998; Kirik *et al.*, 2002). Reversal of the aberrant rotational behavior in this model may require transduction of a significant volume of striatum with the TH therapeutic gene, and this may not be possible with a single intrastriatal injection of a viral vector (Kirik *et al.*, 2002). In contrast, transvascular delivery of the TH gene to brain enables complete normalization of TH enzyme activity in the striatum (Table 2) and normalization of the level of immunoreactive TH in the entire striate body (Fig. 4). These findings are consistent with reversal of apomorphine-induced rotational behavior after a single intravenous administration of the TH gene packaged in the PIL gene delivery system (Fig. 5C). Apomorphine-induced rotation 3 days after treatment with mlgG2a-PIL is increased 50% relative to drug-induced rotation 1 week before treatment (Fig. 5A), and this observation is consistent with the known pharmacodynamics of the 6-hydroxydopamine model. Apomorphine-induced rotations increase 50% by 4 weeks after 6-hydroxydopamine injection as compared with rotations observed 3 weeks after injection (Meshul *et al.*, 2002). The comparison of the two treatment groups 4 weeks after toxin injection is shown in Fig. 5C, and these data show a 70% reduction in rotation behavior after treatment with TfRMAB-targeted PIL.

Normalization of striatal TH activity after a single intravenous administration of TH gene encapsulated in targeted PIL is transient, and the level of TH activity in brain is reduced 50% by 6 days and reduced >90% by 9 days (Fig. 6). This time course in rat brain TH activity parallels prior work, which showed the rat brain activity of β -galactosidase was decreased 50% by 6 days after a single intravenous injection of expression plasmid encapsulated in targeted PIL (Shi *et al.*, 2001b). The organ level of the plasmid DNA, as determined by Southern blotting, was also 50% decreased at 6 days after a single intravenous administration of PIL (Shi *et al.*, 2001b), which suggests that gene expression declines with time owing to degradation of plasmid DNA within the target tissue. Reversible

gene expression by PIL gene-targeting technology is consistent with expression of the gene episomally, without integration of the plasmid DNA within the host genome. Conversely, the expression of exogenous genes is long-lasting after the transfection of brain cells with either retrovirus (Kordower *et al.*, 2000) or adeno-associated virus (Kapli *et al.*, 1994), as these viral vectors randomly and stably integrate into the host genome. The long-term effects of such stable and random integration are not known (Cavazzana-Calvo *et al.*, 2000). Although gene expression is reversible with nonviral, plasmid-based gene therapy, sustained pharmacologic effects can be achieved with repeat administration of the gene medicine. Weekly intravenous administration of plasmid DNA encoding antisense RNA against the human epidermal growth factor receptor caused a 100% increase in survival time for mice with intracranial brain cancer (Zhang *et al.*, 2002a).

A linear dose response is observed as the striatal TH activity ipsilateral to the 6-hydroxydopamine injection is increased in proportion to the dose of TH expression plasmid targeted to brain by TfRMAB-PIL. A maximal effect is observed in rats receiving a 10- μ g dose, whereas the 1- μ g/rat dose is ineffective, and an intermediate response is obtained with the 5- μ g/rat dose (Fig. 7). A per-rat dose of 10 μ g of the 6.0-kb clone 877 plasmid delivers 1.2×10^9 plasmid molecules per gram of brain, because 0.07% of the injected PIL dose is delivered to 1 g of rat brain (Shi and Pardridge, 2000). Given 10^8 cells per gram of brain, the 10- μ g/rat dose delivers approximately 12 plasmid DNA molecules per brain cell. Conversely, only one plasmid molecule per brain cell is delivered with the 1- μ g/rat dose, and this dose has no pharmacologic effect on TH activity in brain (Fig. 7). These findings suggest a relatively high efficiency of transfection of brain cells *in vivo* by the PIL gene-targeting technology, and that pharmacological effects in brain are achieved with the delivery of only 5–10 plasmid DNA molecules per brain cell.

TH enzyme activity in rat liver is also increased by the intravenous administration of clone 877 plasmid DNA encapsulated in TfRMAB-PIL, although the enzyme activity in liver at 3 days (Table 1) is <2% of striatal enzyme activity (Table 2).

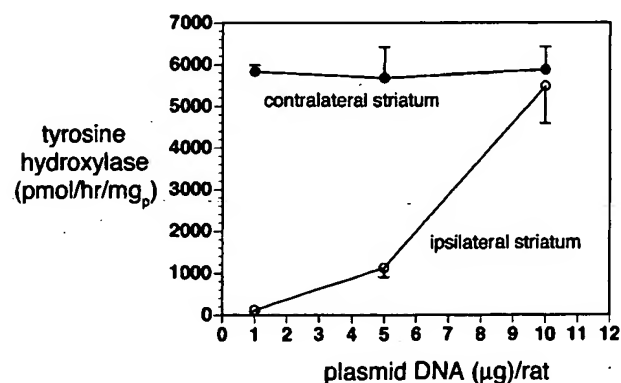


FIG. 7. The striatal tyrosine hydroxylase (TH) activity either ipsilateral or contralateral to the 6-hydroxydopamine lesion is plotted versus the dose of clone 877 plasmid DNA encapsulated in TfRMAB-PIL. Data represent means \pm SD ($n = 3$ rats per point). Striatal TH was measured 3 days after the single intravenous administration of DNA.

The TH gene is expressed in liver because (1) the TfR is highly expressed in this organ (Shi *et al.*, 2001b), and (2) clone 877 plasmid is under the influence of the widely expressed SV40 promoter (see Materials and Methods). However, if the SV40 promoter is replaced with a brain-specific promoter, such as the 5'-flanking sequence of the glial fibrillary acidic protein gene, then extracerebral gene expression is eliminated (Shi *et al.*, 2001a). Therefore, the tissue specificity of expression of the exogenous gene can be controlled by the combined use of gene-targeting technology and tissue-specific gene promoters.

In summary, the intracerebral injection of 6-hydroxydopamine into the medial forebrain bundle caused a 90% decrease in ipsilateral TH enzyme activity and immunoreactive TH in the ipsilateral striatum. TH enzyme activity and immunoreactive TH in the striatum were normalized by a single intravenous injection of a nonviral TH expression plasmid encapsulated in the interior of PIL and targeted to neurons by a TfRMAB. Normalization of striatal TH enzyme activity was associated with a 70% reduction in apomorphine-induced rotation behavior. The pharmacological effect in brain is both time and dose dependent. This work shows that it is possible to achieve pharmacological effects in target tissues by nonviral gene transfer after intravenous administration of the gene.

ACKNOWLEDGMENTS

This work was supported by a grant from the Neurotoxin Exposure Treatment Research Program of the U.S. Department of Defense. F.C. was supported by the Canadian Institutes of Health Research.

REFERENCES

- ANTON, R., KORDOWER, J.H., MAIDMENT, N.T., MANASTER, J.S., KANE, D.J., RABIZADEH, S., SCHUELLER, S.B., YANG, J., RABIZADEH, S., EDWARDS, R.H., MARKHAM, C.H., and BREDESEN, D.E. (1994). Neural-targeted gene therapy for rodent and primate hemiparkinsonism. *Exp. Neurol.* **127**, 207-218.
- ARMSTRONG, R.J.E., HURELBRINK, C.B., TYERS, P., RATCLIFFE, E.L., RICHARDS, A., DUNNETT, S.B., ROSSER, A.E., and BARKER, R.A. (2002). The potential for circuit reconstruction by expanded neural precursor cells explored through porcine xenografts in a rat model of Parkinson's disease. *Exp. Neurol.* **175**, 98-111.
- BANKIEWICZ, K.S., EBERLING, J.L., KOHUTNICKA, M., JAGUST, W., PIVROTTO, P., BRINGAS, J., CUNNINGHAM, J., BUDINGER, T.F., and HARVEY-WHITE, J. (2000). Convection-enhanced delivery of AAV vector in parkinsonian monkeys: In vivo detection of gene expression and restoration of dopaminergic function using pro-drug approach. *Exp. Neurol.* **164**, 2-14.
- BOADO, R.J., and PARDRIDGE, W.M. (1998). Ten nucleotide cis element in the 3'-untranslated region of GLUT1 glucose transporter mRNA increases gene expression via mRNA stabilization. *Mol. Brain Res.* **59**, 109-113.
- BOOIJ, J., BERGMANS, P., WINOGRODZKA, A., SPEELMAN, J.D., and WOLTERS, E.C. (2001). Imaging of dopamine transporters with [¹²³I]FP-CIT SPECT does not suggest a significant effect of age on the symptomatic threshold of disease in Parkinson's disease. *Synapse* **39**, 101-108.
- CAVAZZANA-CALVO, M., HACEIN-BEY, S., DE SAINT BASILE, G., YVON, E., NUSBAUM, P., SELZ, F., HUE, C., CERTAIN, S., CASANOVA, J.L., BOUSSO, P., DEIST, F.L., and FISCHER, A. (2000). Gene therapy of human severe combined immunodeficiency (SCID)-X1 disease. *Science* **288**, 669-672.
- DURING, M.J., NAEGELE, J.R., O'MALLEY, K.L., and GELLER, A.I. (1994). Long-term behavioral recovery in parkinsonian rats by an HSV vector expressing tyrosine hydroxylase. *Science* **266**, 1399-1403.
- DWYER, K.J., BOADO, R.J., and PARDRIDGE, W.M. (1996). Cis-element/cytoplasmic protein interactions within the 3'-untranslated region of GLUT1 glucose transporter mRNA. *J. Neurochem.* **66**, 449-458.
- HIRAYAMA, K., LENTZ, S.I., and KAPATOS, G. (1993). Tetrahydrobiopterin cofactor biosynthesis: GTP cyclohydrolase I mRNA expression in rat brain and superior cervical ganglia. *J. Neurochem.* **61**, 1006-1014.
- HORELLOU, P., GUIBERT, B., LEVIEL, V., and MALLET, J. (1989). Retroviral transfer of a human tyrosine hydroxylase cDNA in various cell lines: Regulated release of dopamine in mouse anterior pituitary AtT-20 cells. *Proc. Natl. Acad. Sci. U.S.A.* **86**, 7233-7237.
- HUWYLER, J., WU, D., and PARDRIDGE, W.M. (1996). Brain drug delivery of small molecules using immunoliposomes. *Proc. Natl. Acad. Sci. U.S.A.* **93**, 14164-14169.
- HWANG, O., BAKER, H., GROSS, S., and JOH, T.H. (1998). Localization of GTP cyclohydrolase in monoaminergic but not nitric oxide-producing cells. *Synapse* **28**, 140-153.
- JEFFERIES, W.A., BRANDON, M.R., HUNT, S.V., WILLIAMS, A.F., GATTERS, K.C., and MASON, D.Y. (1984). Transferrin receptor on endothelium of brain capillaries. *Nature* **312**, 162-163.
- KANEDA, N., SASAKA, T., KOBAYASHI, K., KIUCHI, K., NAGATSU, I., KUROSAWA, Y., FUJITA, K., YOKOYAMA, M., NOMURA, T., KATSUKI, M., and NAGATSU, T. (1991). Tissue-specific and high-level expression of the human tyrosine hydroxylase gene in transgenic mice. *Neuron* **6**, 583-594.
- KAPLITT, M.G., LEONE, P., SAMULSKI, R.J., XIAO, X., PFAFF, D.W., O'MALLEY, K.L., and DURING, M.J. (1994). Long-term gene expression and phenotypic correction using adeno-associated virus vectors in the mammalian brain. *Nat. Genet.* **8**, 148-154.
- KIRIK, D., GEORGIEVSKA, B., BURGER, C., WINKLER, C., MUZYCZKA, N., MANDEL, R.J., and BJORKLUND, A. (2002). Reversal of motor impairments in parkinsonian rats by continuous intrastriatal delivery of L-dopa using rAAV-mediated gene transfer. *Proc. Natl. Acad. Sci. U.S.A.* **99**, 4708-4713.
- KORDOWER, J.H., EMBORG, M.E., BLOCH, J., MA, S.Y., CHU, Y., LEVENTHAL, L., MCBRIDE, J., CHEN, E.-Y., PALFI, S., ROITBERG, B.Z., BROWN, W.D., HOLDEN, J.E., PYZALSKI, R., TAYLOR, M.D., CARVEY, P., LING, Z., TRONO, D., HANTRAYE, P., DEGLON, N., and AEBISCHER, P. (2000). Neurodegeneration prevented by lentiviral vector delivery of GDNF in primate models of Parkinson's disease. *Science* **290**, 767-773.
- LEFF, S.E., RENDAHL, K.G., SPRATT, S.K., KANG, U.J., and MANDEL, R.J. (1998). In vivo L-DOPA production by genetically modified primary rat fibroblast or 9L gliosarcoma cell grafts via co-expression of GTP cyclohydrolase I with tyrosine hydroxylase. *Exp. Neurol.* **154**, 249-264.
- LENTZ, S.I., and KAPATOS, G. (1996). Tetrahydrobiopterin biosynthesis in the rat brain: Heterogeneity of GTP cyclohydrolase I mRNA expression in monoamine-containing neurons. *Neurochem. Int.* **28**, 569-582.
- LEONE, P., MCPHEE, S.W.J., JANSON, C.G., DAVIDSON, B.L., FREESE, A., and DURING, M.J. (2000). Multi-site partitioned delivery of human tyrosine hydroxylase gene with phenotypic recovery in parkinsonian rats. *Neuroreport* **2**, 1145-1151.
- LEVINE, R.A., MILLER, L.P., and LOVENBERG, W. (1981). Tetrahydrobiopterin in striatum: Localization in dopamine nerve terminals and role in catecholamine synthesis. *Science* **214**, 919-921.

- MANDEL, R.J., RENDAHL, K.G., SPRATT, S.K., SNYDER, R.O., COHEN, L.K., and LEFF, S.E. (1998). Characterization of intrastriatal recombinant adeno-associated virus-mediated gene transfer of human tyrosine hydroxylase and human GTP-cyclohydrolase I in rat model of Parkinson's disease. *J. Neurosci.* **18**, 4271-4284.
- MANDEL, R.J., RENDAHL, K.G., SNYDER, R.O., and LEFF, S.E. (1999). Progress in direct striatal delivery of L-dopa via gene therapy for treatment of Parkinson's disease using recombinant adeno-associated viral vectors. *Exp. Neurol.* **159**, 47-64.
- MASH, D.C., PABLO, J., BUCK, B.E., SANCHEZ-RAMOS, J., and WEINER, W.J. (1991). Distribution and number of transferrin receptors in Parkinson's disease and in MPTP-treated mice. *Exp. Neurol.* **114**, 73-81.
- MESHUL, C.K., KAMEL, D., MOORE, C., KAY, T.S., and KRENTZ, L. (2002). Nicotine alters striatal glutamate function and decreases the apomorphine-induced contralateral rotations in 6-OHDA-lesioned rats. *Exp. Neurol.* **175**, 257-274.
- MONNARD, P.-A., OBERHOLZER, T., and LUISI, P. (1997). Entrapment of nucleic acids in liposomes. *Biochim. Biophys. Acta* **1329**, 39-50.
- MOURADIAN, M.M., and CHASE, T.N. (1997). Gene therapy for Parkinson's disease: An approach to the prevention or palliation of levodopa-associated motor complications. *Exp. Neurol.* **144**, 51-57.
- NAGATSU, I., ARAI, R., SAKAI, M., YAMAWAKI, Y., TAKEUCHI, T., KARASAWA, N., and NAGATSU, T. (1997). Immunohistochemical colocalization of GTP cyclohydrolase I in the nigrostriatal system with tyrosine hydroxylase. *Neurosci. Lett.* **224**, 185-188.
- NUSSLER, A.K., LIU, Z.-Z., HATAKEYAMA, K., GELLER, D.A., BILLIAR, T.R., and MORRIS, S.M., JR. (1996). A cohort of supporting metabolic enzymes is coinduced with nitric oxide synthase in human tumor cell lines. *Cancer Lett.* **103**, 79-84.
- PARDRIDGE, W. (2002). Drug and gene targeting to the brain with molecular Trojan horses. *Nat. Rev. Drug Discov.* **1**, 131-139.
- PARDRIDGE, W.M., EISENBERG, J., and YANG, J. (1987). Human blood-brain barrier transferrin receptor. *Metabolism* **36**, 892-895.
- PARDRIDGE, W.M., BUCIAK, J.L., and YOSHIKAWA, T. (1992). Transport of recombinant CD4 through the rat blood-brain barrier in vivo. *J. Pharmacol. Exp. Ther.* **261**, 1175-1180.
- REINHARD, J.F., SMITH, G.K., and NICHOL, C.A. (1986). A rapid and sensitive assay for tyrosine-3-monooxygenase based upon the release of $^3\text{H}_2\text{O}$ and adsorption of ^3H -tyrosine by charcoal. *Life Sci.* **39**, 2185-2189.
- SHI, N., and PARDRIDGE, W.M. (2000). Noninvasive gene targeting to the brain. *Proc. Natl. Acad. Sci. U.S.A.* **97**, 7567-7572.
- SHI, N., ZHANG, Y., BOADO, R.J., ZHU, C., and PARDRIDGE, W.M. (2001a). Brain-specific expression of an exogenous gene following intravenous administration. *Proc. Natl. Acad. Sci. U.S.A.* **98**, 12754-12759.
- SHI, N., BOADO, R.J., and PARDRIDGE, W.M. (2001b). Receptor-mediated gene targeting to tissues in the rat in vivo. *Pharm. Res.* **18**, 1091-1095.
- SHIMOJI, M., HIRAYAMA, K., HYLAND, K., and KAPATOS, G. (1999). GTP cyclohydrolase I gene expression in the brains of male and female hph-1 mice. *J. Neurochem.* **72**, 757-764.
- SHUSTA, E.V., BOADO, R.J., and PARDRIDGE, W.M. (2002). Vascular proteomics and subtractive antibody expression cloning. *Mol. Cell. Proteomics* **1**, 75-82.
- SUMI-ICHINOSE, C., URANO, F., KURODA, R., OHYE, T., KOJIMA, M., TAZAWA, M., SHIRAIISHI, H., YASUMICHI, H., NAGATSU, T., NOMURA, T., and ICHINOSE, H. (2001). Catecholamines and serotonin are differently regulated by tetrahydrobiopterin. *J. Biol. Chem.* **276**, 41150-41160.
- VANN, L.R., PAYNE, S.G., EDSALL, L.C., TWITTY, S., SPIEGEL, S., and MILSTIEN, S. (2002). Involvement of sphingosine kinase in TNF- α -stimulated tetrahydrobiopterin biosynthesis in C6 glioma cells. *J. Biol. Chem.* **277**, 12649-12656.
- ZHANG, Y., ZHU, C., and PARDRIDGE, W.M. (2002a). Antisense gene therapy of brain cancer with an artificial virus gene delivery system. *Mol. Ther.* **6**, 67-72.
- ZHANG, Y., LEE, H.J., BOADO, R.J., and PARDRIDGE, W.M. (2002b). Receptor-mediated delivery of an antisense gene to human brain cancer cells. *J. Gene Med.* **4**, 183-194.
- ZHANG, Y., BOADO, R.J., and PARDRIDGE, W.M. (2003). Marked enhancement in gene expression by targeting the human insulin receptor. *J. Gene Med.* **5**, in press.

Address reprint requests to:
 Dr. William M. Pardridge
 UCLA
 Warren Hall 13-164
 900 Veteran Avenue
 Los Angeles, CA 90024

E-mail: wpardridge@mednet.ucla.edu

Received for publication September 18, 2002; accepted after revision November 13, 2002.

Published online: December 2, 2002.



Organ-specific gene expression in the rhesus monkey eye following intravenous non-viral gene transfer

Yun Zhang,¹ Felix Schlachetzki,^{1,2} Jian Yi Li,¹ Ruben J. Boado,¹ William M. Pardridge¹

¹Department of Medicine, UCLA, Los Angeles, CA; ²Department of Neurology, University of Regensburg, Regensburg, Germany

Purpose: The transfer of exogenous genes to the entire retina and other ocular structures is possible with a vascular route of gene delivery using a non-viral gene transfer method. The present studies examine the extent to which either β -galactosidase or luciferase expression plasmids are targeted to the retina in the adult rhesus monkey following intravenous administration. In addition, these studies examine the pattern of organ expression of the transgene in the rhesus monkey depending on whether the plasmid is under the influence of a widely expressed promoter, the SV40 promoter, or an ocular-specific promoter, the opsin promoter.

Methods: The plasmid DNA with either the SV40 or opsin promoter is encapsulated in the interior of 85 nm pegylated immunoliposomes (PILs), which are targeted across the blood-retinal barrier and into ocular cells with a monoclonal antibody to the human insulin receptor. Following a single intravenous injection of the PIL carrying the transgene, the animals were sacrificed 2, 7, or 14 days later for the measurement of β -galactosidase or luciferase gene expression in the monkey eye and peripheral organs.

Results: Histochemistry showed expression of the β -galactosidase gene throughout the entire primate retina including the photoreceptor cells with either an SV40 or a bovine opsin promoter. Whereas the SV40 promoter enables gene expression in other organs of the primate (brain, liver, spleen), the opsin promoter restricted trans-gene expression to the primate eye, as there was no gene expressed in other organs. The retinal luciferase activity at 2 days after administration was 9.6 ± 0.4 pg luciferase/mg protein, and at 14 days after administration was still comparable to maximal levels of luciferase gene expression in the mouse or rat. Confocal microscopy with antibodies to the insulin receptor and to β -galactosidase demonstrated co-localization in the retina, with high expression of the trans-gene and the insulin receptor in the inner segments of the photoreceptor cells.

Conclusions: The PIL non-viral gene transfer technology makes possible adult transgenics in 24 h. Ectopic expression of exogenous genes in organs other than the target organ is made possible with the use of organ specific promoters, and gene expression in the primate is restricted to the eye when the trans-gene is under the influence of the opsin promoter. Plasmid-based gene expression is still in the therapeutic range for 2-3 weeks after a single intravenous administration. Exogenous genes are expressed throughout the entire primate retina following the delivery of the gene to the eye via a trans-vascular route.

Many forms of blindness are potentially treatable with retinal gene therapy [1,2]. The retinal photoreceptor cells can be transduced with sub-retinal injections of viruses such as adeno-associated virus (AAV) [3]. The portion of the human retina that is transduced with a sub-retinal injection is localized to the injection site [4,5]. Conversely, global expression of an exogenous gene throughout the human retina may be possible with a transvascular route to the eye following intravenous administration. However, viral vectors do not cross the blood-retinal barrier (BRB). In mice a non-viral gene delivery system comprised of pegylated immunoliposomes (PIL) can be targeted across the BRB following intravenous administration, and this leads to expression of an exogenous gene in the eye [6]. In this approach, the therapeutic gene is incorporated in non-viral plasmid DNA, which is encapsulated in the interior of 85 nm anionic liposomes [7,8]. The surface of the

liposome is conjugated with several thousand strands of polyethylene glycol (PEG), which stabilizes the liposome in the circulation, minimizes liposome uptake by the reticulo-endothelial system, and enables a sustained circulation time of the liposome in the blood. The tips of 1-2% of the PEG strands are conjugated with a targeting ligand such as a peptidomimetic monoclonal antibody (MAb). The targeting ligand binds to specific receptors expressed at both the BRB and the plasma membrane of retina and ocular cells to trigger receptor-mediated transcytosis across the BRB and receptor-mediated endocytosis into cells of the eye [6].

Exogenous genes have been targeted to the mouse eye and retinal pigmented epithelium (RPE) with PILs formulated with a MAb to the mouse transferrin receptor (TfR) [6]. This resulted in widespread expression of the exogenous gene throughout the RPE, but there was no measureable gene expression in the photoreceptor cells of the mouse retina [6]. The absence of gene expression in the photoreceptor layer is attributed to the minimal expression of TfR on the plasma membranes in the outer nuclear layer (ONL) of the retina [9,10]. The reduced expression of the TfR in the ONL is con-

Correspondence to: Dr. William M. Pardridge, UCLA, Warren Hall 13-164, 900 Veteran Avenue, Los Angeles, CA, 90024; Phone: (310) 825-8858; FAX: (310) 206-5163; email: wpardridge@mednet.ucla.edu

sistent with very low concentrations of iron and ferritin in this region of the retina [10]. Conversely, the cells of the ONL express high levels of the insulin receptor (IR) [11,12] and a targeting ligand that accesses the IR could deliver genes to the ONL. The 83-14 murine MAb to the human insulin receptor (HIR) is rapidly transported across the blood-brain barrier (BBB) of Old World primates, owing to high expression of the IR on the primate BBB [13]. Gene transfer with the HIRMAb-targeted PIL enables the global delivery of exogenous genes to the brain of the rhesus monkey following intravenous injection [14]. The IR is also expressed at the BRB [11,12]. Therefore, the present studies determine the extent to which endogenous genes are expressed in the Rhesus monkey retina following a single intravenous injection of non-viral plasmid DNA encapsulated in a PIL that is targeted to the HIR. Owing to the genetic similarity between humans and Old World monkeys such as the Rhesus monkey [15], the 83-14 HIRMAb cross-reacts with the Rhesus monkey IR [13]. In the present studies, plasmids encoding either β -galactosidase or luciferase are administered by peripheral venous injection, and gene expression in the primate retina is measured with the luciferase assay, β -galactosidase histochemistry, and confocal microscopy using antibodies directed against β -galactosidase and the HIR. The β -galactosidase expression plasmid, under the influence of the SV40 promoter, is alternatively designated pSV- β -galactosidase or clone 756, as described previously [14]. The luciferase expression plasmid, under the influence of the SV40 promoter, was derived from the pCEP4 plasmid, and is designated clone 790 as described previously [14].

A second goal of the present work was to examine the organ specificity of gene expression with the PIL gene transfer approach. If the exogenous gene is under the influence of a widely expressed promoter, such as the SV40 promoter, then the gene is expressed in multiple organs of the primate, including brain, liver, and spleen, following the intravenous injection of HIRMAb-targeted PILs [14]. In the present study, a β -galactosidase expression plasmid under the influence of the bovine opsin promoter, is injected into the primate following encapsulation in HIRMAb-targeted PILs. The opsin- β -galactosidase plasmid is designated pLacF, as described by Zack et al [16].

METHODS

Materials: POPC (1-palmitoyl-2-oleoyl-*sn*-glycerol-3-phosphocholine) and DDAB (didodecyldimethylammonium bromide) were purchased from Avanti-Polar Lipids Inc. (Alabaster, AL), and distearoylphosphatidylethanolamine (DSPE)-PEG 2000 was obtained from Shearwater Polymers (Huntsville, AL). DSPE-PEG 2000-maleimide was custom synthesized by Shearwater Polymers. [α - 32 P]dCTP (3000 Ci/mmol) was from NEN Life Science Product Inc. (Boston, MA). The nick translation system was from Invitrogen (San Diego, CA). 5-Bromo-4-chloro-3-indoyl- β -D-galactoside (X-gal), IGEAL CA-630 and all other chemicals were purchased from Sigma Chemical Co. (St. Louis, MO). The 2-iminothiolane (Traut's reagent) and bicinchoninic acid (BCA) protein assay reagents

were obtained from Pierce Chemical Co. (Rockford, IL). The 83-14 murine MAb to the HIR was purified by protein G affinity chromatography from hybridoma generated ascites. The luciferase expression plasmid is designated clone 790 and is derived from the pCEP4 plasmid under the control of the SV40 promoter as described previously [17]. The pSV- β -galactosidase expression plasmid driven by the SV40 promoter is designated clone 756 as described previously [7]. The pLacF expression plasmid under the influence of the bovine rhodopsin promoter was provided by Dr. Don Zack of Johns Hopkins University, and was described previously [16], and is designated clone 933. This 8 kb plasmid includes nucleotides -2174 to +70 of the bovine rhodopsin gene. The presence of this portion of the bovine rhodopsin promoter within the plasmid was confirmed by DNA sequencing using a M13 reverse sequencing primer followed by custom sequencing primers. Digestion of the rhodopsin/ β -galactosidase plasmid with BamHI released the 3.0 kb insert from the 5.0 kb vector backbone.

Pegylated immunoliposome synthesis: Pegylated immunoliposomes (PILs) were synthesized from a total of 20 μ mol of lipids, including 18.6 μ mol of POPC, 0.6 μ mol of DDAB, 0.6 μ mol of DSPE-PEG, and 0.2 μ mol of DSPE-PEG-maleimide [7,8]. Clone 756 plasmid DNA, clone 790 plasmid DNA, or pLacF plasmid DNA was produced by Maxiprep (Qiagen; Chatsworth, CA), and the supercoiled plasmid DNA (200 μ g) and 1 μ Ci of 32 P-nick translated plasmid DNA were encapsulated in the pegylated liposomes by serial extrusion through filters of 400, 200, and 100 nm pore size, which forms liposomes of 85 nm diameter [18]. The exteriorized DNA was quantitatively removed by exhaustive nuclease digestion, as described previously [18]. The 83-14 MAb containing a trace amount of 3 H-labeled antibody, was thiolated with Traut's reagent and the thiolated MAb was conjugated to the pegylated liposome overnight at room temperature as described previously [7,19]. The unconjugated MAb, and the degraded exteriorized DNA were separated from the DNA encapsulated within the PIL by elution through a 1.6x18 cm column of Sepharose CL-4B in 0.05 M Hepes, pH 7.0, as described previously [7,19]. The average number of MAb molecules conjugated per liposome was 43 ± 2 (mean \pm SE, $n=3$ syntheses). The final percentage entrapment of 200 μ g of plasmid DNA in the liposome preparation was computed from the 32 P radioactivity and was $35 \pm 7.5\%$ (mean \pm SE, $n=3$ syntheses). The PIL conjugated with the HIRMAb is designated HIRMAb-PIL. The HIRMAb-PIL carrying either plasmid DNA was sterilized before injection into the primate with a 0.22 μ m filter (Millipore Co., Bedford, MA) as described previously [19].

Intravenous gene administration in Rhesus monkeys: Three healthy 5-10 year old, 5-6 kg female Rhesus monkeys were purchased from Covance (Alice, TX) and used in this study. In addition, a fourth rhesus monkey was sacrificed for removal of control tissues from an uninjected primate. Animal care guidelines were comparable to those published by the Institute for Laboratory Animal Research (Guide for the Care and Use of Laboratory Animals) and the US Public Health

Service (Public Health Service Policy on Human Care and Use of Laboratory Animals). The animals were anesthetized with 10 mg/kg ketamine intra-muscular, and 5 ml of sterile HIRMAb-PIL containing 70 μ g of plasmid DNA was injected into the monkey via the saphenous vein with a 18-g catheter. The total dose of HIRMAb that was conjugated to the PIL and administered to each monkey was 1.8 mg or 300 μ g/kg of antibody. The injection dose of PIL encapsulated plasmid DNA was 12 μ g/kg. The eyes were enucleated immediately after euthanasia. In addition, the brain, liver, spleen, lung, heart, kidney, triceps skeletal muscle and omental fat were removed. The conjunctiva, orbital connective and muscular tissues, and vitreous body were removed from the eye. One eye was used for measurement of luciferase activity and the other eye was frozen in powdered dry ice for 30 min, embedded in OCT and re-frozen for cryostat sectioning. Eyes were also removed from a control rhesus monkey (Sierra Biomedical/Charles River; Sparks, NV), not injected with gene, and these eyes were frozen in OCT embedding medium immediately after euthanasia, and processed in parallel with the eyes from the gene injected monkey.

The experimental design involved the injection of either 1 or 2 plasmids in the same animal, so as to minimize the number of terminal primate experiments. Monkey 1 was injected on day 0 with both clone 756 (the SV40 driven β -galactosidase plasmid), and clone 790 (the SV40 driven luciferase plasmid), and sacrificed at 2 days after injection. For the monkey 1 experiment, the clone 756 or clone 790 plasmid DNA was individually encapsulated in separate preparations of HIRMAb-targeted PILs and co-injected into the primate, similar to the experimental design used previously [14]. Monkey 2 was injected with clone 790 on day 0, and injected with clone 933, the pLacF (the rhodopsin promoter driven β -galactosidase plasmid), on day 5, and sacrificed on day 7. Monkey 3 was injected with clone 790 on day 0 and sacrificed on day 14. Monkey 4 was the control, uninjected primate.

β -Galactosidase histochemistry: Frozen sections of 20 μ m thickness were cut on a Mikron cryostat and fixed with 0.2% glutaraldehyde in 0.1 M NaH_2PO_4 for 1 h. The sections were washed with 0.1 M NaH_2PO_4 three times, and incubated overnight at 37 °C in X-gal staining solution (20 mM potassium-ferrocyanide, 20 mM potassium-ferricyanide, 2 mM

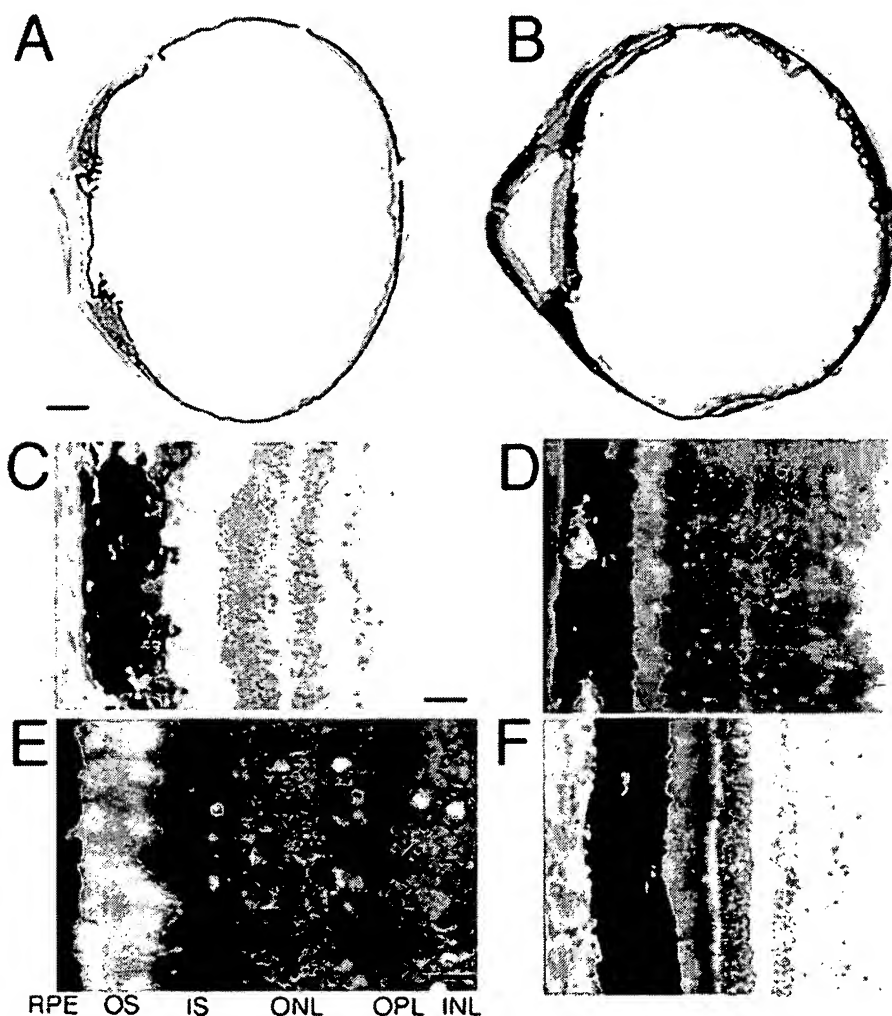


Figure 1. β -Galactosidase histochemistry of primate eyes. β -galactosidase histochemistry in control, un-injected Rhesus monkey eye (Panels A and C) and gene-injected Rhesus monkey eye (Panels B, D, E, and F). Panels A-E show β -galactosidase histochemistry followed by counter-staining with hematoxylin, whereas Panel F shows the retina only counter-stained with hematoxylin. Magnification in Panels A and B is the same; the magnification bar in Panel A represents 2 mm. The magnification in Panels C, D, and F is the same; the magnification bar in Panel C represents 32 μ m. The magnification bar in Panel E represents 13 μ m. Abbreviations in Panel E: INL, inner nuclear layer; OPL, outer plexiform layer; ONL, outer nuclear layer; IS inner segments; OS, outer segments; RPE, retinal pigmented epithelium. All specimens shown in Panels B, D-F were taken 48 h after the intravenous administration of clone 756, the pSV40- β -galactosidase plasmid, in monkey 1 (see Methods).

MgCl₂, 0.02% IGEPAL CA-630, 0.01% Na deoxycholate, and 1 mg/ml X-gal in 0.1 M NaH₂PO₄ at pH 7.3. Prior to coverslipping, the sections were scanned with a UMAX PowerLookIII scanner with transparency adapter, and the image was cropped in Adobe Photoshop 5.5 on a G4 Power Macintosh computer. Control or un-injected rhesus monkey eye was stained in parallel with the eye obtained from the gene-injected animal. Specimens were examined with and without hematoxylin counter-staining.

Confocal Imaging: Frozen sections (20 μ m) of either gene-injected and control monkey eyes were fixed for 5 min in 100% acetone at room temperature (RT). Following air drying, all sections were washed in 0.01 M PBS buffer and non-specific binding was blocked using 10% goat serum in 0.01 M PBS with 0.1% Triton X-100, pH 7.4 for 60 min at RT. Primary antibodies were the 83-14 mouse anti-human insulin receptor, rabbit anti E. coli β -galactosidase polyclonal antibody (Bioscience Int., Saco, ME), mouse IgG2a isotype control, or rabbit IgG, 5 μ g/ml, in 3% bovine serum albumin, 0.01 M PBS with 0.1% Triton X-100, pH 7.4; all primary antibodies were used at 5 μ g/ml. Incubation time was 48 h at 4 °C in a humidified chamber. Secondary antibodies used were 594 Goat anti-mouse IgG and 488 goat anti-rabbit IgG (Molecular Probes; Eugene, OR), 5 μ g/ml, in 1% goat serum, 0.01

M PBS, 0.1% Triton X-100, pH 7.4. Incubation time was 1 h at RT. Confocal imaging was performed with a Zeiss LSM 5 PASCAL confocal microscope with dual argon and helium/neon lasers equipped with Zeiss LSM software for image reconstruction (Zeiss, Jena, Germany). All sections were scanned in multitrack mode to avoid overlap of the fluorescein (excitation at 488 nm) and rhodamine (excitation at 543 nm) channels employing the Plan-Neofluar 40x/0.75 objective. Pinhole size was 126 μ m in both channels, and detector gain, amplifier gain and amplifier offset was identical for the gene-injected and control retina. Two scanning lines were integrated for a 512x512 image matrix. By integrating 4 serial tomographic images stack sizes of 230.3x230.3x4.8 μ m dimension were created. 2D images were visualized by integrating 4 serial tomographs by maximum intensity projection.

Luciferase measurements: Primate retina was homogenized in 4 volumes of lysis buffer for measurement of luciferase activity, as described previously [19]. The data are reported as pg luciferase activity per mg cell protein. Based on the standard curve, 1 pg of luciferase was equivalent to 14,312 \pm 2,679 relative light units (RLU), which is the mean \pm S.E. of 5 assays.

RESULTS

Histochemistry of the retina obtained from a control, un-injected Rhesus monkey shows no measurable β -galactosidase histochemical product (Figure 1A). In contrast, there is global β -galactosidase histochemical product in the primate retina and eye obtained 48 h after the single intravenous injection of the pSV- β -galactosidase plasmid encapsulated in the HIRMAb-PIL (Figure 1B). Exogenous gene expression is detected in multiple structures of the eye including the entire retina, the epithelium of the cornea, the ciliary body, and the iris. Higher magnification of the retina shows no evidence of histochemical product in the eye obtained from the un-injected monkey (Figure 1C), although there is gene expression in most layers of the retina in the gene-injected Rhesus monkey (Figure 1D). There is abundant histochemical product in the cell bodies of the ONL as well as the inner segments (IS) and some measurable histochemical product in the outer segments (OS) of the photoreceptor cells (Figure 1E). Other layers of the retina that are positive for β -galactosidase gene expression include the inner plexiform layer (IPL), the inner nuclear layer (INL), the outer plexiform layer (OPL) and the ganglion cell layer (GCL); see Figure 1D,E. There is no structural damage to the retina caused by the PIL administration as shown by the counter-staining of the primate retina (Figure 1F).

The luciferase gene was also expressed in the retina, and the retinal luciferase activity at 48 h was 9.6 \pm 0.4 pg luciferase/mg protein (mean \pm S.E., n=3 replicates). This is equivalent to 1.4 \times 10⁵ relative light units (RLU)/mg protein (Methods). No luciferase enzyme activity was detected in the retina of the control, uninjected monkey. The retina luciferase activity was also measured in primates at 7 and 14 days after injection, and the retinal luciferase activity decayed exponentially (Figure 2). The half-time of luciferase gene expression decay was 2.0 \pm 0.1 days and the extrapolated Y-intercept [A(0)], which

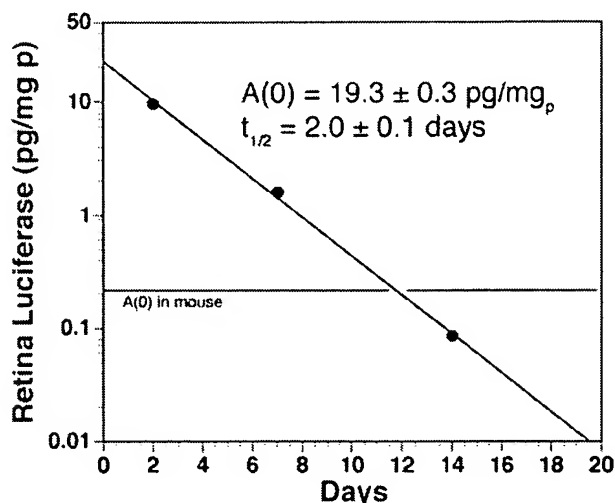


Figure 2. Luciferase gene expression in the primate eye. Retinal luciferase activity in 3 rhesus monkeys sacrificed at 2, 7, or 14 days after intravenous administration of clone 790 in monkeys 1, 2, and 3, respectively (see Methods). The data were fit to a single-exponential equation to yield the slope/half-time ($t_{1/2}$) and the intercept, [A(0)]. The horizontal line shows the A(0) of luciferase activity in control mouse brain, 0.22 \pm 0.08 pg/mg [20], which indicates the level of gene expression in the monkey retina is still above the therapeutic level for at least 2 weeks after injection. The luciferase expression plasmid was under the influence of the SV40 promoter in these studies. The diagonal line through the data points was drawn by eye. Error bars representing the standard deviation are shown over each closed circle.

gives the maximal retinal luciferase level, was 19.3 ± 0.1 pg per mg protein (Figure 2). The horizontal line in Figure 2 is the luciferase A(0) in the mouse [20], which corresponds to the primate retina luciferase activity at 12 days after a single intravenous injection (Figure 2).

Confocal microscopy shows diffuse expression of the IR in the retina of the gene-injected primate with high levels in the IS, OPL, IPL, and intermediate levels of expression in the INL and ONL cell bodies (Figure 3A). The same pattern of retinal expression of the IR is seen in the control monkey (Figure 3D). There is diffuse immunoreactive β -galactosidase in the gene-injected monkey with high levels in the IS, OPL, and IPL (Figure 3B). There is no immunoreactive β -galactosidase in the un-injected control monkey, as the faint autofluorescence seen over the RPE, OPL, and rod outer segments (Figure 3E, left lower corner) was also detected with control rabbit IgG (Figure 3H). The IR/ β -galactosidase overlap images for the gene-injected monkey and un-injected control monkey are shown in Figure 3C,F, respectively. There is a co-localization of β -galactosidase and IR in the gene injected monkey with minimal overlap signal in the un-injected monkey (Figure 3F).

The organ specificity of β -galactosidase gene expression was examined in the primate at 2 days following the intravenous injection of the pLacF plasmid driven by the bovine opsin promoter. Although there was abundant gene expression in multiple structures of the eye (Figure 4A), there was no gene expression in monkey brain, heart, lung, fat, spleen, or

liver (Figure 4C-H). The negative histochemical reaction in these multiple peripheral tissues was not assay related, because the histochemistry was done in parallel with the primate eye (Figure 4A,I) as well as the primate kidney (Figure 4B,J). Control kidney from un-injected animals contains β -galactosidase that is active at neutral pH and is histochemically active in the β -galactosidase assay [7]. Therefore, the histochemistry of kidney tissues serves as a positive control for the β -galactosidase assay. The pattern of cellular gene expression in the layers of the primate retina following administration of the opsin promoter plasmid (Figure 4I) is comparable to that found with the SV40 promoter plasmid as shown in Figure 1E. β -galactosidase gene expression under the influence of the opsin promoter was observed in multiple layers of the retina including the ONL, and the IS and OS of the photoreceptor cells (Figure 4I).

DISCUSSION

The results of these studies support the following conclusions. First, exogenous plasmid-based genes may be targeted to nearly all structures of the primate eye using the PIL gene targeting system and a HIRMAb as the targeting ligand (Figure 1). Second, the IR is expressed in the cell bodies of the ONL (Figure 3A), which enables global expression of exogenous genes in the photoreceptor cells and particularly IS (Figure 1E and Figure 3B). Third, β -galactosidase gene expression in the rhesus monkey is restricted to the eye when the trans-gene is under the influence of an ocular-specific promoter such as the opsin

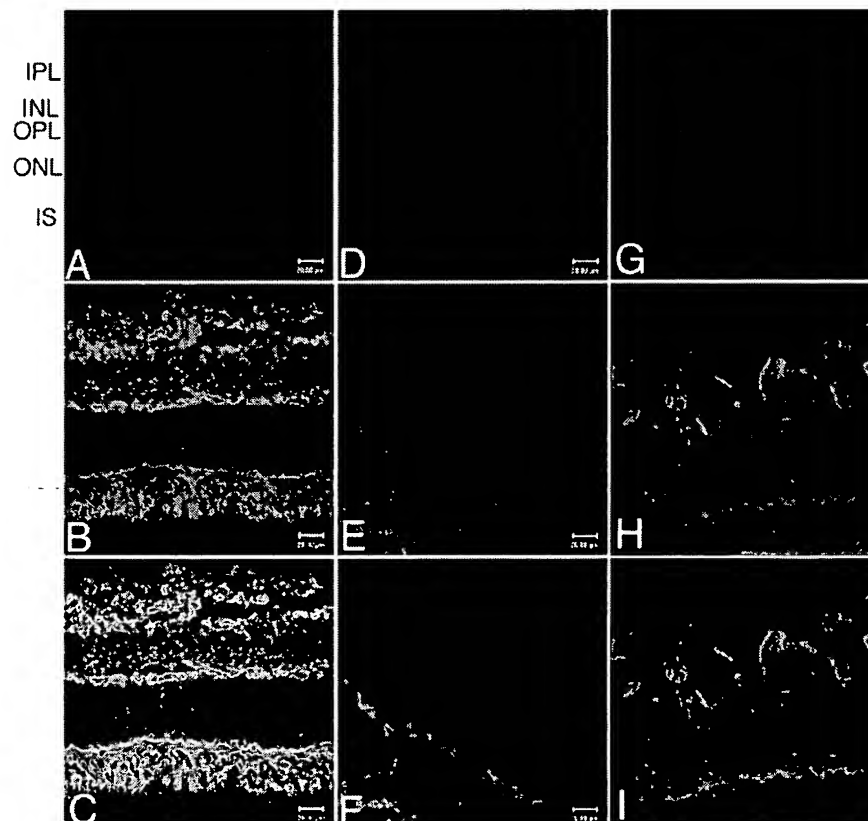


Figure 3. Confocal microscopy of the primate retina. Confocal microscopy of the retina from the gene-injected monkey (A-C, G-I) and from the control, un-injected monkey (D-F). Immunoreactive insulin receptor, stained with rhodamine-labeled secondary antibody, is shown in Panels A and D. Immunoreactive β -galactosidase, stained with the fluorescein-labeled secondary antibody, is shown in Panels B and E. Staining with the pre-immune mouse IgG or the rabbit IgG is shown in Panels G and H. The respective superimposed images are shown in panels C, F, and I. The yellow image in panel C shows co-localization of the β -galactosidase and human insulin receptor in the retina of the gene-injected monkey, including the photoreceptor cells. Scale bar: 20 μ m. Abbreviations in Panel A: IPL, inner plexiform layer; INL, inner nuclear layer; OPL, outer plexiform layer; ONL, outer nuclear layer; IS, inner segments. All specimens shown in Panels A-C were taken 48 h after the intravenous administration of clone 756, the pSV40- β -galactosidase plasmid in monkey 1 (see Methods).

promoter (Figure 4). Fourth, the expression of a reporter gene in the monkey eye declines following a single intravenous injection of plasmid and decays exponentially with a $t_{1/2}$ of 2.0 ± 0.1 days (Figure 2).

The nearly global expression of the exogenous gene delivered to the primate eye via the HIRMAb targeted PIL is shown by the β -galactosidase histochemistry (Figure 1B). There is gene expression in the retina, the cornea, the ciliary body, and the iris, and this global expression in the eye is observed with either the SV40 promoter (Figure 1B) or the bovine opsin promoter (Figure 4A). The sites of β -galactosidase gene expression parallel the sites of expression of the insulin receptor. The IR is expressed in the human eye in the epithelium and endothelium of the cornea, the lens capsular epithelium, and multiple cells within the retina including the inner segments, the ONL, the RPE, GCL, and Müller cells [11,12]. In addition to the widespread expression within the eye of the IR, this receptor is also useful for gene targeting to the nucleus. The IR serves to deliver ligand to the nucleus; prior work has shown that the IR delivers to the nucleus the majority of plasmid DNA taken up by the cell [19,21]. The mechanism of gene delivery to the eye is receptor-mediated, and not a non-specific breakdown of the BRB caused by the PIL injection. Prior work has shown that when the β -galactosidase expression plasmid is encapsulated in a PIL targeted with an isotype control antibody that does not recognize any receptor, then there is no β -galactosidase gene expression observed either in the eye [6], or in any other organ [7,8]. There is normal cellular architecture in the retina following PIL administration (Figure 1F).

The present studies target genes to the primate eye with the HIRMAb and demonstrate gene expression in the primate photoreceptor cells (Figures 1, 3 and 4). In contrast, prior work in mice targeted genes to the retina with the TfRMAb, and no expression of the β -galactosidase gene in the photoreceptor cells of the mouse retina was observed [6]. This observation correlates with the known tissue-specific expression of the TfR within the retina. The TfR is produced in the RPE, IS, OPL, INL, and GCL, but is minimally expressed in the cell bodies of the ONL [9,10]. The low expression of TfR in the ONL is consistent with the very low stores of either iron or ferritin in the ONL [10]. The TfR is expressed on the IS of the photoreceptor cells [6], but PIL entry into the photoreceptor cell at the IS apparently cannot support gene expression [6]. There may be minimal retrograde transport of the PIL from the IS to the cell body of the photoreceptor cell in the ONL. While the TfR is minimally expressed in the cell bodies of the ONL [10], the insulin receptor is expressed in this region of the retina in both humans and rats [11,12]. The present studies demonstrate that the ONL of the primate retina is also a site of abundant insulin receptor expression as shown by confocal microscopy (Figure 3A,D). In parallel with the expression of insulin receptor at the ONL, the β -galactosidase gene is expressed in the photoreceptor cells of the monkey (Figure 1E). The β -galactosidase gene expression is more prominent in the inner segments relative to the outer segments, although β -galactosi-

dase activity in the outer segments is visible by histochemistry (Figure 1E and Figure 4I).

The organ specificity of gene expression is a function of two variables: (a) the organ specificity of the targeting MAb attached to the PIL, and (b) the organ specificity of the pro-

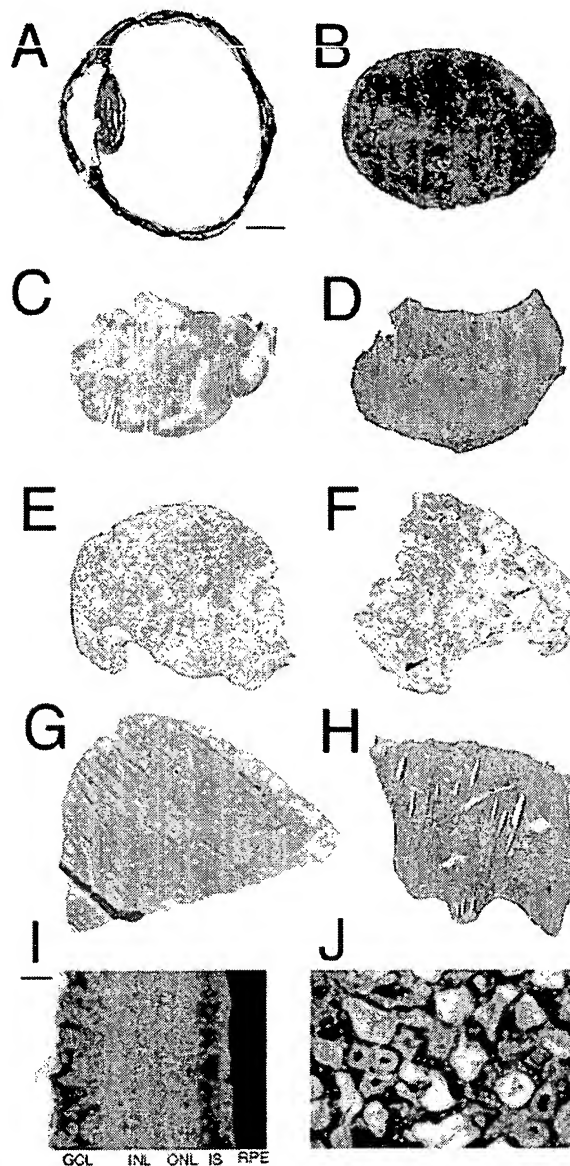


Figure 4. β -Galactosidase histochemistry of primate organs. Organ β -galactosidase histochemistry for Rhesus monkey eye (A and I), kidney (B and J), brain (C), heart (D), lung (E), omental fat (F), spleen (G), and liver (H). Skeletal muscle was also examined (not shown), and like the heart showed no histochemical reaction. The organs were removed from the animal sacrificed at 48 h after an intravenous injection of the opsin promoter-driven pLacF plasmid encapsulated in HIRMAb-targeted PILs, which corresponds to monkey 2 (see Methods). The magnification is the same for panels A-H; the magnification bar in Panel A represents 3 mm. The magnification is the same for panels I-J; the magnification bar in Panel I represents 12 μ m.

moter incorporated in the expression plasmid. In prior work in the rhesus monkey, the pSV- β -galactosidase expression plasmid was under the influence of the widely expressed SV40 promoter. Therefore, gene expression was observed in multiple organs of the primate including brain, liver, and spleen [14]. However, the present studies show that the expression of the β -galactosidase gene is restricted to the eye when the β -galactosidase expression plasmid is under the influence of the bovine opsin promoter (Figure 4). The pLacF β -galactosidase expression plasmid is driven by the 2 kb of the 5'-flanking sequence (FS) of the bovine opsin gene [16]. Under the restriction of the opsin promoter, there is no expression in brain, liver, spleen or other organs following the intravenous administration of HIRMAb-targeted PILs in the rhesus monkey (Figure 4). This observation in the primate of organ-specific gene expression with organ-specific promoters parallels prior work in the mouse and rat [7,8]. Genes driven by the SV40 promoter and encapsulated in TfRMAb-targeted PILs are expressed in multiple TfR-rich peripheral organs including brain, liver, and spleen [7]. However, a different pattern of gene expression is observed if the exogenous gene is driven by a brain-specific promoter such as the 2 kb of the 5'-FS of the glial fibrillary acidic protein (GFAP) gene. If the SV40 promoter is replaced with the GFAP promoter, then gene expression in the brain and eye is preserved [6,7], whereas trans-gene expression in peripheral tissues such as liver or spleen is eliminated [7]. The finding of eye-specific gene expression in the monkey with the pLacF plasmid (Figure 4) parallels prior work with transgenic mice produced with the pLacF gene. Gene expression is confined to the eye in either the germ cell transgenic mouse [16], or the adult rhesus monkey made acutely transgenic with the PIL gene transfer technology (Figure 4).

The bovine opsin promoter restricts transgene expression to the eye, but does not restrict gene expression to the photoreceptor cells in the monkey (Figure 4A). A similar finding was made in transgenic mice produced with the pLacF construct, as these transgenic mice expressed the β -galactosidase gene in the photoreceptor cells, as well as the iris and ciliary body, and the brain [16]. One possible explanation for the diffuse expression of the reporter gene in the eye is selective expression in the photoreceptor cells followed by secretion and diffusion to other parts of the eye. However, this explanation appears unlikely since prior work has shown selective localization of the β -galactosidase enzyme in retinal structures without secretion and diffusion to other parts of the eye [6]. A more likely explanation for the broad spectrum of opsin promoter driven gene expression in the eye is that the other ocular structures are embryologically related to the neural retina. Transfection of iris or ciliary body with the photoreceptor cell specific *Crx* homeobox gene results in the synthesis of rhodopsin in these extra-retinal ocular structures [22]. The restriction of gene expression to the photoreceptor cells may require regulatory gene elements in addition to the 5'-FS of the gene. In the case of brain GFAP gene expression, the 5'-FS confers brain specificity, but does not restrict gene expression within the brain to astrocytes. Astrocyte specific gene expression re-

quires the coordinate interaction of gene elements in both the 5'-FS and the 3'-FS of the GFAP gene [23,24].

The luciferase gene expression decays exponentially with a half-time of 2.0 ± 0.1 days, and the peak luciferase expression, $A(0)$ is 19.3 ± 0.3 pg/mg (Figure 2). The peak luciferase gene expression is 50-fold higher than the $A(0)$ in rodent brain [14,20], and the rodent $A(0)$ is shown by the horizontal line in Figure 2. The higher peak level of gene expression in the primate, relative to the rodent, is attributed to the much higher activity of the HIRMAb as a targeting ligand, as compared to the TfRMAb [21]. The HIRMAb is used to target PILs to primate brain [14], whereas the TfRMAb is used to target PILs to rodent brain [6-8]. The level of gene expression achieved with the TfRMAb is sufficient to cause the desired pharmacological effect. The intravenous administration of TfRMAb-targeted PILs produces a 100% increase in survival time in mice with experimental brain cancer treated with EGFR antisense gene therapy [20], or a 100% normalization of striatal enzyme activity in rats with experimental Parkinsonism treated with tyrosine hydroxylase gene therapy [25]. Therefore, the mouse $A(0)$ shown in Figure 2 represents levels of gene expression that yield therapeutic effects. Owing to the very high initial level of gene expression in the primate with the HIRMAb, the level of retinal gene expression is still in the therapeutic range for more than 2 weeks after a single intravenous injection (Figure 2). Therefore, primates may require repeat administration of gene therapy at intervals of 3-4 weeks.

In summary, these studies show it is possible to achieve global expression of an exogenous gene in photoreceptor cells of the primate retina following a non-invasive, intravenous administration of a non-viral form of the gene. The plasmid replicates episomally and gene expression is reversible (Figure 2). Southern blotting shows no integration of the plasmid DNA into host chromosomal DNA following PIL gene delivery [8]. Similarly, plasmid DNA delivered to organs in vivo with the hydrodynamics injection method is not integrated in the host chromosome [26]. Owing to the transient nature of plasmid-based gene expression, it is necessary to administer the PIL formulation at regular intervals to sustain a therapeutic effect, and this has been done for the treatment of mice with brain cancer [20]. The chronic weekly intravenous administration of PIL encapsulated genes causes no change in organ histology, serum chemistry, or body weights, and causes no inflammation in the central nervous system [27]. Repeat intravenous administration of the PIL formulation is possible, because the only antigenic component of the liposome is the targeting ligand. The immunogenicity of the targeting MAb can be reduced or eliminated with genetic engineering and "humanization" of the original murine MAb. The murine 83-14 HIRMAb has been genetically engineered to produce the chimeric form of this antibody, and the chimeric HIRMAb has an identical affinity for the HIR as the original murine antibody [28]. The chimeric HIRMAb rapidly crosses the primate BBB in vivo [28], and the present studies provide evidence that the HIRMAb also crosses the primate BRB and distributes to the retina and to multiple ocular structures.

ACKNOWLEDGEMENTS

Dafang Wu, Hwa Jeong Lee, Chunni Zhu, Toyofumi Suzuki, and Yufeng Zhang of the UCLA Department of Medicine provided assistance in the primate experiments. This work was supported by grants from the University of California, Davis/ Medical Investigation of Neurodevelopmental Disorders Institute Research Program, and the Neurotoxin Exposure Treatment Research Program of the U. S. Department of Defense. Felix Schlachetzki was supported by a grant from the Ernst Schering Research Foundation (Berlin, Germany). This work was presented in part at the Annual Meeting of the Association for Research in Vision and Ophthalmology (ARVO-2003), Fort Lauderdale, FL, May, 2003.

REFERENCES

- Hauswirth WW, Beaufre L. Ocular gene therapy: quo vadis? *Invest Ophthalmol Vis Sci* 2000; 41:2821-6.
- Dejneka NS, Bennett J. Gene therapy and retinitis pigmentosa: advances and future challenges. *Bioessays* 2001; 23:662-8.
- Hauswirth WW, McInnes RR. Retinal gene therapy 1998: summary of a workshop. *Mol Vis* 1998; 4:11.
- Bennett J, Maguire AM, Cideciyan AV, Schnell M, Glover E, Anand V, Aleman TS, Chirmule N, Gupta AR, Huang Y, Gao GP, Nyberg WC, Tazelaar J, Hughes J, Wilson JM, Jacobson SG. Stable transgene expression in rod photoreceptors after recombinant adeno-associated virus-mediated gene transfer to monkey retina. *Proc Natl Acad Sci U S A* 1999; 96:9920-5.
- Flannery JG, Zolotukhin S, Vaquero MI, LaVail MM, Muzyczka N, Hauswirth WW. Efficient photoreceptor-targeted gene expression in vivo by recombinant adeno-associated virus. *Proc Natl Acad Sci U S A* 1997; 94:6916-21.
- Zhu C, Zhang Y, Pardridge WM. Widespread expression of an exogenous gene in the eye after intravenous administration. *Invest Ophthalmol Vis Sci* 2002; 43:3075-80.
- Shi N, Zhang Y, Zhu C, Boado RJ, Pardridge WM. Brain-specific expression of an exogenous gene after i.v. administration. *Proc Natl Acad Sci U S A* 2001; 98:12754-9.
- Shi N, Boado RJ, Pardridge WM. Receptor-mediated gene targeting to tissues in vivo following intravenous administration of pegylated immunoliposomes. *Pharm Res* 2001; 18:1091-5.
- Davis AA, Hunt RC. Transferrin is made and bound by photoreceptor cells. *J Cell Physiol* 1993; 156:280-5.
- Yefimova MG, Jeanny JC, Guillonneau X, Keller N, Nguyen-Legros J, Sergeant C, Guillou F, Courtois Y. Iron, ferritin, transferrin, and transferrin receptor in the adult rat retina. *Invest Ophthalmol Vis Sci* 2000; 41:2343-51.
- Naeser P. Insulin receptors in human ocular tissues. Immunohistochemical demonstration in normal and diabetic eyes. *Ups J Med Sci* 1997; 102:35-40.
- Gosbell AD, Favilla I, Baxter KM, Jablonski P. Insulin receptor and insulin receptor substrate-1 in rat retinae [published erratum in: *Clin Experiment Ophthalmol* 2000; 28:443]. *Clin Experiment Ophthalmol* 2000; 28:212-5.
- Pardridge WM, Kang YS, Buciak JL, Yang J. Human insulin receptor monoclonal antibody undergoes high affinity binding to human brain capillaries in vitro and rapid transcytosis through the blood-brain barrier in vivo in the primate. *Pharm Res* 1995; 12:807-16.
- Zhang Y, Schlachetzki F, Pardridge WM. Global non-viral gene transfer to the primate brain following intravenous administration. *Mol Ther* 2003; 7:11-8.
- Ford SM. Systematics of the new world monkeys. In: Erwin J, Swindler DR, editors. *Comparative primate biology I: Systematics, evolution, and anatomy*. New York: Alan R. Liss; 1986. p. 23-135.
- Zack DJ, Bennett J, Wang Y, Davenport C, Klaunberg B, Gearhart J, Nathans J. Unusual topography of bovine rhodopsin promoter-lacZ fusion gene expression in transgenic mouse retinas. *Neuron* 1991; 6:187-99.
- Boado RJ, Pardridge WM. Ten nucleotide cis element in the 3'-untranslated region of the GLUT1 glucose transporter mRNA increases gene expression via mRNA stabilization. *Brain Res Mol Brain Res* 1998; 59:109-13.
- Shi N, Pardridge WM. Noninvasive gene targeting to the brain. *Proc Natl Acad Sci U S A* 2000; 97:7567-72.
- Zhang Y, Jeong Lee H, Boado RJ, Pardridge WM. Receptor-mediated delivery of an antisense gene to human brain cancer cells. *J Gene Med* 2002; 4:183-94.
- Zhang Y, Zhu C, Pardridge WM. Antisense gene therapy of brain cancer with an artificial virus gene delivery system. *Mol Ther* 2002; 6:67-72.
- Zhang Y, Boado RJ, Pardridge WM. Marked enhancement in gene expression by targeting the human insulin receptor. *J Gene Med* 2003; 5:157-63.
- Haruta M, Kosaka M, Kanegae Y, Saito I, Inoue T, Kageyama R, Nishida A, Honda Y, Takahashi M. Induction of photoreceptor-specific phenotypes in adult mammalian iris tissue. *Nat Neurosci* 2001; 4:1163-4.
- Kaneko R, Sueoka N. Tissue-specific versus cell type-specific expression of the glial fibrillary acidic protein. *Proc Natl Acad Sci U S A* 1993; 90:4698-702.
- Galou M, Pournin S, Ensergueix D, Ridet JL, Tchelinguerian JL, Lossouarn L, Privat A, Babinet C, Dupouey P. Normal and pathological expression of GFAP promoter elements in transgenic mice. *Glia* 1994; 12:281-93.
- Zhang Y, Calon F, Zhu C, Boado RJ, Pardridge WM. Intravenous nonviral gene therapy causes normalization of striatal tyrosine hydroxylase and reversal of motor impairment in experimental parkinsonism. *Hum Gene Ther* 2003; 14:1-12.
- Stoll SM, Scimienti CR, Baba EJ, Meuse L, Kay MA, Calos MP. Epstein-Barr virus/human vector provides high-level long-term expression of alpha1-antitrypsin in mice. *Mol Ther* 2001; 4:122-9.
- Zhang YF, Boado RJ, Pardridge WM. Absence of toxicity of chronic weekly intravenous gene therapy with pegylated immunoliposomes. *Pharm Res*. In press 2003.
- Coloma MJ, Lee HJ, Kurihara A, Landaw EM, Boado RJ, Morrison SL, Pardridge WM. Transport across the primate blood-brain barrier of a genetically engineered chimeric monoclonal antibody to the human insulin receptor. *Pharm Res* 2000; 17:266-74.

Global Non-Viral Gene Transfer to the Primate Brain Following Intravenous Administration

Yun Zhang, Felix Schiachetzki,* and William M. Pardridge†

Dept. of Medicine, UCLA School of Medicine, Los Angeles, CA 90024

*Present address: Dept. of Neurology, University of Regensburg, Regensburg, Germany

†To whom correspondence should be addressed: Dr. William M. Pardridge, UCLA Warren Hall 13-164, 900 Veteran Avenue, Los Angeles, CA 90024. Phone: (310) 825-8858. Fax: (310) 206-5163. E-mail: Wpardridge@mednet.ucla.edu.

Expression plasmids encoding either luciferase or β -galactosidase were encapsulated in the interior of an "artificial virus" comprised of an 85 nm pegylated immunoliposome, which was targeted to the rhesus monkey brain *in vivo* with a monoclonal antibody (MAB) to the human insulin receptor (HIR). The HIRMAb enables the liposome carrying the exogenous gene to undergo transcytosis across the blood-brain barrier and endocytosis across the neuronal plasma membrane following intravenous injection. The level of luciferase gene expression in the brain was 50-fold higher in the rhesus monkey as compared to the rat. Widespread neuronal expression of the β -galactosidase gene in primate brain was demonstrated by both histochemistry and confocal microscopy. This approach makes feasible reversible adult transgenics in 24 hours.

Key Words: gene therapy, insulin receptor, liposomes, non-viral gene transfer, blood-brain barrier

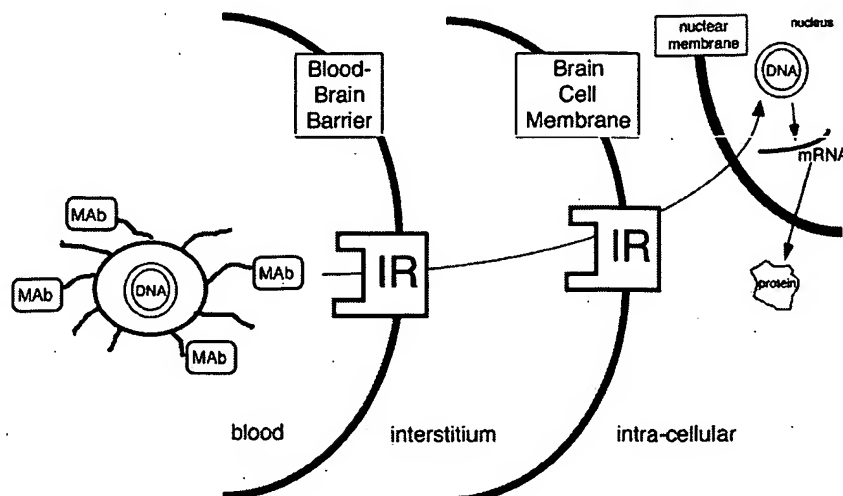
INTRODUCTION

Many diseases of the central nervous system (CNS) are candidates for treatment by gene therapy [1], and for most of these disorders, it is necessary to achieve widespread expression of the exogenous gene throughout the entire CNS. Global, neuronal gene expression in the brain is possible with trans-vascular delivery of the gene following intravenous administration. The cerebral microvasculature, which forms the blood-brain barrier (BBB) *in vivo*, is a very dense network, comprising approximately 400 miles in the human brain. Since virtually every neuron in the brain is perfused by its own blood vessel, the delivery of the gene across the BBB targets the gene to the "doorstep" of every neuron in the brain. Subsequent to transport across the BBB, it is also necessary for the exogenous gene to undergo uptake into brain cells via endocytosis across the brain cell plasma membrane (BCM).

The widespread expression of exogenous genes in rodent brain has been recently demonstrated using non-viral gene transfer technology and pegylated immunoliposomes (PIL). In this approach, the non-viral plasmid DNA is encapsulated in the interior of an 85 nm liposome [2]. The liposome has the same size as many viral vectors, and like a viral vector, the liposome houses the plasmid DNA in the interior of a nanocontainer to prevent degradation of the DNA by endonucleases [3], which are ubiqu-

itous *in vivo*. The blood residence time of the liposome is prolonged by conjugating several thousand strands of 2000 Dalton polyethylene glycol (PEG) to the surface of the liposome [2]. The PEG strands reduce adsorption of serum proteins to the liposome surface, which minimizes uptake of the nanocontainer by the cells lining the reticulo-endothelial system *in vivo* [4]. The pegylated liposome can be targeted to brain cells by tethering to the tips of 1–2% of the PEG strands a receptor-specific targeting ligand, such as a peptidomimetic monoclonal antibody (MAB). The MAB attaches to a receptor expressed on both the BBB and the BCM to enable sequential receptor-mediated transcytosis across the BBB and receptor-mediated endocytosis across the BCM (Figure 1). The targeting MAB acts as molecular Trojan horse to ferry the PIL across biological barriers in the brain via endogenous transport systems [5]. The targeting MAB's are species-specific. Endogenous genes are delivered to mouse brain with the rat 8D3 MAB to the mouse transferrin receptor (TfR) [6], and to rat brain with the murine OX26 MAB to the rat TfR [2,7]. In addition to the targeting specificity of the MAB, tissue-specific gene expression is influenced by the gene promoter. Exogenous genes driven by the SV40 promoter, and targeted to rodent tissues with a TfRMAb are expressed in brain [6,7] or retina [8], as well as peripheral tissues that also express the TfR. However, the SV40 promoter is widely expressed *in vivo* [9]. Replacement of the

FIG. 1. The plasmid DNA is encapsulated in the interior of an 85 nm pegylated immunoliposome (PIL). The surface of the liposome is conjugated with several thousand strands of 2000 Dalton polyethyleneglycol (PEG), and the tips of 1–2% of the PEG strands is tethered with a targeting ligand, such as a insulin receptor (IR)-specific monoclonal antibody (MAb). The MAb-conjugated PIL undergoes receptor-mediated transcytosis across the blood-brain barrier and receptor-mediated endocytosis across the brain cell plasma membrane and enters the nuclear compartment [12].



SV40 promoter with a brain specific promoter eliminates exogenous gene expression in peripheral Tfr-rich organs following intravenous administration [6]. Successful gene therapy of the brain is feasible with intravenous administration of the gene formulated with the PIL gene targeting technology. The survival time is increased 100% in mice with intra-cranial human brain cancer following weekly injections of the targeted PIL carrying plasmid DNA that expresses antisense mRNA to the human epidermal growth factor [10].

The 8D3 or OX26 anti-TfRMAB's are specific for mice and rats, respectively, and are not active in primates or humans [5]. Drug or gene targeting to the brain of Old World primates such as the rhesus monkey is possible with the murine 83-14 MAb to the human insulin receptor (HIR). The rate of transport of the HIRMAb across the primate BBB is nearly 10-fold greater than the rate of transport of an anti-human TfRMAB across the primate BBB *in vivo* [5]. The high activity of the HIRMAb was demonstrated recently with respect to gene targeting to cultured human or rat glioma cells. In these studies, a luciferase expression plasmid was targeted to human glial cells with HIRMAb-conjugated PIL and to rat glial cells with TfRMAB-conjugated PIL [11]. The level of gene expression was > 10-fold greater in human cells targeted with the HIRMAb as compared to rat cells targeted with the TfRMAB.

The purpose of the present study is to evaluate the targeting of exogenous genes to primate brain *in vivo* using the PIL gene targeting technology and the HIRMAb as the targeting ligand. This MAb acts as a molecular Trojan horse to ferry the liposome across the BBB and the BCM in the primate brain *in vivo* (Figure 1). Expression plasmids driven by the SV40 promoter and encoding luciferase or bacterial β -galactosidase were encapsulated in the HIRMAb-PIL and injected intravenously into the

adult Rhesus monkey. The animal was sacrificed 48 hours later and brain expression of the luciferase and β -galactosidase genes in the primate brain was measured. Since luciferase measurements are quantitative, the level of luciferase gene expression in the primate brain targeted with the HIRMAb-PIL was compared to luciferase gene expression in rat brain targeted with the TfRMAB-PIL.

RESULTS

The level of luciferase gene expression in hemispheric gray matter in the primate is high and approximately 10 pg luciferase per mg of brain protein (Figure 2A). The level of luciferase gene expression in the Rhesus monkey brain targeted with the HIRMAb-PIL is nearly 50-fold greater than the level of luciferase gene expression in rat brain targeted with the TfRMAB-PIL (Figure 2B). The luciferase gene, driven by the SV40 promoter, is also expressed in insulin receptor-rich or Tfr-rich organs in the monkey and rat, respectively, such as liver, spleen, and lung (Figure 2) with minimal gene expression in kidney or heart in these species (Figure 2). Luciferase gene expression in primate skeletal muscle was also low, 0.13 ± 0.02 pg luciferase per mg protein. Luciferase gene expression in hemispheric white matter of the primate brain was 3.2 ± 0.3 pg luciferase per mg protein, which is 3-fold lower than luciferase gene expression in gray matter of primate brain (Figure 2A). The level of luciferase gene expression in primate cerebellar gray matter and white matter was 7.0 ± 1.6 and 4.0 ± 0.4 pg luciferase per mg protein, respectively.

The expression of the β -galactosidase gene in primate brain was examined with both histochemistry and confocal microscopy. The histochemistry of frozen sections of primate brain removed 48 hours after the single intravenous injection of the gene shows diffuse and wide-

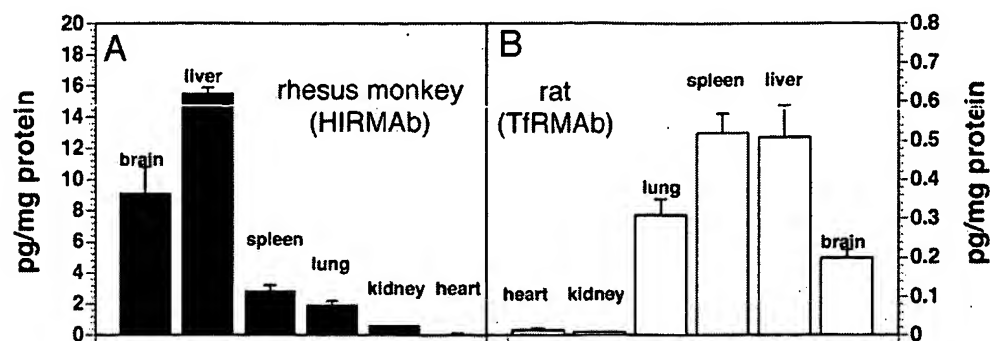


FIG. 2. Luciferase gene expression in the brain and other organs of the adult rhesus monkey (A) and adult rat (B) measured at 48 hours after a single intravenous injection of the PIL carrying the plasmid DNA. Data are mean \pm SE. The plasmid DNA encoding the luciferase gene used in either species is clone 790, which is driven by the SV40 promoter [11,12]. The PIL carrying the DNA was targeted to primate organs with the 83-14 HIRMAb and to rat organs with the OX26 TfRMAb.

spread expression of β -galactosidase in primate brain (Figure 3A, 3C). In contrast, β -galactosidase histochemistry of control or un-injected primate brain shows no β -galactosidase activity (Figure 3B). The gray and white matter

tracts of the brain are delineated in the histochemistry, consistent with a greater level of β -galactosidase gene expression in gray matter relative to white matter. Light micrographs of the primate brain β -galactosidase histo-

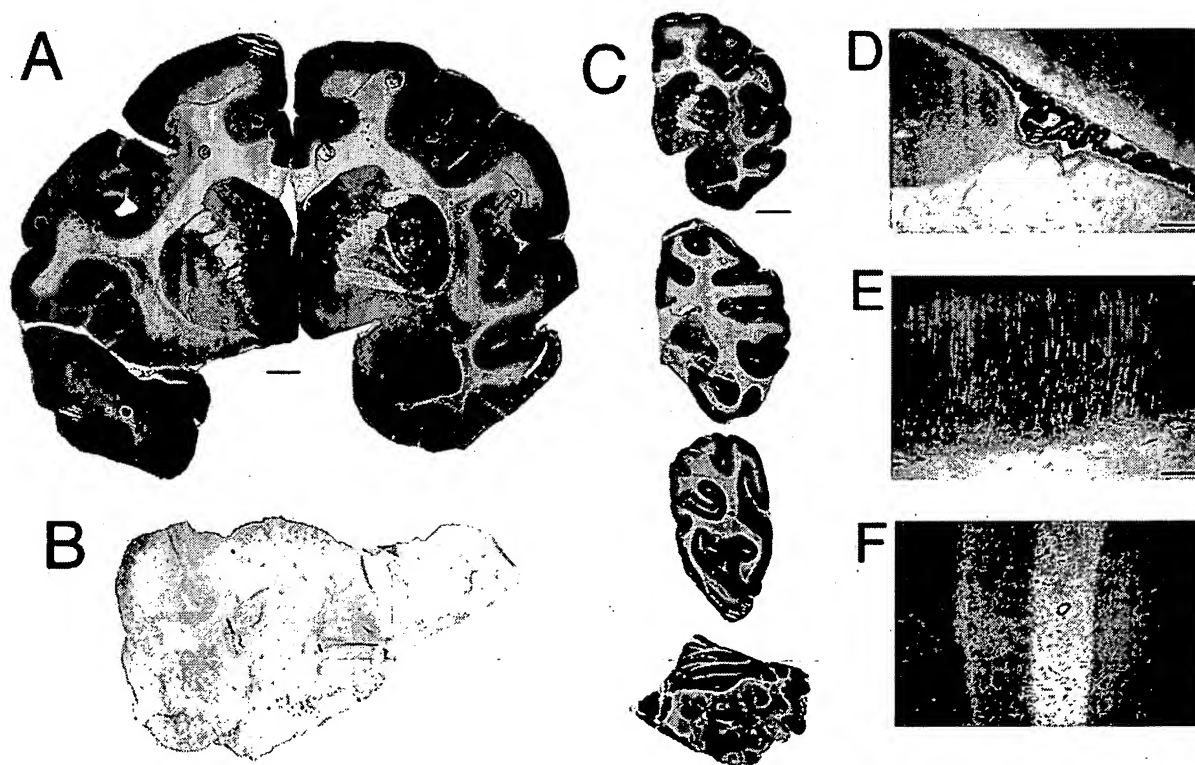
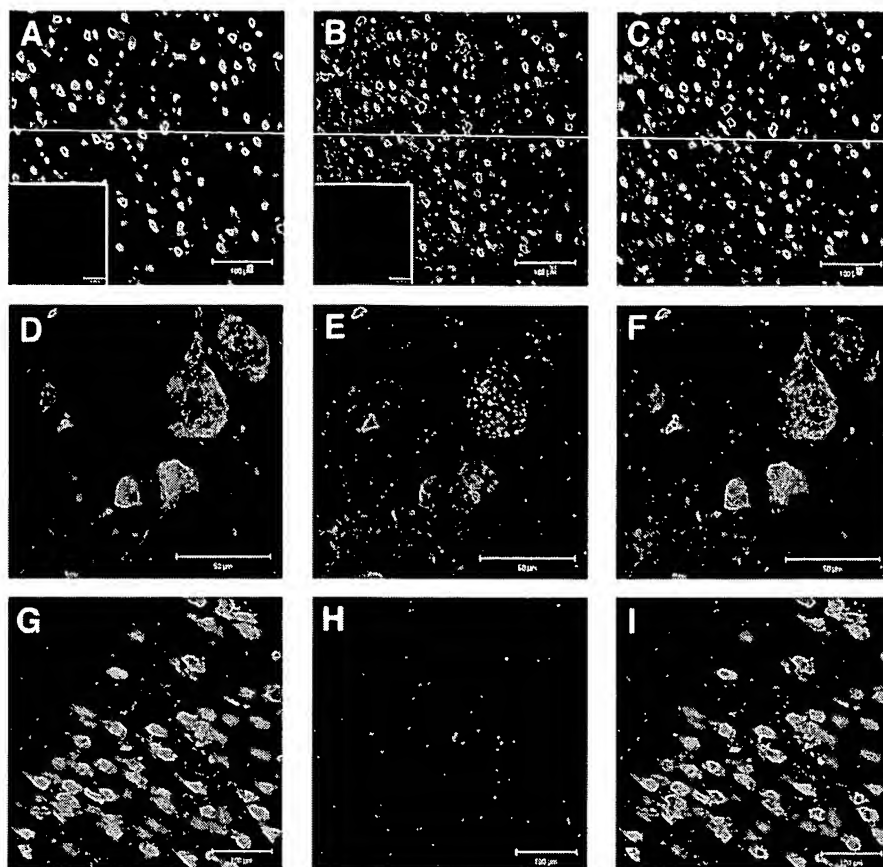


FIG. 3. β -Galactosidase histochemistry of brain removed from either the HIRMAb-PIL injected rhesus monkey (A, C, D, E, and F) or the control, uninjected rhesus monkey (B). The plasmid DNA encapsulated in the PIL is the pSV- β -galactosidase expression plasmid driven by the SV40 promoter. Panel A is a reconstruction of the 2 halves of a coronal section of the forebrain. Panel C shows half-coronal sections through the primate cerebrum and a full coronal section through the cerebellum; the sections from top to bottom are taken from the rostral to caudal parts of brain. Panels D, E, and F are light micrographs of choroid plexus, occipital cortex, and cerebellum, respectively. All specimens are β -galactosidase histochemistry without counter-staining. The magnification in panels A and B is the same and the magnification bar in panel A is 3 mm; the magnification bar in panel C is 8 mm; the magnification bars in panels D-F are 155 μ m.

FIG. 4. Confocal immunofluorescent imaging of β -galactosidase expression in neurons of the gene injected (A–F) and the uninjected control rhesus monkey brain (G–I). Immunoreactive neuronal nuclei (NeuN) are stained with a mouse anti-neuN primary antibody and a fluorescein-labeled secondary antibody, as shown in panels A, D, and G. Immunoreactive β -galactosidase is stained with a rabbit anti-bacterial β -galactosidase primary antibody and a rhodamine-labeled secondary antibody, as shown in panels B, E, and H. The respective superimposed yellow images reveal co-localization of the neuN and β -galactosidase in neurons (C, F). Primate brain was also immunolabeled with the isotype control mouse IgG₁ or rabbit IgG, which showed no specific staining as shown in the insets of panels A and B, respectively. Scale bars in panels A–C and G–I are 100 μ m; scale bars in panels D–F (oil immersion) are 50 μ m. Neurons from the primate supplementary motor cortex are shown in panels A–C, and larger neurons from the primate primary motor cortex are shown in panels G–I.



chemistry are shown in Panels D–F of Figure 3. The choroid plexus bordered by gray matter and white matter is shown in Figure 3D. Gene expression is visible within the choroid plexus epithelium, the ependymal lining of the ventricle, and the capillary endothelium of adjacent white matter (Figure 3D). The β -galactosidase gene expression within the neurons of the occipital cortex is visible and reveals the columnar organization of the occipital cortex of the primate brain (Figure 3E). Dense gene expression in the molecular and granular layers of the cerebellum, as well as the intermediate Purkinje cells, are visible in Figure 3F. Owing to the reduced level of gene expression in the cerebellar white matter, the β -galactosidase enzyme activity is detected in the capillary endothelium within the white matter of the cerebellum (Figure 3F).

Confocal microscopy confirmed neuronal expression of the β -galactosidase gene, as there is overlap of immunoreactive neuN and β -galactosidase in primate brain (Figure 4). Immunostaining of neuN is shown in Figure 4A and 4D in the gene-injected monkey and in Figure 4G for the un-injected control monkey. Immunoreactive β -galactosidase is detected in the brain of the gene injected

monkey (Figure 4B and 4E), but not in the brain of the un-injected control monkey (Figure 4H). The overlap of the immunoreactive neuN and β -galactosidase is shown in Figure 4C and 4F. Control staining with the either mouse IgG₁ or rabbit IgG were negative as shown in the insets of Figures 4A and 4B, respectively.

Histochemistry of primate peripheral organs demonstrated tissue specific expression of the β -galactosidase gene (Figure 5), similar to luciferase gene expression (Figure 2B). Diffuse trans-hepatic gene expression was observed in primate liver (Figure 5A) and light microscopy shows the gene is expressed in hepatocytes (Figure 5B). Diffuse gene expression is observed in spleen (Figure 5C), and light microscopy shows a higher level of gene expression in red pulp as compared to white pulp (Figure 5D). No detectable β -galactosidase gene expression is observed in heart, skeletal muscle, or fat in the primate (Figure 5E–J).

DISCUSSION

The results of these studies are consistent with the following conclusions. First, the PIL gene targeting technology

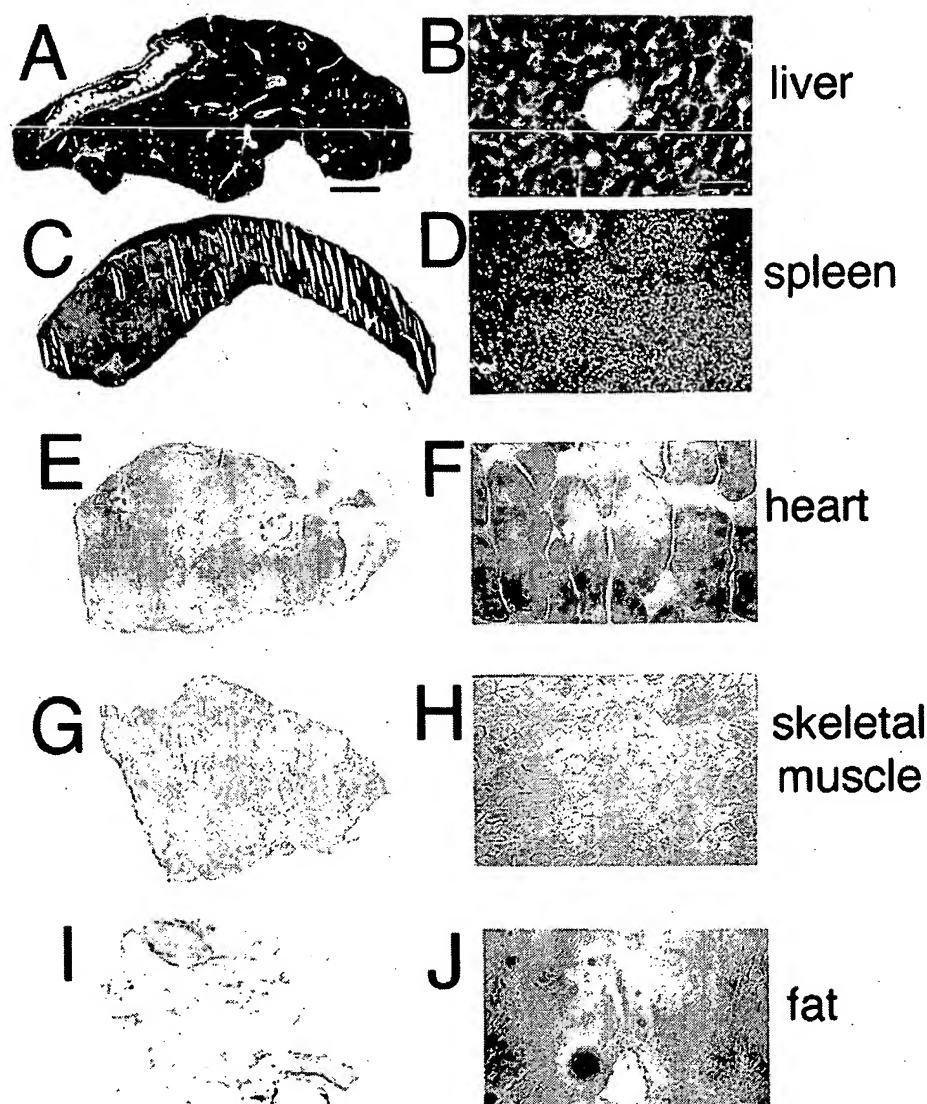


FIG. 5. β -Galactosidase histochemistry of rhesus monkey organs removed 48 hours after intravenous injection of the pSV- β -galactosidase expression plasmid encapsulated in the HIRMAb-PIL, including liver (A,B), spleen (C, D), heart (E, F), biceps skeletal muscle (G, H), and omental fat (I, J). Magnification in panels A, C, E, G, and I is the same and the magnification bar in panel A is 5 mm. Magnification in panels B, D, F, H, and J is the same and the magnification bar in panel B is 65 μ m. The β -galactosidase gene is diffusely expressed in primate liver and spleen, whereas there is no detectable gene expression in heart, skeletal muscle, or fat. No sections are counter-stained.

enables diffuse, widespread expression of exogenous genes in the primate brain (Figure 3). Second, the level of gene expression in the monkey brain targeted with the HIRMAb-PIL is 50-fold greater than gene expression in the rat brain targeted with the TfrMAb-PIL (Figure 2). Third, the exogenous gene is expressed in neurons in the primate brain as shown by co-labeling primate brain sections with antibodies against the neuN neuronal specific antigen and bacterial β -galactosidase (Figure 4). Fourth, the exogenous gene is expressed in primate peripheral tissues expressing the insulin receptor, which have a permeable microvasculature, such as liver or spleen, but not in peripheral tissues which are perfused by a microvasculature with a continuous endothelium, such as heart, skeletal muscle, kidney, or fat (Figures 2, 5).

The PIL is targeted to brain of rats or monkeys because both the brain cell membrane, and the brain microvascular endothelium, which forms the BBB *in vivo*, are enriched in either insulin receptor (IR) or Tfr [5]. However, the extent to which a given gene is expressed is a function of the activity of the targeting antibody and the targeted receptor. The present studies show that the level of gene expression in the primate brain targeted with the HIRMAb-PIL is nearly 50-fold greater than the level of gene expression in the rat brain targeted with the TfrMAb-PIL (Figure 2). This finding parallels recent observations that the level of gene expression in cultured human glial cells targeted with the HIRMAb-PIL is >10-fold greater than the gene expression in cultured rat glial cells targeted with the TfrMAb-PIL [11]. The higher levels of

gene expression following targeting of the insulin receptor may be due to the property of this receptor to target the nuclear compartment [11]. Confocal microscopy of cultured human glial cells shows the HIRMAb-PIL rapidly delivers fluoresceinated plasmid DNA to the nucleus of the cell [12].

The delivery of the exogenous gene to the primate brain is global (Figure 3). Gene expression is higher in gray matter as compared to white matter, based on the β -galactosidase histochemistry (Figure 3). The level of luciferase activity in gray matter is 2–3-fold higher than in primate white matter (Results), and these findings are consistent with the approximate 3-fold greater vascular density of gray matter relative to white matter [13]. Within the gray matter regions of brain, the majority of the neurons within a field express the exogenous gene, as shown by the microscopy of either the occipital cortex (Figure 3E) or the cerebellar cortex (Figure 3F). The PIL gene targeting technology enables the global transduction of the majority of neurons throughout the entire brain, and this is possible because the gene is delivered to brain via the trans-vascular route.

In addition to brain, the PIL-targeted gene is expressed in liver and spleen (Figure 5). These organs are perfused by a leaky sinusoidal vasculature, which allows rapid trans-vascular egress of the PIL into the organ interstitium, and the parenchymal cells in liver or spleen are enriched in IR or TfR [7]. Despite the high expression of the IR on parenchymal cells, gene expression in heart, skeletal muscle, fat, or kidney is minimal (Figures 2, 5), because these organs are perfused by capillaries with continuous endothelium. Unlike the brain, where the IR is expressed on the microvascular endothelial barrier (Figure 1), the IR is not expressed on the endothelium in peripheral organs. The PIL cannot readily enter the extravascular space of these peripheral organs in the absence of endothelial transport mechanisms that enable the receptor-mediated transcytosis across the microvascular endothelial barrier. A similar transport restriction across myocardial capillaries occurs for adenoviral vectors following the intra-coronary infusion of the virus [14]. Both adenovirus and the PIL are about 85 nm in diameter, which is too large to freely traverse the small pore system of the endothelium of continuous capillaries.

Gene expression in primate lung is moderate and less than brain, liver, or spleen (Figure 2A). The modest lung expression of the gene illustrates the marked differences between the PIL gene transfer technology and conventional non-viral gene transfer approaches, which use DNA/cationic liposomes. Cationic liposomes, even pegylated cationic liposomes, are taken up by lung at rates log orders greater than liver or spleen [15]. Cationic liposome/DNA complexes aggregate in physiological saline [16], and these aggregates deposit in the first vascular bed encountered after an intravenous injection, which is the pulmonary circulation. In contrast, the PIL does not ag-

gregate in saline or serum and has prolonged blood residence times [2].

The expression of the exogenous gene in primate peripheral tissues such as liver or spleen is observed because either the luciferase or the β -galactosidase expression plasmids used in these studies is under the influence of the SV40 promoter [17]. If the widely expressed SV40 promoter is replaced with a brain specific promoter such as the 5'-flanking sequence from the human glial fibrillary acidic protein (GFAP) gene, then transgene expression is maintained in brain, but is eliminated in peripheral tissues such as liver or spleen [6]. In addition to the promoter, the targeting MAb conjugated to the PIL restricts the specificity of tissue gene expression. If the targeting MAb is replaced with an isotype IgG control antibody, then there is no gene expression in any organ in rats or mice following intravenous administration of the gene encapsulated in the PIL [2,6,7].

The levels of luciferase gene expression in primate brain, liver, or spleen following an intravenous injection of the HIR-PIL (Figure 2) are comparable to the levels of luciferase gene expression in mice following the intravenous injection of HIV-1-based lentivirus encoding the luciferase gene. The luciferase activity in liver and spleen of mice subjected to multiple intravenous infusions with 10^8 viral units is 2000 and 600 pg luciferase per gram tissue, and there is no luciferase expression in brain [18]. Peripheral organs contain 180 mg protein per gram tissue. Therefore, the luciferase activity in liver and spleen of the lentivirus-injected mice is 11 and 3 pg luciferase per mg protein, and these values are comparable to the luciferase levels generated in primate brain, liver, or spleen with non-viral gene transfer of a luciferase expression plasmid (Figure 2).

In summary, these studies show that it is possible to achieve widespread expression of exogenous genes throughout the primate brain following a single intravenous injection of a non-viral formulation of the gene. The PIL gene targeting technology enables adult transgenics of the brain within 24 hours. The only other way to achieve an experimental result such as that shown in Figure 3 is with the engineering and breeding of transgenic primates producing bacterial β -galactosidase within the brain. The PIL acts as an artificial virus carrying exogenous genes across the biological barriers in brain (Figure 1). The component of the PIL that is potentially immunogenic is the targeting antibody. However, the immunogenicity of the antibody can be reduced or eliminated with genetic engineering and the production of "humanized" monoclonal antibodies. The chimeric form of the murine 83-14 HIRMAb has been produced, and has equal affinity for the HIR as the original murine antibody [19]. Therefore, the technology is now available to deliver therapeutic genes to the human brain with an intravenous administration without the use of viral vectors. The plasmid DNA is episomally expressed in cells and must be given on repeat

occasions depending on the persistence of the transgene. In rats, the gene expression in brain decreases approximately 50% at 6 days following a single intravenous administration of a PIL encapsulated plasmid expressing either β -galactosidase [7] or tyrosine hydroxylase [20]. In mice with intra-cranial experimental brain cancer, therapeutic results were achieved with intravenous administrations of the gene medicine given once per week [10]. In rats with experimental Parkinson's disease, striatal tyrosine hydroxylase is normalized at 3–6 days following the single intravenous injection of the gene, whereas gene expression is minimal at 9 days after administration [20]. Therefore, the persistence of the plasmid expression *in vivo* in the brain is sufficient to allow for the intended pharmacological response, which is reversible owing to the episomal nature of plasmid gene expression [21]. The persistence of plasmid gene expression is enhanced with the administration of either linearized mini-genes [21] or genomic DNA [22]. Therefore, it is possible to prolong the duration of gene expression derived from non-viral, plasmid-based gene therapy.

EXPERIMENTAL PROCEDURES

Materials. POPC (1-palmitoyl-2-oleoyl-*sn*-glycerol-3-phosphocholine) and DDAB (didodecyltrimethylammonium bromide) were purchased from Avanti-Polar Lipids Inc. (Alabaster, AL). Distearoylphosphatidylethanolamine (DSPE)-PEG 2000 was obtained from Shearwater Polymers (Huntsville, AL). DSPE-PEG 2000-maleimide was custom synthesized by Shearwater Polymers. [α - 32 P]dCTP (3000 Ci/mmol) was from NEN Life Science Product Inc. (Boston, MA). The nick translation system was from Life Technologies Inc. (Rockville, MD). 5-Bromo-4-chloro-3-indolyl- β -D-galactoside (X-gal), IGEPAL CA-630 and all other chemicals were purchased from Sigma Chemical Co. (St. Louis, MO). The luciferase reagent and recombinant luciferase were obtained from Promega; 2-mercaptoethanol (Traut's reagent) and bicinechonic acid (BCA) protein assay reagents were obtained from Pierce Chemical Co. (Rockford, IL). The 83-14 murine MAb to the HIR, and the OX26 murine MAb to the rat TfR were purified by protein G affinity chromatography from serum-free hybridoma-conditioned media as described previously [12]. The luciferase expression plasmid is designated clone 790 and is derived from the pCEP4 plasmid under the control of the SV40 promoter as described previously [17]. The pSV- β -galactosidase expression plasmid driven by the SV40 promoter is designated clone 756 as described previously [2,6], and was purchased from Promega (Madison, WI).

Pegylated immunoliposome synthesis. Pegylated immunoliposomes (PILs) were synthesized with a total of 20 μ mol of lipids, including 18.8 μ mol of POPC, 0.4 μ mol of DDAB, 0.6 μ mol of DSPE-PEG, and 0.2 μ mol of DSPE-PEG-maleimide, as described previously [6,7]. The PIL lipid contains 2% cationic lipid (DDAB) and 8% anionic lipid (DSPE-PEG), and has a net anionic charge [7]. Clone 756 plasmid DNA or clone 790 plasmid DNA was produced by Maxiprep (Qiagen, Chatsworth, CA). The supercoiled plasmid DNA (200 μ g) and 1 μ Ci of 32 P-nick translated plasmid DNA were encapsulated in the pegylated liposomes by serial extrusion resulting in liposomes of 85 nm diameter [2]. The exteriorized DNA was removed by nuclease digestion [23], as described previously [2]. The 83-14 HIRMAb or OX26 TfRMAb, containing a trace amount of 3H-labeled antibody, was individually thiolated with Traut's reagent and the thiolated MAb was conjugated to the pegylated liposome overnight at room temperature as described previously [6,12]. The unconjugated MAb, and the degraded exteriorized DNA were separated from the DNA encapsulated within the PIL by elution through a 1.6 \times 18 cm column of Sepharose

CL-4B in 0.05 M Hepes, pH = 7.0, as described previously [6,12]. The average number of MAb molecules conjugated per liposome was 43 ± 2 (mean \pm SE, $n = 3$ syntheses). The final percentage entrapment of 200 μ g of plasmid DNA in the liposome preparation was computed from the 32 P radioactivity and was $35 \pm 7.5\%$ (mean \pm SE, $n = 3$ syntheses). The PIL conjugated with the HIRMAb is designated HIRMAb-PIL and the PIL conjugated with the TfRMAb is designated TfRMAb-PIL. Clone 790 DNA was encapsulated in either HIRMAb-PIL or OX26-PIL for injection into primates or rats, respectively. Clone 756 was encapsulated in HIRMAb-PIL for primate injection. The HIRMAb-PIL carrying either the clone 756 or clone 790 plasmid DNA was sterilized before injection into the primate with a 0.22 μ m filter (Millipore Co., Bedford, MA) as described previously [12].

In vivo gene administration. A 10 year-old 6 kg female Rhesus monkey was purchased from Covance (Alice, TX). The animal was anesthetized with 10 mg/kg ketamine intra-muscular, and 5 ml of sterile HIRMAb-PIL containing 70 μ g of each of clone 756 and clone 790 plasmid DNA was injected into the monkey via the saphenous vein with a 18-g catheter. The total dose of HIRMAb that was conjugated to the PIL and administered to the primate was 1.8 mg. Adult male Sprague-Dawley rats weighing 250g were injected via the femoral vein with OX26-PIL carrying clone 790 plasmid DNA at a dose of 5 μ g of PIL-encapsulated plasmid DNA per rat. The dose of PIL encapsulated plasmid DNA was 12 and 20 μ g/kg, respectively, for the primate and rat. Both species were sacrificed at 48 hours post-injection. The brain and peripheral organs (liver, spleen, heart, skeletal muscle (biceps), and omental fat) were removed immediately after euthanasia. The primate brain weighing approximately 100g was divided into 4 coronal sections, and each section was divided into the left and right hemispheres. The brain slabs and peripheral organs were frozen in powdered dry ice for 30 min, embedded in OCT and re-frozen for cryostat sectioning.

β -galactosidase histochemistry. Frozen sections of 20- μ m thickness were cut on a Mikron cryostat and fixed with 0.2% glutaraldehyde in 0.1 M NaH_2PO_4 (pH = 7.0) for 1 hour. Because an entire coronal section of the primate brain was too large to section on the cryostat, each coronal slab was sectioned as coronal hemisphere slices. The sections were washed with 0.1 M NaH_2PO_4 (pH = 7.0) three times, and incubated overnight at 37 C in X-gal staining solution (20 mM potassium-ferrocyanide, 20 mM potassium-ferricyanide, 2 mM MgCl_2 , 0.02% IGEPAL CA-630, 0.01% Na deoxycholate, and 1 mg/ml of X-gal in 0.1 M NaH_2PO_4) at pH = 7.3. Prior to coverslipping, the sections were scanned with a UMAX PowerLookIII scanner with transparency adapter, and the image was cropped in Adobe Photoshop 5.5 on a G4 Power Macintosh computer. Sections were not counter-stained. Control or un-injected rhesus monkey brain was stained in parallel with the brain obtained from the gene-injected animal. The control rhesus monkey brain was frozen as coronal slabs in Tissue Tek OCT embedding medium immediately after euthanasia by Sierra Biomedical/Charles River (Sparks, NV).

Luciferase measurements. Primate tissue samples were taken from the frontal and occipital poles of the cerebrum, as well as from cerebellum, liver, lung, heart, kidney, spleen, and skeletal muscle (biceps). The tissues were homogenized in 4 volumes of lysis buffer for measurements of organ luciferase activity, as described previously [12]. Luciferase activity in rat brain, liver, lung, heart, kidney and spleen were measured in the same way. The data are reported as pg luciferase activity per mg cell protein. Based on the standard curve, 1 pg of luciferase was equivalent to $14,312 \pm 2,679$ relative light units (RLU), which is the mean \pm S.E. of 5 assays [11]. No luciferase enzyme activity was detectable in brain from the control, uninjected monkey.

Confocal microscopy. Frozen sections were fixed for 20 min in 2% paraformaldehyde in 0.1 M Na_2HPO_4 , pH = 7.4 at 4C. The slides were blocked in 0.01 M PBS buffer with 0.1% Triton X, and 10% goat serum. Primary antibodies were mouse anti-neuronal nuclei (neuN) monoclonal antibody (Chemicon Int., Temecula, CA), rabbit anti E.coli β -galactosidase polyclonal antibody (Bioscience Int., Saco, ME), mouse IgG1 isotype control, and rabbit IgG control at a concentration of 6.7 μ g/ml in PBS, pH = 7.4, 0.1% Triton X-100, and 3% bovine serum albumin. Secondary antibodies

used were 488-goat anti-mouse IgG (fluorescein channel) and 594-goat anti-rabbit IgG (rhodamine channel) (Molecular Probes, Eugene, OR) at a concentration of 6.7 µg/ml in PBS, pH = 7.4, 0.1% Triton X-100, and 1% goat serum. Confocal imaging was performed with a Zeiss LSM 5 PASCAL confocal microscope with dual argon and helium/neon lasers equipped with Zeiss LSM software for image reconstruction. All sections were scanned in multitrack mode to avoid overlap of the fluorescein and rhodamine channels.

ACKNOWLEDGMENTS

Dr. Ruben Boado provided valuable discussions. Drs. Dafang Wu, Hwa Jeong Lee, and Chunni Zhu provided assistance in the primate experiment. This work was supported by a grant from the University of California, Davis/Medical Investigation of Neural Developmental Disorders Institute Research Program, and the Neurotoxin Exposure Treatment Research Program of the U.S. Dept. of Defense. Felix Schlachetzki was supported by a grant from the Ernst Schering Research Foundation (Berlin, Germany).

RECEIVED FOR PUBLICATION SEPTEMBER 12; ACCEPTED NOVEMBER 5, 2002.

REFERENCES

- Martin, J. B. (1995). Gene therapy and pharmacological treatment of inherited neurological disorders. *Trends Biotechnol* 13: 28–35.
- Shi, N., and Pardridge, W. M. (2000). Non-invasive gene targeting to the brain. *Proc. Natl. Acad. Sci. USA* 97: 7567–7572.
- Mok, K. W. C., Lam, A. M. I., and Cullis, P. R. (1999). Stabilized plasmid-lipid particles: factors influencing plasmid entrapment and transfection properties. *Biochem. Biophys. Acta* 1419: 137–150.
- Semple, S. C., Chonn, A., and Cullis, P. R. (1998). Interactions of liposomes and lipid-based carrier systems with blood proteins: relation to clearance behaviour in vivo. *Adv. Drug Deliv. Rev.* 32: 3–17.
- Pardridge, W. M. (2001). *Brain Drug Targeting: The Future of Brain Development*. Cambridge University Press, Cambridge, United Kingdom, 1–370.
- Shi, N., Zhang, Y., Boado, R. J., Zhu, C., and Pardridge, W. M. (2001). Brain-specific expression of an exogenous gene following intravenous administration. *Proc. Natl. Acad. Sci. USA* 98: 12754–12759.
- Shi, N., Boado, R. J., and Pardridge, W. M. (2001). Receptor-mediated gene targeting to tissues in the rat in vivo. *Pharm. Res.* 18: 1091–1095.
- Zhu, C., Zhang, Y., and Pardridge, W. M. (2002). Widespread expression of an exogenous gene in the eye following intravenous administration. *Invest. Ophthalmol. Vis. Sci.* 43: 3075–3080.
- Strayer, D. S. (1996). SV40 as an effective gene transfer vector in vivo. *J. Biol. Chem.* 271: 24741–24746.
- Zhang, Y., Zhu, C., and Pardridge, W. M. (2002). Antisense gene therapy of brain cancer with an artificial virus gene delivery system. *Mol. Ther.* 6: 67–72.
- Zhang, Y., Boado, R. J., and Pardridge, W. M. (2003). Marked enhancement in gene expression by targeting the human insulin receptor. *J. Gene Med.*, in press.
- Zhang, Y., Lee, H. J., Boado, R. J., and Pardridge, W. M. (2002). Receptor-mediated delivery of an antisense gene to human brain cancer cells. *J. Gene Med.* 4: 183–194.
- Lierse, W., and Horstmann, E. (1959). Quantitative anatomy of the cerebral vascular bed with especial emphasis on homogeneity and inhomogeneity in small parts of the gray and white matter. *Acta Neurol.* 14: 15–19.
- Nevo, N., Chossat, N., Gagnach, W., Logeart, D., Mercadier, J.-J., and Michel, J.-B. (2001). Increasing endothelial cell permeability improves the efficiency of myocyte adenoviral vector infection. *J. Gene Med.* 3: 42–50.
- Hong, K., Zheng, W., Baker, A., and Papahadjopoulos, D. (1997). Stabilization of cationic liposome-plasmid DNA complexes by polyamines and poly(ethylene glycol)-phospholipid conjugates for efficient in vivo gene delivery. *FEBS Lett.* 400: 233–237.
- Plank, C., Tang, M. X., Wolfe, A. R., and Szoka, F. C. Jr. (1999). Branched cationic peptides for gene delivery: role of type and number of cationic residues in formation and in vitro activity of DNA polyplexes. *Hum. Gene Ther.* 10: 319–332.
- Boado, R. J., and Pardridge, W. M. (1998). Ten nucleotide cis element in the 3'-untranslated region of the GLUT1 glucose transporter mRNA increases gene expression via mRNA stabilization. *Mol. Brain Res.* 59: 109–113.
- Peng, K.-W., Pham, L., Ye, H., Zufferey, R., Trono, D., Cosset, F.-L., and Russell, S. J. (2001). Organ distribution of gene expression after intravenous infusion of targeted and untargeted lentiviral vectors. *Gene Ther.* 8: 1456–1463.
- Coloma, M. J., Lee, H. J., Kurihara, A., Landaw, E. M., Boado, R. J., Morrison, S. L., and Pardridge, W. M. (2000). Transport across the primate blood-brain barrier of a genetically engineered chimeric monoclonal antibody to the human insulin receptor. *Pharm. Res.* 17: 266–274.
- Zhang, Y., Calon, F., Zhu, C., Boado, R. J., Pardridge, W. M. (2003). Intravenous non-viral gene therapy causes normalization of striatal tyrosine hydroxylase and reversal of motor impairment in experimental Parkinsonism. *Human Gene Therapy* 14: 1–12.
- Chen, Z.-Y., Yant, S. R., He, C.-Y., Meuse, L., Shen, S., and Kay, M. A. (2001). Linear DNAs concatemize in vivo and result in sustained transgene expression in mouse liver. *Mol. Ther.* 3: 403–410.
- Stoll, S. M., Scimmenti, C. R., Baba, E. J., Meuse, L., Kay, M. A., and Calos, M. P. (2002). Epstein-Barr virus/human vector provides high-level, long-term expression of α_1 -antitrypsin in mice. *Mol. Ther.* 4: 122–129.
- Monnard, P.-A., Oberholzer, T., and Luisi, P. L. (1997). Entrapment of nucleic acids in liposomes. *Biochem. Biophys. Acta* 1329: 39–50.

Widespread Expression of an Exogenous Gene in the Eye after Intravenous Administration

Chunni Zhu, Yun Zhang, and William M. Pardridge

PURPOSE. Gene-targeting technology and tissue-specific gene promoters were used to produce widespread expression of an exogenous gene throughout the eye, including the retinal pigmented epithelium, after noninvasive intravenous administration of a nonviral plasmid formulation.

METHODS. An expression plasmid encoding bacterial β -galactosidase, under the influence of either the simian virus (SV)40 promoter or the glial fibrillary acidic protein (GFAP) gene promoter, was packaged in the interior of 85-nm pegylated immunoliposomes (PIL) targeted to transferrin receptor (TfR)-rich structures with the rat 8D3 monoclonal antibody (mAb) to the mouse TfR. Plasmid DNA was packaged in the 8D3-PIL and injected intravenously into adult female BALB/c mice at a dose of 5 μ g DNA per mouse. The eyes were removed 48 hours later, and frozen sections were prepared for β -galactosidase histochemistry and rhodopsin, TfR, or GFAP immunocytochemistry.

RESULTS. There was diffuse expression of the SV40/ β -galactosidase gene in the retinal pigmented epithelium. The cellular specificity of gene expression was influenced by the promoter used in the gene construct, evidenced by the fact that gene expression in the inner retina was induced with the GFAP promoter. The β -galactosidase gene was also widely expressed in the TfR-rich epithelial structures of the eye, including the ciliary body, the iris, the sebaceous glands of the tarsal plate, and the epithelium of the cornea. When the anti-TfR mAb on the PIL was replaced with the rat IgG isotype control, there was no gene expression in the eye.

CONCLUSIONS. Widespread expression of an exogenous gene throughout the retina pigmented epithelium or other structures of the eye is possible with a noninvasive intravenous administration of a nonviral plasmid that is reformulated with gene-targeting technology. The cellular specificity of gene expression in the eye can be regulated with the use of cell-specific gene promoters. (*Invest Ophthalmol Vis Sci.* 2002;43:3075-3080)

Many disorders of the retina and other structures of the eye are potentially amenable to treatment with gene therapy.¹ In the case of retinitis pigmentosa (RP), many of the gene defects that cause the disease are known.²⁻³ The limiting factor in gene therapy for the eye is the gene delivery system. Both viral and nonviral cationic liposome systems have been used to target exogenous genes to the retina and other structures of the eye. Because neither the viral nor the cationic liposome

gene delivery system crosses the blood-retinal barrier (BRB), it is necessary to inject the gene directly into either the vitreous cavity or the subretinal space. The exogenous gene is expressed at the local site of injection, with no gene expression in the retina at distances as little as 100 μ m away from the injection site.⁴ It has been estimated that only 6% of the human retina would be transduced after a single subretinal injection of an exogenous gene.¹

It would be advantageous to have a retinal gene-targeting system that transduces essentially 100% of the retina with the therapeutic gene. This would require targeting the exogenous gene through the retinal microvasculature comprising the BRB, which would allow for gene distribution to all parts of the retina. In this approach, the exogenous gene is administered noninvasively, by an intravenous or subcutaneous route, for example. This would be possible if a retinal gene-targeting technology were developed that is capable of delivering an exogenous gene across the two principle barriers that segregate the blood from the intracellular space of the retina: the BRB and the plasma membrane of cells within the retina.

The widespread expression of an exogenous gene throughout the target organ after an intravenous (IV) injection is possible with gene-targeting technology that uses nonviral expression plasmids encapsulated in pegylated immunoliposomes (PIL).⁵ The double-stranded, supercoiled plasmid DNA is encapsulated in the interior of a 75- to 100-nm liposome (Fig. 1A). This encapsulation in the interior of the liposome renders the exogenous gene resistant to the ubiquitous endonucleases present in vivo. The liposome is stabilized for in vivo circulation and prolonged plasma residence time by conjugating to the surface of the liposome several thousand strands of 2000-dalton polyethylene glycol (PEG), designated PEG²⁰⁰⁰ (Fig. 1A). A receptor-specific monoclonal antibody (mAb) is tethered to approximately 1% to 2% of the tips of the PEG²⁰⁰⁰ strands.⁵ The mAb targets a receptor present on both the BRB and the plasma membrane of cells within the retina or other ocular structures. In the formulation used in the present studies for gene targeting to the mouse retina, the rat 8D3 mAb to the mouse transferrin receptor (TfR) was used.⁶ The TfR is widely expressed at both the BRB and the plasma membrane of cells in the retina and other structures of the eye.⁷⁻¹¹

Once the exogenous gene is delivered to cells, the expression of the gene is regulated by the promoter that is inserted in the expression plasmid (Fig. 1A). Prior work has shown that gene expression is observed in both brain and peripheral TfR-rich organs, when the widely active simian virus (SV)40 promoter is used to drive the expression of the exogenous gene.^{5,12} Conversely, brain-specific expression of an exogenous gene after IV administration is possible with a combined use of the PIL gene-targeting technology and a brain-specific promoter, such as the glial fibrillary acidic protein (GFAP) gene promoter.⁶ The GFAP gene is expressed in the normal retina in the ganglion cell layer (GCL).¹³ Therefore, with the rat 8D3 mAb to the mouse TfR, we examined the expression of an exogenous gene, bacterial β -galactosidase, that was controlled by either the SV40 promoter or the human GFAP promoter and was packaged in the interior of a PIL targeted to the mouse retina.

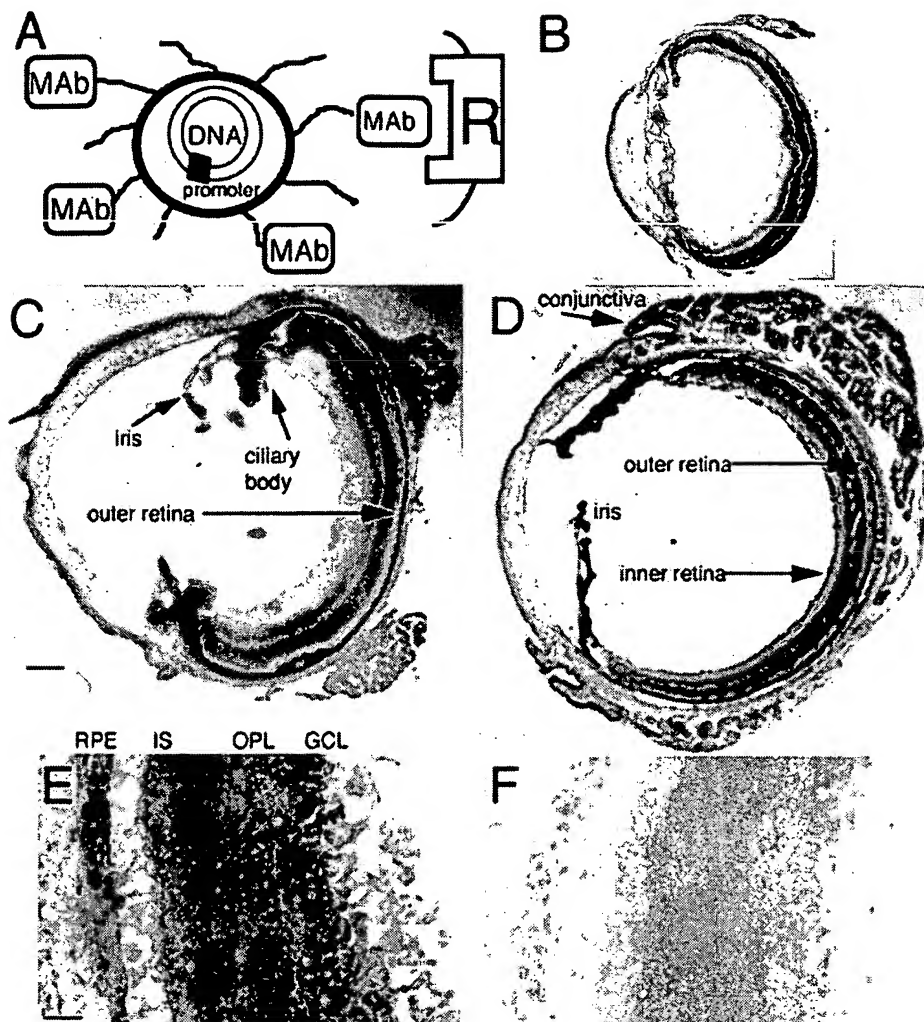
From the Department of Medicine, UCLA School of Medicine, Los Angeles, California.

Submitted for publication November 27, 2001; revised April 16, 2002; accepted May 20, 2002.

Commercial relationships policy: P (WMP); N (all others).

The publication costs of this article were defrayed in part by page charge payment. This article must therefore be marked "advertisement" in accordance with 18 U.S.C. §1734 solely to indicate this fact.

Corresponding author: William M. Pardridge, UCLA Warren Hall 13-164, 900 Veteran Avenue, Los Angeles, CA 90024; wpardridge@mednet.ucla.edu.



mouse TfR. (F) Immunocytochemistry of mouse retina with the rat IgG control antibody. All specimens were counterstained with hematoxylin. (E, F) Immunopositive TfR is reddish brown and the counterstain is purple. Scale bars: (C, D) 106 μ m; (E, F) 27 μ m.

MATERIALS AND METHODS

Materials

Adult female BALB/c albino mice (25–30 g) were purchased from Harlan (Indianapolis, IN). The pSV- β -galactosidase expression plasmid under the influence of the SV40 promoter was obtained from Promega (Madison, WI). The β -galactosidase staining kit was purchased from Invitrogen (San Diego, CA). The pGfa-lacZ β -galactosidase expression plasmid was provided by Jose Segovia of the Center of Investigation and Advanced Studies (San Pedro Zacatenco, Mexico). In this plasmid, the lacZ gene is driven by the human GFAP promoter, as described previously.^{14,15} The 8D3 hybridoma line, secreting a rat IgG to the mouse TfR,¹⁶ was obtained from Britta Engelhardt of the Max Planck Institute (Bad Nauheim, Germany), and the 8D3 mAb was purified as described previously.⁶ The 1D4 mouse mAb against bovine rhodopsin¹⁷ was obtained from Dean Bok of the UCLA School of Medicine (Los Angeles, CA). The immunodetection kit (Vector MOM), 3-amino-9-ethylcarbazole (AEC) substrate kit for peroxidase, and hematoxylin QS counterstain were purchased from Vector Laboratories (Burlingame, CA). Optimal cutting temperature compound (OCT; Tissue-Tek) was purchased from Sakura FineTek (Torrance, CA). The mouse mAb against porcine GFAP, pooled rat immunoglobulin G (IgG), and all other reagents were purchased from Sigma (St. Louis, MO).

In Vivo Administration of Pegylated Immunoliposomes

The preparation of the 8D3-PIL carrying either the pSV- β -galactosidase (designated SV40/ β -galactosidase) or the pGfa-lacZ (designated GFAP/ β -galactosidase) has been described previously.^{5,6} All animal procedures were approved by the UCLA Animal Research Committee and adhered to the ARVO Statement for the Use of Animals in Ophthalmic and Vision Research. Female BALB/c mice of 25 to 30 g body weight were anesthetized with intraperitoneal ketamine (50 mg/kg) and xylazine (4 mg/kg). Experimental animals ($n = 8$) were injected intravenously through the femoral vein with 8D3-PIL carrying either pSV- β -galactosidase plasmid DNA ($n = 3$) or the pGfa-lacZ plasmid DNA ($n = 5$) at a dose of 5 to 6 μ g per mouse. For control studies, the plasmid DNA was encapsulated within PILs targeted with the rat IgG isotype control antibody, and mice ($n = 5$) were injected intravenously with 5 to 6 μ g per mouse of plasmid DNA carried by the rat IgG-PIL. Prior work has shown that if the targeting mAb is replaced with an isotype control antibody that does not recognize the targeted receptor, then there is no gene expression in brain, liver, spleen, lung, or heart in either rats or mice.^{5,6,12}

Mice injected with either the 8D3-PIL or the rat IgG-PIL were killed at 48 hours after the single IV injection of the gene. Eyes were removed and frozen in OCT embedding medium on dry ice and stored at -70°C .

FIGURE 1. (A) A nonviral, supercoiled, double-stranded plasmid DNA driven by a cell-specific promoter was packaged in the interior of a 75- to 100-nm liposome. The surface of the liposome was labeled with several thousand strands of PEG²⁰⁰⁰, and the tips of 1% to 2% of the PEG strands were conjugated with a receptor (R)-specific targeting mAb. The mAb triggered the receptor-mediated transcytosis of the pegylated immunoliposome across the blood-retinal barrier, and triggered the receptor-mediated endocytosis of the PIL into cells of the eye expressing the targeted receptor. The PIL was prepared with either the rat 8D3 mAb to the mouse TfR or the rat IgG isotype control antibody. The control rat IgG antibody did not target the TfR. (B) β -Galactosidase histochemistry in an eye of a mouse injected with the GFAP/ β -galactosidase plasmid encapsulated in PILs targeted with nonspecific rat IgG showed no expression of the β -galactosidase gene. (C) β -Galactosidase histochemistry in an eye obtained 48 hours after IV injection of the SV40/ β -galactosidase plasmid encapsulated within the PIL targeted with the 8D3 mAb. There was diffuse expression of the transgene in the RPE and in the iris and ciliary body. (D) β -Galactosidase histochemistry in the mouse eye obtained 48 hours after IV injection of the GFAP/ β -galactosidase plasmid encapsulated within the PIL targeted with the 8D3 mAb. There is diffuse expression of the transgene in the inner retina and at the RPE and in the iris and conjunctival epithelium. (E) Immunocytochemistry of mouse retina with the rat 8D3 mAb to the

Alternatively, some mice underwent perfusion fixation with 4% paraformaldehyde in situ before removal of the eyes. These eyes were immersion fixed in 4% paraformaldehyde, cryoprotected overnight in 30% sucrose, and frozen in OCT medium before preparation of frozen sections. Mouse kidney was also removed as a positive control for the β -galactosidase histochemistry.^{6,12}

β -Galactosidase Histochemistry

β -Galactosidase histochemistry was performed on frozen sections of eyes similar to prior work reported in brain tissue.^{5,6,12} Horizontal frozen sections of 18- μ m thickness were cut on a microtome cryostat (model HM505; Micron Instruments, San Diego, CA) and fixed with 0.5% glutaraldehyde in 0.01 M PBS (pH 7.4) for 5 minutes. After a wash in PBS, sections were incubated in 5-bromo-4-chloro-3-indoyl- β -D-galactoside (X-gal) staining solution (4 mM potassium ferricyanide, 4 mM potassium ferrocyanide, 2 mM $MgCl_2$, and 1 mg/mL X-gal [pH 7.4]) at 37°C overnight. After the staining, sections were briefly washed in distilled water and lightly counterstained with hematoxylin. Frozen sections of mouse kidney were also processed in the histochemistry assay. Unlike the eye, kidneys from control, uninjected rodents express endogenous β -galactosidase-like enzyme activity that gives a positive histochemical reaction at a neutral pH.^{6,12} Therefore, including kidney sections in the β -galactosidase histochemistry assay serves as a positive internal control, particularly for eye specimens taken from rat IgG-PIL-injected animals that show no evidence of β -galactosidase gene expression.

Immunohistochemistry

Immunohistochemistry for rhodopsin, GFAP, or mouse TfR was performed with the avidin biotin complex (ABC) immunoperoxidase method (Vector Laboratories). Frozen sections of the eyes from the control and experimental animals were fixed in 2% paraformaldehyde for 20 minutes at 4°C. Endogenous peroxidase was blocked with 0.3% H_2O_2 in 0.3% horse serum for 5 minutes. Nonspecific binding of proteins was blocked with mouse immunoglobulin blocking solution (MOM; Vector) for 1 hour, when a mouse primary antibody was used. Sections were then incubated in the primary antibody for 30 minutes at room temperature, and three primary antibodies were used: the 1D4 mouse anti-bovine rhodopsin mAb (5 μ g/mL), the mouse anti-porcine GFAP mAb (8 μ g/mL), and the rat 8D3 mAb to the mouse TfR (10 μ g/mL). Control primary antibodies were either mouse or rat IgG at the same concentration. After a wash in PBS, sections were incubated in biotinylated secondary antibody for 10 minutes and then in ABC horseradish peroxidase (Vectastain Elite; Vector) for 5 minutes. After development with AEC, sections were lightly counterstained with hematoxylin and mounted with glycerol-gelatin. The thickness of the layers of the retina in different sections varied, owing to differences in sectioning angle of frozen, unfixed eyes.

RESULTS

β -Galactosidase histochemistry was performed on eye sections obtained from mice that were injected with the β -galactosidase plasmid encapsulated within the control rat IgG-PIL, and the histochemistry shows the absence of any endogenous β -galactosidase enzyme product (Fig. 1B). The β -galactosidase histochemistry of the eye removed 48 hours after a single IV injection of the 8D3-PIL carrying the β -galactosidase expression plasmid driven by the SV40 promoter is shown in Figure 1C. This demonstrates diffuse expression of the exogenous gene in the outer retina corresponding to the retinal pigmented epithelium (RPE), as well as gene expression in the ciliary body and iris (Fig. 1C).

Ocular expression of the β -galactosidase gene was examined at 48 hours after a single IV injection of the GFAP/ β -galactosidase plasmid encapsulated within the 8D3-PIL. The gene was expressed in both the inner retina and the RPE, as

shown in Figure 1D. The β -galactosidase gene driven by the GFAP promoter was also expressed in the conjunctival epithelium and in the epithelium of the ciliary body and the iris (Fig. 1D).

The reactivity of the rat 8D3 mAb to the mouse TfR with ocular structures was examined by immunocytochemistry using either the 8D3 mAb (Fig. 1E) or the control rat IgG (Fig. 1F). Immunoreactive TfR was present in the ganglion cell layer (GCL), the outer plexiform layer (OPL), the inner segments (IS) of the photoreceptor cells, and the RPE (Fig. 1E).

High-magnification microscopy of the retina removed from control mice shows the absence of the endogenous β -galactosidase histochemical product (Fig. 2A). After the IV administration of the SV40/galactosidase plasmid encapsulated within the 8D3-PIL, the predominant site of gene expression was the RPE (Fig. 2B). There was minimal gene expression in the inner retina after the administration of the SV40/galactosidase plasmid (Fig. 2B).

The administration of the GFAP/ β -galactosidase plasmid resulted in increased gene expression in the inner retina corresponding to the GCL and the inner nuclear layer (INL; Fig. 2C). GFAP immunocytochemistry was performed on parallel sections (data not shown), and there was overlap of the GFAP-immunopositive cells in the inner retina and the β -galactosidase histochemical product (Fig. 2C).

Higher-magnification views of the outer retina are shown in Figures 2D and 2H for β -galactosidase histochemistry and for rhodopsin immunocytochemistry, respectively. The outer segments (OS) and the IS of the photoreceptor cells, which were immunopositive and immunonegative, respectively, for rhodopsin are visible in Figure 2H. Based on comparison of the β -galactosidase histochemistry (Fig. 2D) and the rhodopsin immunocytochemistry (Fig. 2H), it appears that exogenous gene expression in the outer retina was restricted to the RPE when either the SV40 or GFAP promoter was used.

The exogenous gene was also expressed in the epithelium of the ciliary body and iris (Fig. 2E). The tarsal plate sebaceous gland epithelium, with the characteristic foamy appearance, expressed the exogenous gene (Fig. 2F). The epithelium of the cornea demonstrated expression of the transgene (Fig. 2G).

DISCUSSION

The results of these studies lead to the following conclusions: First, it is possible to target an exogenous gene throughout the entire RPE and other structures of the eye with a simple IV injection, if gene-targeting technology is used. Second, the expression of the exogenous gene in different cell layers of the retina can be modulated with cell-specific promoters, as shown by the selective expression of the β -galactosidase gene in the GCL after administration of the expression plasmid driven by the GFAP promoter (Fig. 2C). The use of tissue-specific promoters can eliminate gene expression in peripheral tissues, as shown in the mouse.⁶ Gene expression in the eye was demonstrated in the present studies at a single time point, 48 hours, after IV injection (Figs. 1, 2), although prior work with either Southern blot or histochemical analysis for either brain or liver has demonstrated that expression of the exogenous gene is detectable for at least 6 days after a single IV administration of the gene.¹²

The nonviral PIL formulation (Fig. 1A) used in the present investigations can be contrasted with conventional nonviral cationic liposome-DNA mixtures. The latter form layered structures of DNA and lipid in aqueous solutions of low ionic strength.¹⁸ However, cationic liposomes rapidly aggregate into structures of more than 1 μ m in physiologic saline,¹⁹ and cationic liposomes are inhibited by serum proteins.²⁰ Cationic

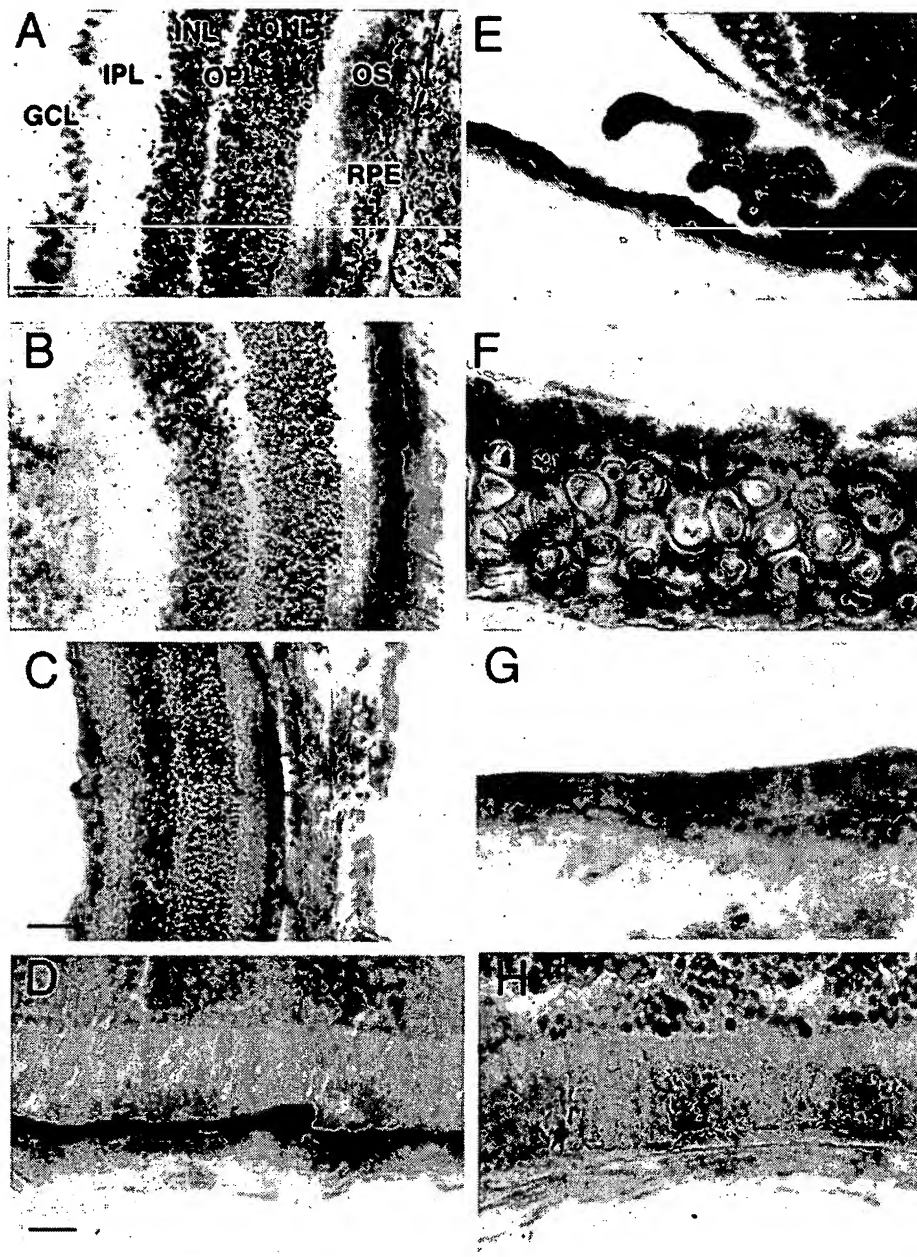


FIGURE 2. β -Galactosidase histochemistry: (A) The eye of a control, uninjected mouse. (B) The retina of a mouse injected with the SV40/ β -galactosidase plasmid encapsulated within the 8D3-PIL showing diffuse expression in the RPE with minimal gene expression in the inner retina or GCL. (C) An eye of a mouse injected with the GFAP/ β -galactosidase expression plasmid encapsulated within the 8D3-PIL, showing gene expression in the RPE, the GCL of the inner retina, and at the border of the IPL and the INL. (D) The outer retina in a high-magnification view. A comparison of the distribution of rhodopsin, shown in (H) indicates the transgene is expressed in the RPE. (E) Expression of the transgene in the epithelium of the iris and ciliary body. (F) Expression of the transgene in the foamy epithelia of the sebaceous gland of the conjunctival tarsal plate. (G) Expression of the transgene in the epithelium of the cornea. (H) Rhodopsin immunocytochemistry. All specimens were counterstained with hematoxylin. The specimens used for histochemistry (A–G) were fixed in 0.5% glutaraldehyde for 5 minutes, and that used for immunocytochemistry (H) was fixed in 2% paraformaldehyde for 20 minutes. Scale bars: (A, B, E) 37 μ m; (C) 60 μ m; (D, F, G, H) 15 μ m.

liposomes aggregate in blood, and more than 99% of organ gene expression is found in the pulmonary vascular bed after IV administration of cationic liposomes.^{21,22} There is no gene expression in the brain after IV injection of cationic liposomes.²³ In contrast to the cationic liposomes, with which the DNA is exposed to blood constituents, the plasmid DNA is packaged in the interior of the PIL (Fig. 1A). The PIL does not aggregate in saline solution and has prolonged plasma residence times, owing to the use of pegylation technology.⁵ Pegylation of the liposome is accomplished by conjugation of several thousand strands of PEG²⁰⁰⁰ to the surface of the liposome (Fig. 1A). A pegylated liposome, per se, would be inert in vivo and would not be specifically targeted to cells in vivo after IV administration.²⁴ When a nonspecific IgG molecule is conjugated to the tips of the PEG strands, in lieu of the targeting mAb (Fig. 1A), and injected intravenously in rats or mice, there is no expression of the exogenous gene in brain or peripheral tissues that express the TfR.^{5,6,12} In the present

studies, there was no gene expression in the mouse eye when the PIL was targeted with a nonspecific isotype control IgG (Fig. 1B). However, the PIL was delivered to tissues based on the tissue-specific expression of the targeted receptor (Fig. 1A, R), if a targeting mAb was conjugated to the PEG strands. An mAb to the TfR was used to target the PIL carrying the DNA to cells in vivo. Gene expression in brain cells is possible with the PIL gene-targeting technology, because the TfR is expressed on both the brain capillary endothelium, which forms the blood-brain barrier (BBB),²⁵ and on the plasma membrane of brain cells.²⁶

The anti-TfR mAb can also be used to target exogenous genes to the eye, owing to the abundant expression of the TfR in ocular structures.⁸ The TfR is expressed on the plasma membrane of multiple cells of the eye, including cells of the GCL, the INL, the RPE, and the IS of the photoreceptor cells.^{7–9} This pattern of retinal TfR expression was confirmed in the present studies with immunocytochemistry with the 8D3 mAb

to the mouse TfR (Fig. 1E), which is the same mAb used to target exogenous genes to the eye (Figs. 1C, 1D). The TfR is also expressed in the epithelium of the conjunctiva, the iris, the ciliary body, and the cornea.^{10,11} The pattern of gene expression in the eye (Figs. 1C, 1D) parallels the diffuse expression of the TfR in the eye. Owing to the dual expression of the TfR on both the BRB and the plasma membrane of ocular cells, the PIL can deliver the exogenous gene across the different cellular barriers separating the blood from the intracellular compartment of cells within the eye. Once inside the retinal cells, the expression of the exogenous gene is influenced by the tissue specificity of the promoter.⁶ The GFAP/ β -galactosidase gene was expressed in epithelial structures such as the iris and the ciliary body, indicating the GFAP promoter is expressed in these structures (Figs. 1C, 1D). This observation correlates with results in prior studies showing GFAP expression in both the iris²⁷ and the ciliary body²⁸ of the rodent eye. The GFAP/ β -galactosidase gene was expressed in cells within the inner retina (Fig. 2C), which appeared to be Müller cell processes located primarily within the GCL and, to a lesser extent, in the INL (Fig. 2C). This pattern of GFAP/ β -galactosidase gene expression correlates with the cellular distribution of GFAP expression in the normal retina, which includes Müller cell processes within the GCL, and to a lesser extent in the IPL and INL.²⁹ There was minimal expression of the β -galactosidase gene in the GCL when the plasmid was under the control of the SV40 promoter (Fig. 2B). The correlation of the β -galactosidase histochemistry (Fig. 2D) and rhodopsin immunocytochemistry (Fig. 2H) suggest gene expression is located primarily in the RPE, with minimal expression in the photoreceptor cells. However, it may be possible to induce expression of an exogenous gene in the photoreceptor segments, if an opsin gene promoter is inserted in the expression plasmid, as has been shown previously with viral delivery systems.³⁰

In summary, the present studies demonstrate that it is possible to obtain diffuse expression of an exogenous gene throughout the RPE after an IV injection of a nonviral formulation. With the expression plasmid used in the present studies, the exogenous gene is expressed within cells as an extrachromosomal episome, and gene expression is necessarily transient. The half-life of expression of an exogenous gene driven by the SV40 promoter and delivered with the PIL system to organs in the rat is approximately 6 days.¹² Therefore, an exogenous gene therapy would have to be administered repeatedly at periodic intervals, based on the persistence of the transgene. Repeated administration of the PIL should be possible, because the only immunogenic component of the formulation is the mAb, and the immunogenicity of the mAb in humans can be reduced or eliminated with genetic engineering and the production of humanized antibodies.

Alternatively, it may be desirable to have long-term expression of the transgene in the retina, and this can be achieved with viral vectors, such as adeno-associated virus (AAV) or lentivirus.^{30,31} However, both of these viral vectors result in stable integration into the host genome, and the long-term effects of such viral integration in humans is unknown. The risk of such viral integration may not be acceptable until it is demonstrated that the therapeutic gene has the intended effect on visual function in humans. The transient and reversible expression of a therapeutic gene in the retina is possible with the PIL gene-targeting technology. The therapeutic gene can be targeted across the BRB in humans with a genetically engineered humanized mAb. If the transient effect on visual function in humans of the therapeutic gene is favorable, then the decision could be made to transduce the retina long-term with viral vectors that integrate into the host genome.

The PIL gene-targeting technology described in the present studies could be used in humans by replacement of the anti-TfR

mAb with an mAb to the human insulin receptor (HIR).³² A genetically engineered HIR mAb readily crosses the primate BBB in vivo and binds to the human BBB in vitro, owing to the high level of expression of the insulin receptor at the BBB.³³ Because the insulin receptor is also expressed at the BRB,³⁴ the genetically engineered HIR mAb may also target PIL-encapsulated genes into the retina in humans. The HIR mAb is particularly suited for targeting therapeutic genes, because this antibody targets the nucleus and yields very high levels of expression of the therapeutic gene in human cells.³⁵

References

- Flannery JG, Zolotukhin S, Vaquero MI, LaVail MM, Muzyczka N, Hauswirth WW. Efficient photoreceptor-targeted gene expression in vivo by recombinant adeno-associated virus. *Proc Natl Acad Sci USA*. 1997;94:6916-6921.
- Phelan JK, Bok D. A brief review of retinitis pigmentosa and the identified retinitis pigmentosa genes. *Mol Vis*. 2000;6:116-124.
- Dejneka NS, Bennett J. Gene therapy and retinitis pigmentosa: advances and future challenges. *Bioessays*. 2001;23:662-668.
- Bennett J, Maguire AM, Cideciyan AV, et al. Stable transgene expression in rod photoreceptors after recombinant adeno-associated virus-mediated gene transfer to monkey retina. *Proc Natl Acad Sci USA*. 1999;96:9920-9925.
- Shi N, Pardridge WM. Non-invasive gene targeting to the brain. *Proc Natl Acad Sci USA*. 2000;97:7567-7572.
- Shi N, Zhang Y, Boado RJ, Zhu C, Pardridge WM. Brain-specific expression of an exogenous gene following i.v. administration. *Proc Natl Acad Sci USA*. 2001;98:12754-12759.
- Davis AA, Hunt RC. Transferrin is made and bound by photoreceptor cells. *J Cell Physiol*. 1993;156:280-285.
- Holash JA, Stewart PA. The relationship of astrocyte-like cells to the vessels that contribute to the blood-ocular barriers. *Brain Res*. 1993;629:218-224.
- Yefimova MG, Jeanny JC, Guillonnet X, et al. Iron, ferritin, transferrin, and transferrin receptor in the adult rat retina. *Invest Ophthalmol Vis Sci*. 2000;41:2343-2351.
- Baudouin C, Brignole F, Fredj-Reygrobelle D, Negre F, Bayle J, Gastaud P. Transferrin receptor expression by retinal pigment epithelial cells in proliferative vitreoretinopathy. *Invest Ophthalmol Vis Sci*. 1992;33:2822-2829.
- Tan PH, King WJ, Chen D, et al. Transferrin receptor-mediated gene transfer to the corneal endothelium. *Transplantation*. 2001;71:552-560.
- Shi N, Boado RJ, Pardridge WM. Receptor-mediated gene targeting to tissues in vivo following intravenous administration of pegylated immunoliposomes. *Pharm Res*. 2001;18:1091-1095.
- Zhuo L, Sun B, Zhang CL, Fine A, Chiu SY, Messing A. Live astrocytes visualized by green fluorescent protein in transgenic mice. *Dev Biol*. 1997;187:36-42.
- Brenner M, Kisseberth WC, Su Y, Besnard F, Messing A. GFAP promoter directs astrocyte-specific expression in transgenic mice. *J Neurosci*. 1994;14:1030-1037.
- Segovia J, Vergara P, Brenner M. Differentiation-dependent expression of transgenes in engineered astrocyte cell lines. *Neurosci Lett*. 1998;242:172-176.
- Kissel K, Hamm S, Schulz M, Vecchi A, Garlanda C, Engelhardt B. Immunohistochemical localization of the murine transferrin receptor (TfR) on blood-tissue barriers using a novel anti-TfR monoclonal antibody. *Histochem Cell Biol*. 1998;110:63-72.
- MacKenzie D, Arendt A, Hargrave P, McDowell JH, Molday RS. Localization of binding sites for carboxyl terminal specific anti-rhodopsin monoclonal antibodies using synthetic peptides. *Biochemistry*. 1984;23:6544-6549.
- Radler JO, Koltover I, Salditt T, Safinya CR. Structure of DNA-cationic liposome complexes: DNA intercalation in multilamellar membranes in distinct interhelical packing regimes. *Science*. 1997;275:810-814.
- Plank C, Tang MX, Wolfe AR, Szoka FC. Branched cationic peptides for gene delivery: role of type and number of cationic resi-

- dues in formation and in vitro activity of DNA polyplexes. *Hum Gene Ther.* 1999;10:319-332.
20. Zelphati O, Uyechi LS, Barron LG, Szoka FC Jr. Effect of serum components on the physico-chemical properties of cationic lipid/oligonucleotide complexes and on their interactions with cells. *Biochim Biophys Acta.* 1998;1390:119-133.
 21. Hoffland HE, Nagy D, Liu JJ, et al. In vivo gene transfer by intravenous administration of stable cationic lipid/DNA complex. *Pharm Res.* 1997;14:742-749.
 22. Barron LG, Uyechi LS, Szoka FC Jr. Cationic lipids are essential for gene delivery mediated by intravenous administration of lipopolyplexes. *Gene Ther.* 1999;6:1179-1183.
 23. Osaka G, Carey K, Cuthbertson A, et al. Pharmacokinetics, tissue distribution, and expression efficiency of plasmid [32 P]DNA following intravenous administration of DNA/cationic lipid complexes in mice: use of a novel radionuclide approach. *J Pharm Sci.* 1996;85:612-618.
 24. Huwyler J, Wu D, Pardridge WM. Brain drug delivery of small molecules using immunoliposomes. *Proc Natl Acad Sci USA.* 1996;93:14164-14169.
 25. Pardridge WM, Eisenberg J, Yang J. Human blood-brain barrier transferrin receptor. *Metabolism.* 1987;36:892-895.
 26. Mash DC, Pablo J, Flynn DD, Efange SM, Weiner WJ. Characterization and distribution of transferrin receptors in the rat brain. *J Neurochem.* 1990;55:1972-1979.
 27. Bjorklund H, Dahl D. Glial fibrillary acidic protein (GFAP)-like immunoreactivity in the rodent eye. *J Neuroimmunol.* 1985;8:331-345.
 28. Villarroya H, Klein C, Thillaye-Goldenberg, B, Eclancher F. Distribution in ocular structures and optic pathways of immunocompetent and glial cells in an experimental allergic encephalomyelitis (EAE) relapsing model. *J Neurosci Res.* 2001;63:525-535.
 29. Chen H, Weber AJ. Expression of glial fibrillary acidic protein and glutamine synthetase by Müller cells after optic nerve damage and intravitreal application of brain-derived neurotrophic factor. *Glia.* 2002;38:115-125.
 30. Miyoshi H, Takahashi M, Gage FH, Verma IM. Stable and efficient gene transfer into the retina using an HIV-based lentiviral vector. *Proc Natl Acad Sci USA.* 1997;94:10319-10323.
 31. Acland GM, Aguirre GD, Ray J, et al. Gene therapy restores vision in a canine model of childhood blindness. *Nat Genet.* 2001;28:92-95.
 32. Pardridge WM, Kang YS, Buciak JL, Yang J. Human insulin receptor monoclonal antibody undergoes high affinity binding to human brain capillaries in vitro and rapid transcytosis through the blood-brain barrier in vivo in the primate. *Pharm Res.* 1995;12:807-816.
 33. Coloma MJ, Lee HJ, Kurihara A, et al. Transport across the primate blood-brain barrier of a genetically engineered chimeric monoclonal antibody to the human insulin receptor. *Pharm Res.* 2000;17:266-274.
 34. Naeser P. Insulin receptors in human ocular tissues: immunohistochemical demonstration in normal and diabetic eyes. *Ups J Med Sci.* 1997;102:35-40.
 35. Zhang Y, Lee HJ, Boado RJ, Pardridge WM. Receptor-mediated delivery of an antisense gene to human brain cancer cells. *J Gene Med.* 2002;4:183-194.

Absence of Toxicity of Chronic Weekly Intravenous Gene Therapy with Pegylated Immunoliposomes

Yu-feng Zhang,¹ Ruben J. Boado,¹ and William M. Pardridge^{1,2}

Received April 29, 2003; accepted July 16, 2003

Purpose. Plasmid DNA-based gene therapy involves episomal gene expression and must be given on a chronic basis. Therefore, the purpose of the present study was to examine for toxic side effects of the chronic weekly intravenous administration of plasmid DNA delivered with a nonviral gene transfer method using pegylated immunoliposomes (PIL).

Methods. A 7-kb expression plasmid encoding for rat tyrosine hydroxylase (TH) was encapsulated in PILs targeted with either the murine OX26 monoclonal antibody (MAb) to the rat transferrin receptor (TfR) or with the mouse IgG2a isotype control antibody. Rats were treated with weekly intravenous injections of 5 µg/rat/week of the TH expression plasmid DNA encapsulated in either the TfRMAb-targeted PIL or the mouse IgG2a-targeted PIL for a total period of 6 weeks. A third control group of rats was treated with saline.

Results. The animals treated with either saline, the TfRMAb-PIL, or the mouse IgG2a-PIL had no measurable differences with respect to body weights, 14 serum chemistries, or organ histology of brain, liver, spleen, kidney, heart, or lung. Immunocytochemistry showed no evidence of inflammation in brain. The delivery to brain of the TH expression plasmid was confirmed with Southern blotting.

Conclusions. The PIL nonviral gene transfer method causes no toxic side effects following chronic weekly intravenous administration in rats.

KEY WORDS: gene therapy; brain; liposomes; nonviral gene transfer; inflammation.

INTRODUCTION

An important issue with either viral or nonviral gene delivery systems is organ toxicity associated with the delivery vector (1). In the case of either adenovirus or Herpes simplex virus, the preexisting immunity to these viruses causes an inflammatory reaction (2,3). A single injection of either adenovirus or Herpes simplex virus into the brain causes inflammation leading to demyelination (4,5). More than 90% of the human population has a preexisting immunity to adeno-associated virus (6). Therefore, there is a need to establish nonviral gene transfer technology with minimal toxicity. The principal forms of nonviral gene transfer include the use of complexes of DNA/cationic polymers or the hydrodynamic injection method. Cationic polyplexes have a relatively narrow therapeutic index. A nitrogen/phosphate (N/P) ratio of 6–10 is necessary for gene expression in the lung following the intravenous injection of the cationic polymer/plasmid DNA

complexes, whereas an N/P ratio >20 is lethal (7). The hydrodynamic method involves the rapid intravenous injection of a volume of saline greater than the existing blood volume of the animal. This results in transitory right heart failure and hepatic congestion causing a selective expression of plasmid DNA in the liver (8). This gene delivery method results in an increase in liver enzymes, and the mortality with this method can be as high as 40% depending on the salt solution injected (8).

An alternative form of nonviral gene transfer involves the use of pegylated immunoliposomes (PIL). In this formulation, the nonviral plasmid DNA is encapsulated in the interior of an 85-nm liposome that has a net anionic charge (9). The surface of the liposome is pegylated with several thousand strands of 2000-Da polyethyleneglycol (PEG). The pegylated liposome is then targeted to distant sites by conjugating a transporting ligand to the tips of 1–2% of the PEG strands. Peptidomimetic monoclonal antibodies (MAb) to either the transferrin receptor (TfR) or the insulin receptor (IR) have been used to target PILs carrying expression plasmids to distant sites following intravenous injection (9,10). The PILs do not aggregate in saline and have prolonged blood residence times (11). PILs have been administered intravenously to mice on a weekly basis for the treatment of brain cancer (12), and PILs have been given to rats for the treatment of experimental Parkinson's disease (13). PILs targeted with the TfRMAb have been used to deliver nonviral plasmid DNA to brain. Because of the expression of the TfR on both the blood–brain barrier (BBB) and the neuronal plasma membrane, the TfRMAb-targeted PIL delivers the plasmid DNA to brain as well as other organs rich in TfR, such as liver and spleen (9,14). However, to date, there has been no evaluation of the potential toxicity of repeat intravenous administration of PILs.

The purpose of the present study was to examine the potential toxicity of repeat weekly intravenous administration of PIL-encapsulated plasmid DNA that was targeted to tissues in the rat with either the murine OX26 MAb to the rat TfR, or PILs targeted with the corresponding mouse IgG2a isotype control antibody. The plasmid DNA used in the present studies is the clone 877 DNA, which encodes for rat tyrosine hydroxylase (TH), as described previously (13). The delivery of the TH expression plasmid to brain with the TfRMAb-targeted PIL results in a normalization of striatal TH enzyme activity in brain of rats lesioned with a neurotoxin (13). For the present toxicity study, the TH expression plasmid DNA was encapsulated in either the TfRMAb-PIL or the mIgG2a-targeted PIL and was injected weekly for 6 weeks at a dose of 5 µg/rat of PIL-encapsulated plasmid DNA. Body weights of the animals were determined during the treatment period, and at the end of the 6-week treatment, blood was obtained for measurement of 14 parameters of serum chemistry reflecting liver and renal function. Major organs were removed at the end of the treatment period for pathologic analysis. In addition, brain was examined in detail with immunocytochemistry using antibodies to multiple antigens that reflect underlying tissue inflammation. Immunocytochemistry of brain was performed with the mouse OX1 MAb to rat leukocytes, the mouse OX2 MAb to the rat class II multiple histocompatibility complex (MHC) antigen, the mouse OX18

¹ Department of Medicine, UCLA, Los Angeles, CA 90024.

² To whom correspondence should be addressed. (email: wpardridge@mednet.ucla.edu)

MAB to the rat class I MHC antigen, the mouse OX35 MAB to the rat lymphocyte CD4 receptor, and the mouse OX42 MAB to the rat macrophage. Finally, the present studies used Southern blotting to confirm distribution of the TH expression plasmid in brain following targeting with the TfRMAb-PIL.

METHODS

Materials

1-Palmitoyl-2-oleoyl-*sn*-glycerol-3-phosphocholine (POPC) and didodecyltrimethylammonium bromide (DDAB) were purchased from Avanti-Polar Lipids Inc. (Alabaster, AL). Distearoylphosphatidylethanolamine (DSPE)-PEG²⁰⁰⁰ was obtained from Shearwater Polymers (Huntsville, AL), where PEG²⁰⁰⁰ is polyethylene glycol (PEG) of 2000 Daltons. DSPE-PEG²⁰⁰⁰-maleimide was custom-synthesized by Shearwater Polymers. The LiposoFAST-Basic extruder and polycarbonate filters were from Avestin (Ottawa, Canada). [α -³²P]dCTP (3000 Ci/mmol) was from NEN Life Science Products Inc. (Boston, MA). *N*-Succinimidyl[2,3-³H]propionate ([³H]NSP, 101 Ci/mmol), Sepharose CL-4B, and Protein G-Sepharose CL-4B were from Amersham Pharmacia Biotech (Arlington Heights, IL). The nick translation system was purchased from Invitrogen Life Technologies (Carlsbad, CA). Exonuclease III was purchased from Promega (Madison, WI); 2-iminothiolane (Traut's reagent) was obtained from Pierce Chemical Co. (Rockford, IL). Mouse myeloma ascites containing IgG2a (κ) (mIgG2a), pancreatic DNase I with a specific activity of 2000 Kunitz units/mg, horse serum, mouse IgG1 isotype, mouse anti-glia fibrillary acidic protein (GFAP) monoclonal antibody (MAB), and glycerol-gelatin were from Sigma Chemical Co. (St. Louis, MO). The antitransferrin receptor monoclonal antibody (TfRMAb) used in these studies is the murine OX26 MAB to the rat TfR, which is a mouse IgG2a. TfRMAb and mIgG2a were individually purified by protein G affinity chromatography from hybridoma-generated ascites. The biotinylated horse anti-mouse IgG, Vectastain ABC kit, and 3-amino-9-ethylcarbazole (AEC) substrate kit were purchased from Vector Laboratories (Burlingame, CA). Mouse antirat class I multiple histocompatibility complex (MHC) monoclonal antibody (OX18), mouse antirat leukocyte CD45 (OX-1), mouse antirat lymphocyte CD4 (OX-35), mouse antirat class II MHC (OX-6), and mouse antirat macrophage CD11b (OX42) were purchased from Serotec (Raleigh, NC). Optimal cutting temperature (O.C.T.) compound (Tissue-Tek) was purchased from Sakura FineTek (Torrance, CA). Adult male Sprague-Dawley rats (weighing from 180–220 g) were obtained from Harlan Breeders (Indianapolis, IN).

Plasmid DNA Preparation and Radiolabeling

The tyrosine hydroxylase expression plasmid, driven by the SV40 promoter and designated clone 877, was constructed as described previously (13). Clone 877 plasmid DNA was purified from *E. coli* with the Plasmid Maxi Kit and desalted per the manufacturer's instructions (Qiagen, Chatsworth, CA). The size of the DNA was confirmed by 0.8% agarose gel electrophoresis. DNA was labeled with [³²P]dCTP using nick translation. The specific activity of

[³²P]DNA was 15–20 μ Ci/ μ g. The trichloroacetic acid precipitability was 99%.

PEGylated Liposome Synthesis and Plasmid Encapsulation

POPC (18.8 μ mol), DDAB (0.6 μ mol), DSPE-PEG²⁰⁰⁰ (0.6 μ mol), and DSPE-PEG²⁰⁰⁰-maleimide (0.2 μ mol) were dissolved in chloroform, followed by evaporation, as described previously (14). The lipids were dispersed in 0.2 ml of 0.05 M Tris-HCl buffer (pH 7.0) and vortexed for 1 min, followed by 2 min of bath sonication. Supercoiled DNA (200 μ g) and 1 μ Ci of [³²P]DNA were added to the lipids. The dispersion was frozen in ethanol/dry ice for 5 min and thawed at room temperature for 25 min, and this freeze-thaw cycle was repeated five times to produce large vesicles with the DNA loosely entrapped inside. The large vesicles were converted into small (85-nm-diameter) liposomes by extrusion. The liposome dispersion was diluted to a lipid concentration of 40 mM, followed by extrusion five times each through two stacks each of 200- and 100-nm pore size polycarbonate membranes with a hand-held LiposoFAST-Basic extruder as described previously (11). The mean vesicle diameters were determined by quasielastic light scattering using a Microtrac Ultrafine Particle Analyzer (Leeds-Northrup, St. Petersburg, FL) as described previously (11).

The plasmid adsorbed to the exterior of the liposomes was removed by nuclease digestion, and 6 U of pancreatic endonuclease I and 33 U of exonuclease III were added in 5 mM MgCl₂ to the liposome/DNA mixture after extrusion. After incubation at 37°C for 1 h, the reaction was stopped by adding 20 mM EDTA. The nuclease digestion removed any exteriorized plasmid DNA, as demonstrated by agarose gel electrophoresis and ethidium bromide staining of aliquots taken before and after nuclease treatment, as described previously (11). The formulation before antibody conjugation is designated a pegylated liposome (PL), and the formulation after antibody conjugation is called a pegylated immunoliposome (PIL).

MAB Conjugation to the PEGylated Liposome Encapsulated with DNA

TfRMAb or mIgG2a was thiolated and individually conjugated to the maleimide moiety of the PEGylated liposome to produce the PIL with the desired receptor specificity. PIL conjugated with the OX26 MAB is designated TfRMAb-PIL, and PIL conjugated with the mIgG2a isotype control is designated mIgG2a-PIL. Either MAB or mIgG2a was radiolabeled with [³H]NSP as described previously (15). [³H]MAB had a specific activity of >0.11 μ Ci/ μ g and a TCA precipitability of >97%. The MAB (3.0 mg, 20 nmol) was thiolated with 40:1 molar excess of 2-iminothiolane (Traut's reagent), as described previously (15). The thiolated MAB, which contained a trace amount of ³H-labeled MAB, was conjugated overnight to the PEGylated liposome with encapsulated plasmid DNA containing a trace amount of [³²P]DNA. The unconjugated MAB and the oligonucleotides produced by nuclease treatment were separated from the PIL by Sepharose CL-4B column chromatography as described previously (11). The number of MAB molecules conjugated per liposome was calculated from the total ³H-labeled MAB radioactivity in the liposome pool and the specific activity of the labeled MAB,

assuming 100,000 lipid molecules per liposome, as described previously (15). The average number of MAb molecules conjugated per liposome was 57 ± 12 (mean \pm SD, $n = 4$ syntheses). The final percentage entrapment of 200 μ g of plasmid DNA in the liposome preparation was computed from the 32 P radioactivity and was $30 \pm 2\%$ (mean \pm SD, $n = 4$ syntheses), or 60 μ g of plasmid DNA.

Chronic Intravenous Administration of PIL-Encapsulated DNA

Adult male Sprague-Dawley rats weighing 200–220 g were anesthetized with ketamine (50 mg/kg) and xylazine (4 mg/kg) intraperitoneally. Animals were divided into three groups. PIL or saline was injected i.v. via femoral vein with a 30-g needle. The first group was injected with TfRMAB-PIL carrying clone 877 plasmid DNA at a dose of 5 μ g per rat. The second group was injected with mIgG2a-PIL carrying clone 877 plasmid DNA at a dose of 5 μ g per rat. The third group was injected with saline. The average intravenous injection volume for all treatments was 300 μ L. These intravenous treatments were given once a week for 6 consecutive weeks. Each week before injection, the body weight for each rat was measured. At 3 days following the sixth injection, the rats were anesthetized, and blood was collected from the vena cava. Serum was stored at -20°C for serum chemistry measurements by autoanalyzer in the UCLA Medical Center Clinical Laboratory. The rats were then sacrificed, and organs were removed for immunocytochemistry.

Immunocytochemistry

Immunocytochemistry was performed by the avidin-biotin complex (ABC) immunoperoxidase method (Vector Laboratories). Brains were removed immediately after sacrifice, and cut into three sagittal slabs. One slab was immersion fixed in cold 4% paraformaldehyde in 0.01 M phosphate-buffered saline (PBS) for 24 h at 4°C . The second slab was fixed in cold 100% methanol for 24 h at -20°C . These slabs were cryoprotected in 20% sucrose in 0.1 M phosphate-buffered water, pH 7.4 (PBW), for 24 h at 4°C , and 30% sucrose in PBW for 24 h at 4°C . Brains were embedded in O.C.T. medium and frozen in dry ice powder. Frozen sections (20 μ m) of rat brain were cut on a Mikron HM505E cryostat. Endogenous peroxidase was blocked with 0.3% H_2O_2 in 0.3% horse serum-phosphate-buffered saline (PBS) for 30 min. Nonspecific binding of proteins was blocked with 10% horse serum in PBS for 30 min. Sections were then incubated in primary antibodies overnight at 4°C . Based on either results provided by the manufacturer or on pilot studies, the fixative (methanol or paraformaldehyde) was chosen to preserve the target antigenicity in the fixed tissue. For methanol-fixed brain sections, OX1 (5 μ g/ml), OX18 (5 μ g/ml), or OX35 (5 μ g/ml) was used as the primary antibody; for paraformaldehyde-fixed brain sections, OX6 (5 μ g/ml), OX42 (5 μ g/ml), or mouse anti-GFAP MAb (1 μ g/ml) was used as the primary antibody. Identical concentrations of isotype control antibody were also used as primary antibody. Mouse IgG1 was used as the isotype control antibody for OX18, OX1, OX6, and GFAP, and mouse IgG2a was used as the isotype control antibody for OX35 and OX42. After incubation and wash in PBS, sections were incubated in biotinylated horse antimouse IgG for 30

min. After development in AEC, sections were mounted with glycerol-gelatin and examined by light microscopy.

Hematoxylin and Eosin Staining of Rat Organs

The third sagittal slab of brain, as well as liver, spleen, kidney, heart, and lung of each rat were removed and immersion fixed in 10% formalin in 0.1 M phosphate buffer for 48 h at 4°C . The fixed organs were embedded in paraffin and stained with hematoxylin and eosin and examined by light microscopy.

Southern Blotting

Plasmid DNA was isolated with the Hirt procedure (16) from rat brain 3 days following the intravenous injection of saline, clone 877 encapsulated in TfRMAB-PIL, or clone 877 encapsulated in mIgG2a-PIL. Rat brain (100 mg) was homogenized in 2 ml lysis buffer (20 mM Tris pH 7.5, 10 mM EDTA, 1% SDS) containing 15 μ g/ml DNase-free RNase A using a Polytron PT-MR 3000 homogenizer (Littau, Switzerland) at full speed for 10 s. Samples were incubated for 30 min at 37°C . Proteinase K was added to a final concentration of 1 mg/ml and samples incubated for 2 h at 37°C . Nuclear DNA was precipitated overnight at 4°C in the presence of 1.1 M NaCl. Samples were centrifuged at 14,000 rpm and 4°C for 30 min. Supernatants were extracted with phenol:chloroform, and plasmid DNA precipitated with ethanol in the presence of 10 μ g glycogen carrier. Aliquots of precipitated material were resolved by gel electrophoresis in 0.8% agarose and blotted onto a GeneScreen Plus membrane (14). To prevent hybridization with the endogenous rat TH genomic DNA, membranes were hybridized with [32 P]pGL2 clone 734 (17), which contains the clone 877 backbone but without the rat TH cDNA insert (13). Southern blot hybridization was performed as previously reported (14). Autoradiograms were developed with Kodak X-Omat Blue film and intensifying screens for 24 h at -70°C . Films were scanned with a Umax PowerLook III scanner, and images imported and cropped in Adobe Photoshop 5.5 on a G4 Power Macintosh.

Statistical Analysis

Statistical differences at the $p < 0.05$ level among different groups were evaluated by analysis of variance with Bonferroni correction.

RESULTS

The animals were divided into three groups depending on whether the rat was treated with weekly intravenous injections of (a) saline, (b) the TH expression plasmid encapsulated in mouse IgG2a targeted PILs, or (c) the TH expression plasmid encapsulated in the OX26 TfRMAB-targeted PILs. The body weights of the animals in the three treatment groups are shown in Fig. 1, and there was no significant difference between the body weights of the animals in the three groups throughout the treatment period.

The results of the chemistry analysis of the serum taken 3 days after the sixth weekly injection are shown in Table I. There are no significant differences in any of the 14 different serum chemistries for any of the three treatment groups

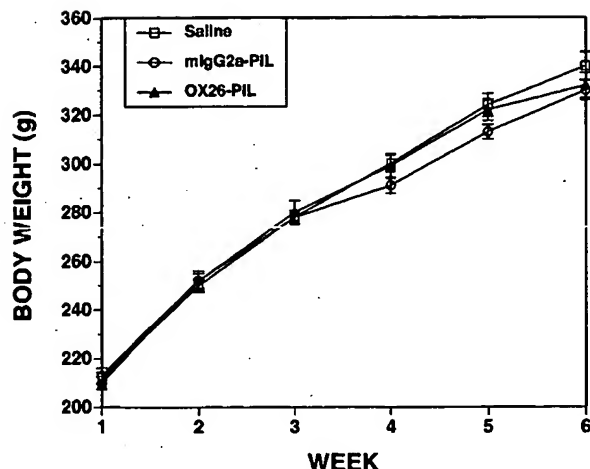


Fig. 1. The body weight of each rat in the three treatment groups was measured weekly during the course of treatment, and the mean \pm SE ($n = 6$ rats per group) is shown. The OX26-PIL is the TIRMAb-targeted PIL, and the mIgG2a-PIL is the PIL targeted with the non-specific mouse IgG2a, which is the isotype control antibody for the OX26 MAb.

(Table I). The organ histology in the rats sacrificed 3 days following the sixth weekly treatment is shown in Fig. 2 for brain cerebellum (Fig. 2A), lung (Fig. 2B), spleen (Fig. 2C), liver (Fig. 2D), heart (Fig. 2E), and kidney (Fig. 2F). The histology shown in Fig. 2 is for organs removed from rats treated with the TIRMAb-PIL. The organ histology of these animals was normal (Fig. 2) and was no different from the histology of organs taken from animals treated with either saline or the mIgG2a-PIL.

The results of the brain immunocytochemistry are given in Table II. No OX1-immunoreactive leukocytes were found in brain in any of the three treatment groups, although there was immunopositive choroidal endothelium staining in all groups (Table II). There was an occasional OX6-immunoreactive class II antigen-presenting cell in the meningeal surface of all three treatment groups with no evidence of any parenchymal infiltration of class II immunopositive cells in any of the treatment groups (Table II). OX18 immunore-

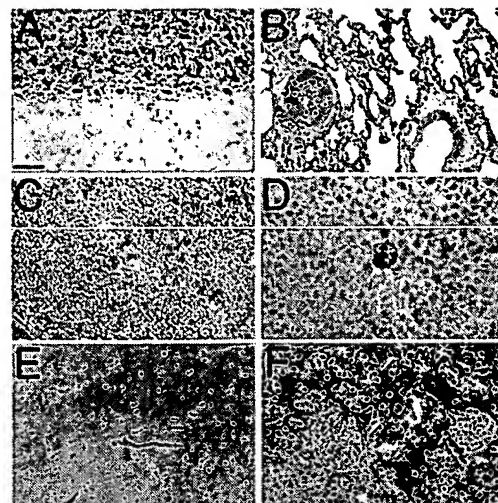


Fig. 2. Hematoxylin and eosin staining of formalin fixed cerebellum (A), lung (B), spleen (C), liver (D), heart (E), and kidney (F), removed 3 days after the sixth weekly intravenous injection of the TH expression plasmid encapsulated in the OX26 TIRMAb-targeted PIL. The magnification is the same in all panels, and the magnification bar in panel A is 37 μ m.

activity indicative of the class I MHC antigen was found on capillary endothelium and in focal subependymal microglia, and the same staining pattern was found in all three treatment groups (Table II). OX35-immunoreactive CD4 lymphocytes were rare in brain with the same pattern in all three treatment groups (Table II). OX42-immunoreactive microglia were found diffusely in the parenchyma throughout the cerebrum and cerebellum, with an identical pattern in all treatment groups (Table II). Immunoreactive GFAP astrocytes were found diffusely throughout the cerebrum and cerebellum, with the same pattern in all three treatment groups (Table II). There was no immunoreactivity in brain with the nonspecific mouse IgG1 (mIgG1), which is the isotype control antibody for the OX1, OX18, OX6, and the GFAP antibodies (Table II). There was no immunocytochemical staining of brain using the nonspecific mouse IgG2a (mIgG2a), which is the isotype control antibody for the OX35 and OX42 antibodies (Table II).

The delivery of the TH expression plasmid to brain was verified with Southern blotting as shown in Fig. 3 (Lane 3). No signal was detected in the saline-treated animals (Lane 1, Fig. 3) because these animals were not administered DNA. No hybridization signal was detected in the brain of animals treated with the expression plasmid encapsulated in the mIgG2a-PIL (Lane 2, Fig. 3) because this isotype control antibody was unable to target the PIL across the BBB and into brain cells.

DISCUSSION

These studies show that the repeat weekly intravenous administration of the PIL-based gene therapy in rats for 6 weeks causes no measurable toxicity in brain or peripheral tissues. In addition, these studies show that the chronic weekly intravenous administration of a TH expression plasmid encapsulated in TIRMAb-PILs causes no inflammation within the target organ, the central nervous system (CNS).

Table I. Summary of Serum Chemistry

Assay	Units	Saline	mIgG2a-PIL	OX26-PIL
Sodium	mM	143 \pm 1	142 \pm 1	140 \pm 1
Potassium	mM	4.4 \pm 0.1	4.6 \pm 0.1	4.6 \pm 0.2
Chloride	mM	100 \pm 1	100 \pm 1	100 \pm 1
CO ₂	mM	29 \pm 1	29 \pm 1	27 \pm 1
Glucose	mg/dl	168 \pm 8	160 \pm 6	163 \pm 4
Creatinine	mg/dl	0.45 \pm 0.03	0.40 \pm 0.01	0.45 \pm 0.02
Urea nitrogen	mg/dl	19 \pm 1	21 \pm 2	18 \pm 1
Total protein	g/dl	5.2 \pm 0.1	5.3 \pm 0.1	5.3 \pm 0.1
Albumin	g/dl	1.4 \pm 0.1	1.4 \pm 0.1	1.4 \pm 0.1
Bilirubin, total	mg/dl	0.35 \pm 0.03	0.25 \pm 0.05	0.33 \pm 0.02
Alk phos	U/L	231 \pm 27	212 \pm 25	281 \pm 11
AST (SGOT)	U/L	65 \pm 5	59 \pm 2	74 \pm 6
ALT (SGPT)	U/L	54 \pm 2	52 \pm 3	59 \pm 1
Calcium	mg/dl	9.4 \pm 0.1	9.5 \pm 0.2	9.2 \pm 0.1

Data are mean \pm SE ($n = 6$ rats in each of the three treatment groups).

Table II. Summary of Immunocytochemistry

Antibody	Parameter	Fixative	Findings
OX1	Leukocytes	Methanol	Positive choroidal endothelium Same pattern in all 3 treatment groups
OX6	Class II MHC	Para. ^a	Occasional positive cell in meninges Same pattern in all 3 treatment groups
OX18	Class I MHC	Methanol	Weak staining of capillary endothelium Focal subependymal microglia Same pattern in all 3 treatment groups
OX35	CD4-lymphocytes	Methanol	Minimal staining of brain and equal to mouse IgG2a control Same pattern in all 3 treatment groups
OX42	Macrophages	Para.	Diffuse immunoreactive microglia throughout cerebrum and cerebellum Same pattern in all 3 treatment groups
GFAP	Astrocytes	Para.	Diffuse immunoreactive astrocytes throughout cerebrum and cerebellum Same pattern in all 3 treatment groups
Mouse IgG1	Control	Methanol Para.	No reaction (control for OX1, OX18) No reaction (control for OX6, GFAP)
Mouse IgG2a	Control	Methanol, Para.	No reaction (control for OX35) No reaction (control for OX42)

Para., paraformaldehyde.

There is no general systemic toxicity following weekly PIL administration based on the observation that the body weights of the animals increase over the 6 week treatment period at the same rate for all 3 treatment groups (Fig. 1). The PIL targets the plasmid DNA to Tfr-rich organs such as the brain, liver, or spleen (9,14). The serum chemistries show normal hepatic function tests and an absence of an increase in serum bilirubin or liver enzymes (Table I). In contrast, the intravenous injection of adenovirus in primates results in increased liver enzymes secondary to hepatic inflammation caused by reaction to the immunogenic viral vector (18). There is no change in serum electrolytes or other renal function tests (Table I). The normal serum chemistry is paralleled by the normal organ histology for liver, spleen, kidney, heart, lung, and brain (Fig. 2). The serum chemistry and organ histology were examined at 3 days following the sixth weekly injection because prior work has shown the TH gene expression following PIL injection is maximal at this time (13).

The intracerebral injection of viral vectors, such as adenovirus or Herpes simplex virus, leads to inflammation of the brain, as evidenced by perivascular cuffing with lymphocytes and increased immunoreactivity for class I and class II MHC antigens in brain (2-5). Therefore, the present studies performed a detailed immunocytochemical analysis of brain to examine for any evidence of inflammation in the brain

following the chronic delivery to brain of a TH expression plasmid encapsulated in a TfrMAB-targeted PIL. The brain immunocytochemistry of the animals treated weekly with the TfrMAB-targeted PIL was compared to that of control groups of rats treated weekly with either saline or with mIgG2a-targeted PILs. There is an identical pattern of immunoreactivity in rat brain using OX1, OX6, OX18, OX35, OX42, and GFAP antibodies in immunocytochemical analysis of brain for all three treatment groups (Table II). In these studies, the brain was fixed with either methanol or paraformaldehyde, depending on which was the optimal fixative for each antigen (Methods), to preserve antigen recognition in the fixed brain. Chronic delivery of TfrMAB-targeted PILs to brain caused (a) no elevations in parenchymal class I (OX18) or II MHC (OX6), (b) no elevations in parenchymal infiltration by lymphocytes (OX35), leukocytes (OX1), or macrophages (OX42), and (c) no elevations in parenchymal gliosis (GFAP).

In summary, these studies demonstrate that nonviral expression plasmids can be delivered to organs with the PIL gene transfer method without toxic side effects when administered at a PIL-encapsulated plasmid DNA dose of 25 µg/kg. The chronic weekly intravenous administration of this dose of plasmid DNA encoding for rat TH and encapsulated in TfrMAB-targeted PILs causes no evidence of toxicity in ei-

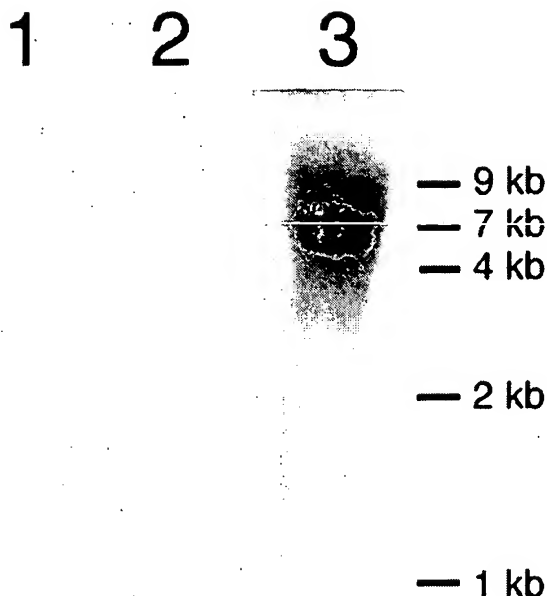


Fig. 3. Southern blot analysis of rat brain with [32 P]pGL2 clone 734. Lane 1, brain isolated from a saline-treated rat; lane 2, brain isolated from a rat injected with the TH expression plasmid encapsulated in the mIgG2a-targeted PIL; and lane 3, brain isolated from a rat injected with the TH expression plasmid encapsulated in the TfRMAB-targeted PIL. The migration of the DNA standards is indicated in the figure. The expected ~7-kb plasmid DNA corresponding to the size of the TH expression plasmid is seen only in the brain of the rats treated with the TfRMAB-targeted PIL (lane 3).

ther the target organ, brain, or in peripheral tissues, such as liver, spleen, kidney, heart, or lung. It is possible that toxic effects may be observed at higher doses, but the dose used in this study in rats was chosen because this dose is therapeutic in rats (13). Moreover, a much higher dose, 200 μ g/kg, of PIL-encapsulated plasmid DNA has been administered weekly to mice without evidence of toxicity (12). The need for high dosing of plasmid DNA with the PIL gene-targeting method is unlikely because a dose of 12 μ g/kg of PIL-encapsulated plasmid DNA in adult primates results in levels of gene expression that are 50-fold higher than in rodents (10). The finding of a lack of toxicity following chronic PIL administration is important because the PIL gene transfer method delivers to the target organ a nonviral plasmid that directs gene expression for only a finite duration (12,13). The expression plasmid is transcribed episomally and is not permanently or randomly integrated into the host genome. Therefore, in order to sustain a pharmacologic effect with plasmid DNA-based gene therapy, it is necessary to administer the gene medicine on a chronic basis. The frequency of the administration is a function of the persistence of plasmid expression in the target organ. Long-term gene expression is possible with viral vectors that permanently integrate into the host genome, but this approach is associated with the risk of insertional mutagenesis (1). An alternative approach to gene therapy is chronic treatment with episomal-based plasmid DNA that is formulated in such a way that the DNA is able to target distant sites following intravenous administration. Prior work has shown that the PIL gene-targeting method enables widespread expression of the exogenous gene in dis-

tant sites such as brain in mice, rats, and rhesus monkeys (9–11). The present studies show that PIL-based gene therapy can be given chronically without the development of tissue toxicity in either the target organ, brain, or in peripheral tissues.

ACKNOWLEDGMENTS

This work was supported by a grant from the Neurotoxin Exposure Treatment Research Program of the U.S. Department of Defense. Dr. Felix Schlachetzki assisted with the immunocytochemistry.

REFERENCES

1. S. Hacein-Bey-Abina, C. von Kalle, M. Schmidt, F. LeDeist, N. Wulffraat, E. McIntyre, I. Radford, J. L. Villeval, C. C. Fraser, M. Cavazzana-Calvo, and A. Fischer. A serious adverse event after successful gene therapy for X-linked severe combined immunodeficiency. *N. Engl. J. Med.* 348:255–256 (2003).
2. M. M. McMenamin, A. P. Byrnes, H. M. Charlton, R. S. Coffin, D. S. Latchman, and M. J. A. Wood. A γ 34.5 mutant of herpes simplex 1 causes severe inflammation in the brain. *Neuroscience* 83:1225–1237 (1998).
3. Y. Stallwood, K. D. Fisher, P. H. Gallimore, and V. Mautner. Neutralisation of adenovirus infectivity by ascitic fluid from ovarian cancer patients. *Gene Ther.* 7:637–643 (2000).
4. R. A. Dewey, G. Morrissey, C. M. Cowdell, D. Stone, F. Bolognani, N. J. F. Dodd, T. D. Southgate, D. Klatzmann, H. Lassmann, M. G. Castro, and P. R. Lowenstein. Chronic brain inflammation and persistent herpes simplex virus 1 thymidine kinase expression in survivors of syngeneic glioma treated by adenovirus-mediated gene therapy: Implications for clinical trials. *Nature Med.* 5:1256–1263 (1999).
5. M. J. A. Wood, H. M. Charlton, K. J. Wood, K. Kajiwarra, and A. P. Byrnes. Immune responses to adenovirus vectors in the nervous system. *Trends Neurosci.* 19:497–501 (1996).
6. N. Chirmule, K. J. Propert, S. A. Magosin, Y. Qian, R. Qian, and J. M. Wilson. Immune responses to adenovirus and adeno-associated virus in humans. *Gene Ther.* 6:1574–1583 (1999).
7. S. M. Zou, P. Erbacher, J. S. Remy, and J. P. Behr. Systemic linear polyethylenimine (L-PEI)-mediated gene delivery in the mouse. *J. Gene Med.* 2:128–134 (2000).
8. G. Zhang, V. Budker, and J. A. Wolff. High levels of foreign gene expression in hepatocytes after tail vein injections of naked plasmid DNA. *Hum. Gene Ther.* 10:1735–1737 (1999).
9. N. Shi, Y. Zhang, R. J. Boado, C. Zhu, and W. M. Pardridge. Brain-specific expression of an exogenous gene following intravenous administration. *Proc. Natl. Acad. Sci. USA* 98:12754–12759 (2001).
10. Y. Zhang, F. Schlachetzki, and W. M. Pardridge. Global non-viral gene transfer to the primate brain following intravenous administration. *Mol. Ther.* 7:11–18 (2003).
11. N. Shi and W. M. Pardridge. Noninvasive gene targeting to the brain. *Proc. Natl. Acad. Sci. USA* 97:7567–7572 (2000).
12. Y. Zhang, C. Zhu, and W. M. Pardridge. Antisense gene therapy of brain cancer with an artificial virus gene delivery system. *Mol. Ther.* 6:67–72 (2002).
13. Y. Zhang, F. Calon, C. Zhu, R. J. Boado, and W. M. Pardridge. Intravenous nonviral gene therapy causes normalization of striatal tyrosine hydroxylase and reversal of motor impairment in experimental parkinsonism. *Hum. Gene Ther.* 14:1–12 (2003).
14. N. Shi, R. J. Boado, and W. M. Pardridge. Receptor mediated gene targeting to tissues *in vivo* following intravenous administration of pegylated immunoliposomes. *Pharm. Res.* 18:1091–1095 (2001).

15. J. Huwyler, D. Wu, and W. M. Pardridge. Brain drug delivery of small molecules using immunoliposomes. *Proc. Natl. Acad. Sci. USA* **93**:14164-14169 (1996).
16. D. Duan, P. Sharma, J. Yang, Y. Yue, L. Dudus, Y. Zhang, K. J. Fisher, and J. F. Engelhardt. Circular intermediates of recombinant adeno-associated virus have defined structural characteristics responsible for long-term episomal persistence in muscle tissue. *J. Virology* **72**:8568-8577 (1998).
17. R. J. Boado and W. M. Pardridge. Ten nucleotide cis element in the 3'-untranslated region of the GLUT1 glucose transporter mRNA increases gene expression via mRNA stabilization. *Molec. Brain Res.* **59**:109-113 (1998).
18. J. N. Lozier, G. Csako, T. H. Mondoro, D. M. Krizek, M. E. Metzger, R. Costello, J. G. Vostal, M. E. Rick, R. E. Donahue, and R. A. Morgan. Toxicity of a first-generation adenoviral vector in rhesus macaques. *Hum. Gene Ther.* **13**:113-124 (2002).

Receptor-Mediated Gene Targeting to Tissues *In Vivo* Following Intravenous Administration of Pegylated Immunoliposomes

Ningya Shi,¹ Ruben J. Boado,¹ and William M. Pardridge^{1,2}

Received March 5, 2001; accepted April 17, 2001

Purpose. Gene therapy has been limited by the immunogenicity of viral vectors, by the inefficiency of cationic liposomes, and by the rapid degradation *in vivo* following the injection of naked DNA. The present work describes a new approach that enables the non-invasive, non-viral gene therapy of the brain and peripheral organs following an intravenous injection.

Methods. The plasmid DNA encoding β -galactosidase is packaged in the interior of neutral liposomes, which are stabilized for *in vivo* use by surface conjugation with polyethyleneglycol (PEG). The tips of about 1% of the PEG strands are attached to a targeting monoclonal antibody (MAb), which acts as a "molecular Trojan Horse" to ferry the liposome carrying the gene across the biological barriers of the brain and other organs. The MAb targets the transferrin receptor, which is enriched at both the blood-brain barrier (BBB), and in peripheral tissues, such as liver and spleen.

Results. Expression of the exogenous gene in brain, liver, and spleen was demonstrated with β -galactosidase histochemistry, which showed persistence of gene expression for at least 6 days after a single intravenous injection of the pegylated immunoliposomes. The persistence of the transgene was confirmed by Southern blot analysis.

Conclusions. Widespread expression of an exogenous gene in brain and peripheral tissues is induced with a single intravenous administration of plasmid DNA packaged in the interior of pegylated immunoliposomes. The liposomes are formulated to target specific receptor systems that enable receptor-mediated endocytosis of the complex into cells *in vivo*. This approach allows for non-invasive, non-viral gene therapy of the brain.

KEY WORDS: gene delivery; transferrin receptor; blood-brain barrier; β -galactosidase.

INTRODUCTION

Current approaches to gene delivery *in vivo* use either viral vectors (1,2) or cationic liposome/DNA formulations (3,4). In a third approach, plasmid DNA is attached to a receptor ligand to trigger receptor-mediated endocytosis into the target cell. In the receptor-mediated approach, the plasmid DNA is complexed to the targeting ligand with a polylysine bridge and this method has worked in cell culture and in some *in vivo* applications (5–7). However, the DNA is attached to the conjugate of polylysine and the targeting ligand only by electrostatic interactions and these DNA/polycation interactions may be disrupted in the circulation immediately after injection into the bloodstream. In addition,

the plasmid DNA is unprotected and is subject to degradation by endonucleases, which are not found in tissue culture medium, but which are ubiquitous *in vivo* (8). In contrast, viral vector systems house the exogenous gene in the interior of the viral capsid, which protects the DNA from endonucleases *in vivo*.

In the present approach to targeting an exogenous gene to tissues *in vivo*, a molecular formulation was designed to keep the advantages of both viral vectors and receptor-mediated gene targeting. As shown in Fig. 1A, the supercoiled non-viral plasmid DNA is packaged in the interior of a liposome (9). This formulation makes the plasmid DNA resistant to endonucleases *in vivo* (10), and should be contrasted with conventional cationic liposome/DNA mixtures, where the DNA is exteriorized. Liposomes are immediately coated on the surface by serum proteins and this triggers rapid uptake by cells lining the reticuloendothelial system (RES) in the body *in vivo*. This rapid uptake by the RES can be reduced by conjugation of polymeric strands to the surface of the liposome (11). In the present formulation, the surface of a 75 nm liposome is conjugated with approximately 3000 strands of polyethyleneglycol (PEG) of 2000 Dalton molecular weight, designated PEG²⁰⁰⁰ (Fig. 1A). Pegylated liposomes have prolonged circulation times *in vivo* compared to conventional liposomes (11). However, pegylated liposomes are relatively inert and are not targeted specifically to any tissue. Tissue targeting can be achieved by the conjugation of the tips of the PEG²⁰⁰⁰ strands with a targeting ligand (12). The targeting ligand may be either an endogenous peptide or a peptidomimetic monoclonal antibody (MAb) that undergoes receptor-mediated endocytosis into cells. In the present formulation, the murine OX26 MAb to the rat transferrin receptor (TfR) is used to target the pegylated immunoliposome carrying the plasmid DNA to tissues *in vivo* that express the TfR (9).

Gene targeting to brain and peripheral organs with pegylated immunoliposomes has been reported using luciferase as the exogenous gene (9). However, prior work with luciferase demonstrated a low level of persistence of the transgene *in vivo* with a peak of gene expression at 48 h, followed by return to baseline activity at 72 h after intravenous injection of pegylated immunoliposomes (9). The luciferase expression vector used in prior work contained a heterologous intron in the 3'-untranslated region (UTR), and such inserts can decrease gene expression *in vivo* (3). Therefore, the present studies examine β -galactosidase gene expression in brain and peripheral tissues following the administration of pegylated immunoliposomes carrying a β -galactosidase gene packaged in an expression plasmid with a short 3'-UTR lacking a heterologous intron (pSV- β -galactosidase, Promega). Gene expression is measured at 2, 4, and 6 days after a single intravenous administration using β -galactosidase histochemistry. The persistence of the transgene *in vivo* was confirmed with Southern blotting.

METHODS

Synthesis of Pegylated Immunoliposome with Encapsulated Gene

The liposome was formulated as described previously (9) with 19.2 μ mol of 1-palmitoyl-2-oleoyl-*sn*-glycerol-3-

¹ Department of Medicine, UCLA School of Medicine, Los Angeles, California.

² To whom correspondence should be addressed at UCLA Warren Hall (13-164), 900 Veteran Ave., Los Angeles, California 90024. (e-mail: wpardridge@mednet.ucla.edu)

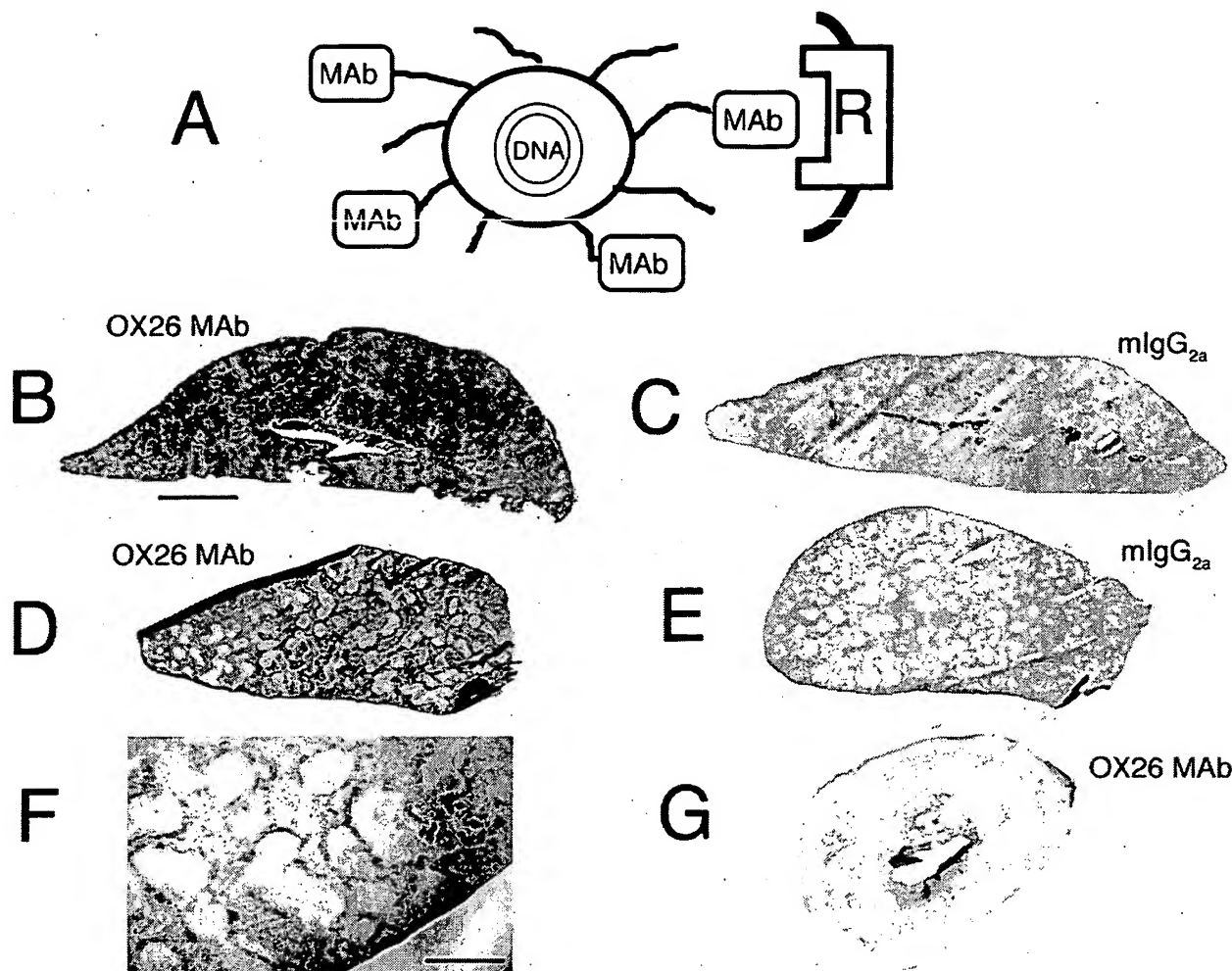


Fig. 1. (A) A double-stranded super-coiled plasmid DNA is packaged in the interior of an 75 nm liposome and the surface of the liposome is conjugated with approximately 3000 strands of polyethyleneglycol (PEG) of 2000 Dalton molecular weight (PEG²⁰⁰⁰). About 1% of the PEG²⁰⁰⁰ strands are conjugated with a targeting ligand (9). In the present formulation, a monoclonal antibody (MAb) to the transferrin receptor (TfR) is used. (B) Liver histochemistry at 2 days after intravenous injection of OX26 pegylated immunoliposomes carrying the pSV- β -galactosidase plasmid. (C) Liver histochemistry at 2 days after intravenous injection of pegylated immunoliposomes carrying the pSV- β -galactosidase plasmid and conjugated with mouse (m) IgG_{2a}. (D) Spleen histochemistry at 2 days after intravenous injection of OX26 pegylated immunoliposomes carrying the pSV- β -galactosidase plasmid. (E) Spleen histochemistry at 2 days after intravenous injection of mouse IgG_{2a} pegylated immunoliposomes carrying the pSV- β -galactosidase plasmid. (F) High magnification of spleen β -galactosidase histochemistry at 2 days after intravenous injection of OX26 pegylated immunoliposomes encapsulated with the pSV- β -galactosidase plasmid. (G) Heart histochemistry at 2 days after intravenous injection of OX26 pegylated immunoliposomes carrying the pSV- β -galactosidase plasmid. The magnification in panels B, C, D, E, and G is the same and the magnification bar in panel B is 3.3 mm. The magnification bar in panel F is 0.94 mm. Only the specimen in panel F was counterstained whereas all other specimens were not counterstained.

phosphocholine (POPC), 0.2 μ mol of didodecyldimethylammonium bromide (DDAB), and 0.6 μ mol of distearoylphosphatidylethanolamine (DSPE)-PEG²⁰⁰⁰. The DSPE-PEG²⁰⁰⁰ was comprised of DSPE-PEG²⁰⁰⁰ and DSPE-PEG²⁰⁰⁰-maleimide in a ratio of 95:5 (9). The surface charge of the empty liposome was not measured directly, but would be expected to be negative, given the 3-fold molar excess of the anionic lipid, DSPE-PEG²⁰⁰⁰, relative to the cationic lipid, DDAB. The bifunctional PEG derivative, DSPE-PEG²⁰⁰⁰-maleimide, enabled conjugation of the thiolated MAb to the tip of the PEG strands (9). Following initial mixing of the lipids in chloroform, evaporation of chloroform, resuspension in 0.05 M Tris (pH = 8.0), and sonication, 100 μ g of super-

coiled plasmid and 1 μ Ci of nick-translated plasmid labeled with ³²P, were added to the lipids. The liposomes were formed by series of freeze/thaw cycles and extrusion through 400, 200, and 100 nm pore-sized polycarbonate membranes as described previously (9). Plasmid DNA bound to the exterior of the pegylated liposome was quantitatively removed by treatment with exonuclease III/DNase I (9). The thiolated OX26 MAb or thiolated mouse IgG_{2a}, which contained a trace amount of [¹²⁵I] labeled IgG, was conjugated to the pegylated liposome overnight and unconjugated MAb was separated by Sepharose CL4B gel filtration chromatography as described previously (9). The final percent entrapment of the DNA within the interior of the liposome was determined

by measuring the total ^{32}P radioactivity in the liposome peak, and this entrapment was typically 20% of the starting plasmid DNA, which included loss of material in the dead volume of the extruder. The number of MAb molecules conjugated to each liposome was computed as described previously (9,12), and ranged from 35-50 MAb molecules per individual liposome. The diameter of the pegylated immunoliposomes was measured by quasielastic light scattering as described previously (9,12) and ranged from 45 nm (10%) to 114 nm (90%) with a mean diameter of 73 nm in a unimodal pattern.

In Vivo Administration and Organ Histochemistry

The pegylated immunoliposomes carrying the DNA were injected intravenously into anesthetized adult male Sprague Dawley rats (250 g) at a dose of 10 μg of plasmid DNA per rat. The pharmacokinetics and organ uptake of these structures has been reported previously (9). Animals were sacrificed at 2, 4, or 6 days after intravenous injection and brain, heart, kidney, spleen, and liver were removed, and processed for β -galactosidase histochemistry with 5-bromo-4-chloro-3-indoyl- β -D-galactoside (X-Gal, Promega) as described previously (9). The presence of endogenous β -galactosidase-like enzyme activity was examined in control tissues obtained from un-injected rats. These studies showed that brain, liver, spleen, and heart contain no endogenous β -galactosidase-like enzyme activity. However, there was abundant β -galactosidase-like activity in control rat kidney, and no further studies with kidney were performed. Slides were scanned with a 1200 dpi UMAX flatbed scanner with transilluminator and cropped with Adobe Photoshop 5.5 with a G4 Power Macintosh. Sections of organs from animals treated with either OX26 or mouse IgG_{2a} pegylated immunoliposomes were scanned simultaneously.

Southern Blotting

Genomic DNA was isolated from rat liver using the Genomic Isolation Kit (Qiagen) and the yield averaged $1.32 \pm 0.17 \mu\text{g}$ DNA/mg tissue (mean \pm SE, $n = 4$). The OD_{260/280} was 1.7 for all samples. Ten μg DNA aliquots were digested with 15 U EcoRI for 1 h at 37°C, resolved by gel electrophoresis in 0.8 % agarose, blotted to a GeneScreen Plus membrane and hybridized with the ^{32}P -pSV- β -galactosidase DNA. Autoradiograms were performed with Kodak X-Omat Blue film for 3 h at 22°C. Ethidium bromide staining of the agarose gel before blotting showed the expected smear of partially digested genomic DNA ranging from 23-0.6 kb in all samples.

RESULTS

The 6.8 kb pSV- β -galactosidase plasmid (Promega) was incorporated in the interior of pegylated immunoliposomes that were conjugated with one of two different targeting ligands: either the OX26 MAb to the rat TfR or a mouse IgG_{2a} isotype control antibody (Fig. 1A). Organs were removed at 2, 4, or 6 days after administration for β -galactosidase histochemistry or Southern blot analysis. After administration of the mouse IgG_{2a} pegylated immunoliposomes, there was no measurable β -galactosidase gene expression in liver (Fig. 1C), spleen (Fig. 1E), brain (Fig. 3C), or heart (data not shown). No plasmid was detectable by Southern blot in liver at 48 h after intravenous administration of the mouse IgG_{2a} pe-

gylated immunoliposomes (Fig. 2, lane 1). However, if the β -galactosidase expression plasmid was incorporated in the interior of pegylated immunoliposomes that were formulated with the OX26 MAb, there was abundant β -galactosidase gene expression in liver (Fig. 1B) or spleen (Fig. 1D) at 48 h after a single intravenous injection of the formulation. The exogenous plasmid DNA was also detected by Southern blot in liver at 2, 4, and 6 days after intravenous injection (Fig. 2). In contrast, there was no measurable β -galactosidase gene expression in heart (Fig. 1G) because of the insignificant expression of the TfR on endothelium comprising the continuous capillaries of the myocardium. The β -galactosidase histochemistry of liver (Fig. 1B) shows the gene is nearly evenly expressed throughout the hepatic lobule, which parallels the distribution of transferrin receptor in the normal rat liver (13). The high magnification of β -galactosidase histochemistry in spleen shows a prominent expression of the gene in the red pulp of spleen with less gene expression in splenic white pulp (Fig. 1F).

The pegylated immunoliposome formulation depicted in Fig. 1A enables widespread expression of an exogenous gene in the brain as shown in Figure 3. The expression of the β -galactosidase transgene in brain persists for at least 6 days after a single intravenous injection of the pegylated immunoliposome, as shown in Fig. 3B. There is also persistent expression of the β -galactosidase transgene in liver or spleen at 6 days after a single intravenous injection, and the histochemical pattern for liver or spleen at 6 days after injection was comparable to that shown for these organs at 2 days after injection (Fig. 1B,D). Measurements were also made at 4 days after intravenous injection and these histochemistry studies

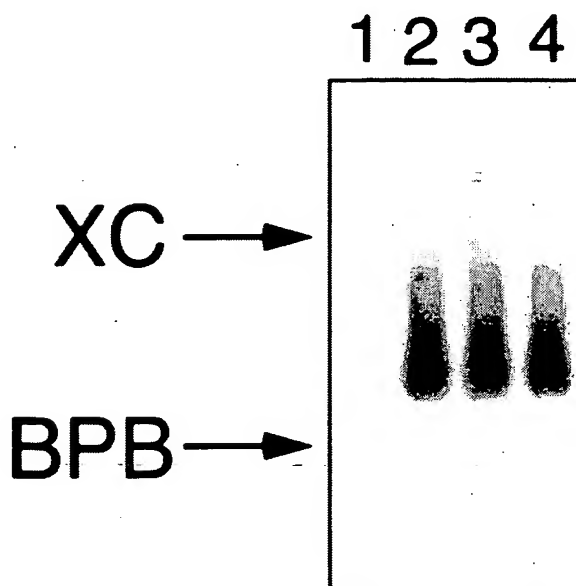


Fig. 2. Southern blot of rat liver with ^{32}P -pSV- β -gal DNA. Lane 1: liver at 2 days after intravenous administration of mouse IgG_{2a} pegylated immunoliposomes carrying the pSV- β -galactosidase plasmid. Lanes 2, 3, and 4: liver at 2, 4, and 6 days, respectively, after intravenous injection of OX26 MAb pegylated immunoliposomes carrying the pSV- β -galactosidase plasmid. The migration of the xylene cyanol (XC) and bromophenol blue (BPB) tracking dyes are indicated; the XC and the BPB dyes migrate near the 4.4 and 0.6 kb DNA sizing standards, respectively.

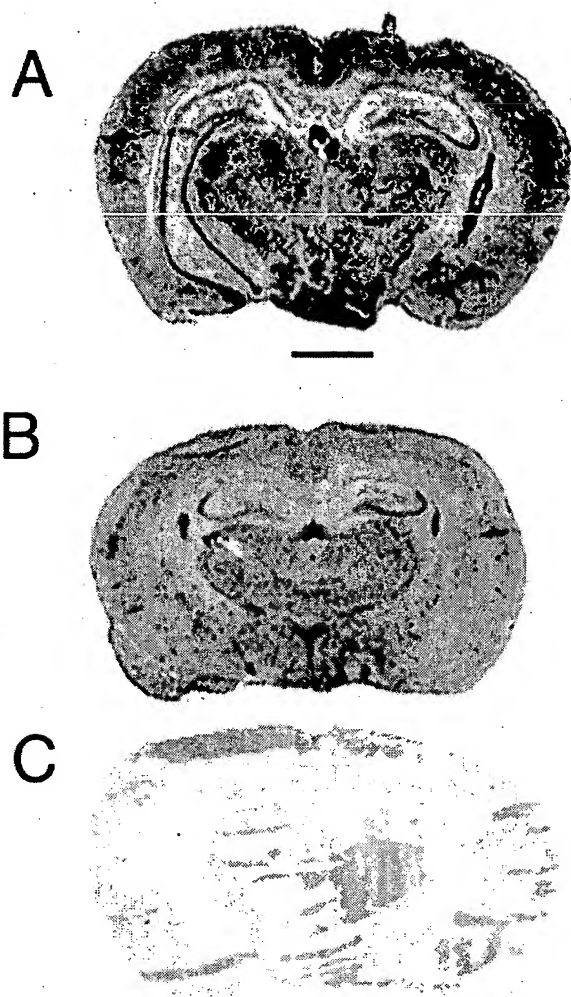


Fig. 3. Brain histochemistry showing β -galactosidase gene expression at either 2 days (panels A and C) or 6 days (panel B) after intravenous injection of pegylated immunoliposomes carrying the β -galactosidase plasmid and conjugated with either the OX26 MAb (panels A and B) or mouse IgG_{2a} isotype control (panel C). None of the specimens were counterstained. The magnification bar in panel A is 3.1 mm.

showed the level of β -galactosidase gene expression in liver, spleen, or brain was intermediate between the 2 day or 6 day activity (data not shown).

DISCUSSION

These studies demonstrate the widespread expression of an exogenous gene following intravenous administration of pegylated immunoliposomes carrying a non-viral plasmid gene packaged in the *interior* of the liposome (Fig. 1A). The exogenous gene is expressed deep within the parenchyma of organs targeted by the anti-TfR MAb, such as liver, spleen, and brain (Fig. 1 and 3). Gene expression persists for at least 6 days after a single intravenous injection of the pegylated immunoliposome (Fig. 3). The β -galactosidase histochemistry is confirmed by Southern blot analysis (Fig. 2), which indicates the persistence of β -galactosidase enzyme activity in the tissues arises from the persistence of the trans-gene *in vivo*.

The packaging of the exogenous gene in the interior of the pegylated immunoliposome protects the gene against the ubiquitous endonucleases that exist *in vivo* (8), which is analogous to packaging an exogenous gene in the interior of a virus. However, unlike viruses, which express immunogenic coat proteins, the immunogenicity of the targeting MAb can be eliminated by "humanization" and genetic engineering of the MAb (14). The pegylated immunoliposome formulation shown in Fig. 1A also contrasts with cationic liposomes, which form a complex with DNA that is exposed to plasma. These structures rapidly aggregate *in vivo* (15) leading to deposition at the pulmonary microvasculature following intravenous administration (16). In the formulation used in the present studies, the surface of the liposome is pegylated, which stabilizes the structure in the blood, minimizes rapid uptake by the reticuloendothelial system, and enables a prolonged plasma residence time (9).

The specificity of the pegylated immunoliposome is a function of the MAb attached to the tips of the PEG strands (Fig. 1A). The gene expression in liver and spleen is due to the high expression of TfR on parenchymal cells in these tissues, and is not a non-specific result of clearance of particulate liposomes by the reticuloendothelial system. This is demonstrated by the observation that substitution of the anti-TfR MAb with the mouse IgG_{2a} isotype control leads to a loss of β -galactosidase gene expression in liver and spleen (Fig. 1C,E). Similarly, prior work with a luciferase reporter plasmid showed the absence of gene expression with mouse IgG_{2a} pegylated immunoliposomes in multiple organs in the rat (9). The anti-TfR MAb targets liver, spleen, and brain, but not heart (Fig. 1). Targeting exogenous genes to organs such as liver or spleen is a "one-barrier" gene delivery problem. Owing to the high porosity of the sinusoids perfusing either liver or the red pulp of spleen, 75 nm structures such as pegylated immunoliposomes freely gain access to the extravascular space in these tissues (17). Once in the extravascular compartment, the liposomes carrying the targeting ligand may then bind to the TfR on the parenchymal cells of liver or spleen.

Gene targeting to organs such as brain, which have continuous capillaries of restricted permeability, is a "two-barrier" gene targeting problem. The pegylated immunoliposome must first traverse the microvascular endothelial barrier, and then must traverse the plasma membrane of the target cell within the organ (9). The expression of the TfR on both barriers in brain enables gene expression in neurons (9). Prior work using high magnification microscopy demonstrated widespread expression of the β -galactosidase gene in neurons in the brain (9). The pegylated immunoliposome first undergoes receptor-mediated transcytosis across the BBB *in vivo*, owing to expression of the TfR on the BBB (18), and then undergoes receptor-mediated endocytosis into neurons within brain, owing to expression of the TfR on the neuronal plasma membrane (19). The BBB TfR is a bidirectional transcytosis system (20), and mediates the movement of the pegylated immunoliposomes through the endothelial barrier into brain interstitial space. The phospholipids forming the liposome fuse with the intracellular endosomal membrane subsequent to endocytosis and release the plasmid DNA into the cytosol of the target cell (21). Once inside the cytosol, the plasmid may diffuse to the nucleus for transcription. These studies show a persistence of gene expression in brain and

other organs *in vivo* for at least 6 days following a single intravenous injection of the plasmid.

In summary, persistent expression of an exogenous gene in tissues *in vivo* may be achieved with a non-invasive, non-viral approach to gene targeting *in vivo* (Fig. 1A). The targeting specificity of the formulation is a function of the targeting ligand that is tethered to the tips of the polyethylene glycol strands on the surface of the liposome. Multiple ligands could be conjugated to the surface of the pegylated liposome to enable tissue-specific targeting of exogenous genes *in vivo*.

ACKNOWLEDGMENTS

This work was supported by a grant from the U.S. Department of Defense.

REFERENCES

1. A. H. Hamawy, L. Y. Lee, R. G. Crystal, and T. K. Rosengart. Cardiac angiogenesis and gene therapy: A strategy for myocardial revascularization. *Curr. Opinion in Cardiology*. 14:515-522 (1999).
2. G. R. Akkaraju, J. Huard, E. P. Hoffman, W. F. Goins, R. Pruchnic, S. C. Watkins, J. B. Cohens, and J. C. Glorioso. Herpes simplex virus vector-mediated dystrophin gene transfer and expression in MDX mouse skeletal muscle. *J. Gene Med.* 1:280-289 (1999).
3. Y. Liu, D. Liggitt, W. Zhong, G. Tu, K. Gaensler, and R. Debs. Cationic liposome-mediated intravenous gene delivery. *J. Biol. Chem.* 270:24864-24870. (1995).
4. C. J. Wheeler, P. L. Flegner, Y. J. Tsai, J. Marshall, L. Sukhu, S. G. Doh, J. Hartikka, J. Nietupski, M. Manthorpe, M. Nichols, M. Plewe, X. Liang, J. Norman, A. Smith, and S.H. Cheng. A novel cationic lipid greatly enhances plasmid DNA delivery and expression in mouse lung. *Proc. Natl. Acad. Sci. USA* 93:11454-11459 (1996).
5. C. H. Wu, J. M. Wilson, and G. Y. Wu. Targeting genes: delivery and persistent expression of a foreign gene driven by mammalian regulatory elements *in vivo*. *J. Biol. Chem.* 264:16985-16987 (1989).
6. M. Cotton, F. Langle-Rouault, H. Kirlappos, E. Wagner, K. Metchler, M. Zenke, H. Beug, and M. L. Birnstiel. Transferrin-polycation-mediated introduction of DNA into human leukemic cells: stimulation by agents that affect the survival of transfected DNA or modulate transferrin receptor levels. *Proc. Natl. Acad. Sci. USA* 87:4033-4037 (1990).
7. T. Ferkol, J.C. Perales, F. Mularo, and R.W. Hanson. Receptor-mediated gene transfer into macrophages. *Proc. Natl. Acad. Sci. USA* 93:101-105 (1996).
8. M. E. Barry, D. Pinto-Gonzalez, F. M. Orson, G. J. McKenzie, G. R. Petry, and M. A. Barry. Role of endogenous endonucleases and tissue site in transfection and CpG-mediated immune activation after naked DNA injection. *Hum. Gene Ther.* 10:2461-2480 (1999).
9. N. Shi and W. M. Pardridge. Non-invasive gene targeting to the brain. *Proc. Natl. Acad. Sci. USA* 97:7567-7572 (2000).
10. P. A. Monnard, T. Oberholzer, and P. Luisi. Entrapment of nucleic acids in liposomes. *Biochim. Biophys. Acta.* 1329:39-50 (1997).
11. D. Papahadjopoulos, T. M. Allen, A. Gabizon, E. Mayhew, K. Matthey, S. K. Huang, K. D. Lee, M. C. Woodle, D. D. Lasic, C. Redemann, *et al.* Sterically stabilized liposomes: Improvements in pharmacokinetics and antitumor therapeutic efficacy. *Proc. Natl. Acad. Sci. USA* 88:11460-11464 (1991).
12. J. Huwyler, D. Wu, and W.M. Pardridge. Brain drug delivery of small molecules using immunoliposomes. *Proc. Natl. Acad. Sci. USA* 93:14164-14169 (1996).
13. K. A. Basclain and G. P. Jeffrey. Coincident increase in periportal expression of iron proteins in the iron-loaded rat liver. *J. Gastroenterol. Hepatol.* 14:659-668 (1999).
14. M. J. Coloma, H. J. Lee, A. Kurihara, E. M. Landaw, R. J. Boado, S. L. Morrison, and W. M. Pardridge. Transport across the primate blood-brain barrier of a genetically engineered chimeric monoclonal antibody to the human insulin receptor. *Pharm. Res.* 17:266-274 (2000).
15. C. Plank, M. X. Tang, A. R. Wolfe, and F. C. Szoka. Branched cationic peptides for gene delivery: role of type and number of cationic residues in formation and in vitro activity of DNA polyplexes. *Hum. Gene Ther.* 10:319-332 (1999).
16. H. E. J. Hofland, D. Nagy, J.J. Liu, K. Spratt, Y. L. Lee, O. Danos, and S. M. Sullivan. *In vivo* gene transfer by intravenous administration of stable cationic lipid/DNA complex. *Pharm. Res.* 14:742-749 (1997).
17. J. Huwyler, J. Yang, and W. M. Pardridge. Targeted delivery of daunomycin using immunoliposomes: pharmacokinetics and tissue distribution in the rat. *J. Pharmacol. Exp. Ther.* 282:1541-1546 (1997).
18. J. Huwyler and W. M. Pardridge. Examination of blood-brain barrier transferrin receptor by confocal fluorescent microscopy of unfixed isolated rat brain capillaries. *J. Neurochem.* 70:883-886 (1998).
19. D. C. Mash, J. Pablo, D. D. Flynn, S. M. Efange, and W. J. Weiner. Characterization and distribution of transferrin receptors in the rat brain. *J. Neurochem.* 55:1972-1979 (1990).
20. Y. Zhang and W. M. Pardridge. Rapid transferrin efflux from brain to blood across the blood-brain barrier. *J. Neurochem.* 76: 1597-1600 (2001).
21. K. W. C. Mok, A. M. I. Lam, and P. R. Cullis. Stabilized plasmid-lipid particles: factors influencing plasmid entrapment and transfection properties. *Biochim. Biophys. Acta.* 1419:137-150 (1999).